

MULTIPLE CODING AND SPACE-TIME MULTI-USER DETECTION IN MULTIPLE  
ANTENNA SYSTEMS

A DISSERTATION SUBMITTED TO THE GRADUATE DIVISION OF THE  
UNIVERSITY OF HAWAII IN PARTIAL FULFILLMENT  
OF THE REQUIREMENTS FOR THE DEGREE OF

DOCTOR OF PHILOSOPHY

IN

ELECTRICAL ENGINEERING

MAY 2005

By  
Jianhan Liu

Dissertation Committee:

Anders Høst-Madsen, Chairperson  
Marc P. C. Fossorier  
James B. Nation  
N. Thomas Gaarder  
Todd R. Reed

Copyright 2004

by

Jianhan Liu

iii

To my wife  
Xin  
and my parents.

## Acknowledgements

I am very glad to take this opportunity to thank a few wonderful people with whom I had studied and worked. Foremost, I would like to express my gratitude to my advisor Dr. Anders Høst-Madsen for his guidance and support throughout the past four years. No matter how busy he was, his office door has always been open to me. I have tremendously benefited from his extensive knowledge, great intuition and technical insight. I greatly appreciate his patience on the guidance, his concern on my research, and his help to my life. In fact, I received his help in all aspects: from how to write good technical papers to how to give impressive presentations. Without his encouragement and advices, this dissertation could not be finished.

I would like to extend my thanks to Dr. Marc P. C. Fossorier for his unselfish help and valuable advices. Working with him is a true pleasure to me. I am deeply indebted to his ideas, insights and even technical writing. I have been influenced by his enthusiasm and industriousness on research and I thank him for introducing me to the world of error control coding.

I am also grateful to Dr. Todd Reed, Dr. Thomas Gaarder, and Dr. James B. Nation, for serving as my committee members, and giving me suggestions to improve this dissertation. I want to extend my thanks to Dr. Anthony Kuh and Dr. James Yee for teaching me interesting courses.

I am thankful to my friends and fellow colleagues: Jinghu, Juntan, Seungjae, Nenad, Zigui, Henning, Xiangang, Wenyi and Yige, for the memorable experience of working together in POST 325. I want to thank them for every help I received. I could not forget to thank my good friend Mu Feng, who provided me innumerable help during these years.

Finally, I want to dedicate this dissertation to my wife Xin, who has shared all the hardships and joys with me in these years; to my parents, who consistently support me with their unconditional love and care.

## ABSTRACT

We study transmit power adaption and capacity-approaching coding/decoding in multiple-input-multiple-output (MIMO) Rayleigh fading channels under the assumption that perfect channel state information is known at both the transmitter and the receiver. The capacity of MIMO systems with transmitter channel state information can be achieved via two schemes: a multiple coding scheme with temporal and spatial water filling and a single coding scheme with temporal and spatial water filling. The former requires an infinite number of different codes and the latter requires inter-block coding and therefore a very long code. We propose three different simple, but powerful, methods for transforming the MIMO fading channel into a set of additive white noise Gaussian channels, to which standard codes for the Gaussian channel can then be applied. We show through a number of examples that these methods can closely approach channel capacity. The code length of the proposed multiple-coding scheme can be much shorter since it can adapt its rate to fading conditions. Also the code length is determined solely by the length of codes chosen for the AWGN channel(s), not the fading dynamics.

We study the applications of space-time block codes in DS-CDMA system. We propose subspace-based blind decoders for the downlink which can blindly suppress the multiple access interferences from other users and exploit the advantages provided by multiple antennas simultaneously. Our schemes can be used for quite a few existing space-time block codes because we *borrow* the structure of linear dispersion codes. We also propose non-coherent blind decoders for the downlink of DS-CDMA system equipped with multiple antennas. Our non-coherent blind decoders can suppress the multiple access interferences and exploit diversity gain without knowing the channel state information either at the base station or at the mobile station. Our simulations results show that the proposed blind decoders significantly outperform the traditional method currently used.

# Contents

<b>Acknowledgements</b>	<b>v</b>
<b>Abstract</b>	<b>vi</b>
<b>List of Tables</b>	<b>ix</b>
<b>List of Figures</b>	<b>x</b>
<b>1 Introduction</b>	<b>1</b>
1.1 Contributions of the Dissertation . . . . .	4
1.2 Organization of the Dissertation . . . . .	5
1.3 Notations in the dissertation . . . . .	7
<b>2 MIMO Fading Channels: An Overview</b>	<b>8</b>
2.1 MIMO Fading Channel Model . . . . .	8
2.2 Ergodic Capacity of MIMO Fading Channels . . . . .	9
2.2.1 Ergodic Capacity with NCSI . . . . .	10
2.2.2 Ergodic Capacity with CSIR . . . . .	11
2.2.3 Ergodic Capacity with CSIT and CSIR . . . . .	11
2.3 Transmission Techniques for MIMO Fading Channels . . . . .	12
2.3.1 Space-time Coding . . . . .	13
2.3.2 Differential Space-time Coding . . . . .	16
2.4 Diversity-Multiplexing Tradeoff . . . . .	17
<b>3 Multiple Coding for MIMO Rayleigh Fading Systems</b>	<b>19</b>
3.1 Motivations . . . . .	19
3.2 System Model with CSIT and CSIR . . . . .	21
3.3 Marginal pdf of the Eigenvalues . . . . .	23
3.3.1 Marginal pdf of the Unordered Eigenvalues . . . . .	23
3.3.2 Marginal pdf of the Ordered Eigenvalues . . . . .	24
3.4 The Beamforming Case . . . . .	25
3.5 The Multiple Eigen-Beamforming Case . . . . .	30

3.5.1	Unordered Multiple Eigen-Beamforming . . . . .	33
3.5.2	Ordered Multiple Eigen-Beamforming . . . . .	36
3.5.3	Discussions . . . . .	39
3.6	Extended to Correlated MIMO Rayleigh Fading Systems . . . . .	43
3.6.1	System Description . . . . .	44
3.6.2	Capacity and Achievable Rate with Different Signaling Schemes . . . . .	47
3.6.3	Examples and Discussion . . . . .	49
<b>4</b>	<b>Blind Decoders of Space-time Block Codes in Downlink DS-CDMA Systems</b>	<b>55</b>
4.1	Introduction . . . . .	55
4.2	Blind Decoders of Linear Dispersion Codes . . . . .	57
4.2.1	Linear Dispersion Codes . . . . .	57
4.2.2	System Model . . . . .	58
4.2.3	Direct Subspace-based Blind Decoder . . . . .	60
4.2.4	Subspace-based Blind Sphere Decoder . . . . .	62
4.2.5	Decimation-combining Processing . . . . .	64
4.2.6	Simulation Examples . . . . .	65
4.3	Non-coherent Blind Decoders for Differential STBC . . . . .	68
4.3.1	System Model . . . . .	69
4.3.2	Encoding and Decoding of Differential STBC . . . . .	71
4.3.3	Non-coherent Detection with Blind Linear Multiuser Estimator . . . . .	72
4.3.4	For MISO DS-CDMA System . . . . .	74
4.3.5	For MIMO DS-CDMA System . . . . .	76
4.3.6	Simulation Examples . . . . .	77
<b>5</b>	<b>Conclusions</b>	<b>82</b>
	<b>Bibliography</b>	<b>84</b>

# List of Tables

1.1	Table of some abbreviations. . . . .	4
3.1	Algorithm for numerically calculating $C_e$ . . . . .	30

# List of Figures

2.1	Capacity with CSIT and CSIR V.S Capacity with CSIR. . . . .	12
2.2	Space-time trellis code, QPSK, 2bits/s/Hz for $N_t = 2$ . . . . .	14
3.1	The illustration of truncated partitioned channel inversion. . . . .	26
3.2	Capacity of beamforming in SISO and SIMO Rayleigh fading channels. . .	31
3.3	Capacity of beamforming in MIMO Rayleigh fading channels. . . . .	32
3.4	Capacity of unordered multiple eigen-beamforming for $(n, 2)$ MIMO Rayleigh fading channels. . . . .	35
3.5	Capacity of unordered multiple eigen-beamforming for $(3, 3)$ and $(4, 4)$ MIMO Rayleigh fading channels. . . . .	36
3.6	Comparison between the method with optimal partition and our heuristic partition method. . . . .	37
3.7	Capacity of ordered multiple eigen-beamforming for $(n, 2)$ MIMO Rayleigh fading channels. . . . .	40
3.8	Capacity of ordered multiple eigen-beamforming for $(3, 3)$ and $(4, 4)$ MIMO Rayleigh fading channels. . . . .	41
3.9	Comparison between ordered and unordered multiple eigen-beamforming for $(3, 3)$ and $(4, 4)$ MIMO Rayleigh fading channels. . . . .	42
3.10	Comparison with the capacity of CSI at receiver only in MIMO Rayleigh fading channels. . . . .	43
3.11	Capacities of $(N_t = n, N_r = 2)$ highly correlated ( $r = 0.9$ ) MIMO fading channels at different SNR. . . . .	50
3.12	Effect of exponential correlation parameter on capacities and achievable rates of the $(N_t = 4, N_r = 2)$ correlated MIMO fading channels at $SNR = 5dB$ . . . . .	51
3.13	Effect of exponential correlation parameter on capacities and achievable rates of the $(N_t = 3, N_r = 3)$ correlated MIMO fading channels at $SNR = 5dB$ . . . . .	52
3.14	Capacities and achievable rates of the $(N_t = 3, N_r = 3)$ slightly correlated ( $r = 0.1$ ) MIMO fading channels at different SNR. . . . .	53
3.15	Capacities and achievable rates of the $(N_t = 3, N_r = 3)$ highly correlated ( $r = 0.9$ ) MIMO fading channels at different SNR. . . . .	54

4.1	Convergence speed of subspace-method blind decoders for $N_t = 2, N_r = 1, T = Q = 2$ in $K = 8$ users DS-CDMA system. . . . .	65
4.2	Performance of different decoders for LD code with $N_t = 2, N_r = 1, T = Q = 2$ in $K = 8$ users DS-CDMA system. . . . .	66
4.3	Convergence speed of subspace-method blind Decoders for $N_t = 2, N_r = 2, T = 2, Q = 4$ LD code in $K=4$ users DS-CDMA system. . . . .	67
4.4	Performance of different decoders for $N_t = 2, N_r = 2, T = 2, Q = 4$ LD code in $K=4$ users DS-CDMA system. . . . .	68
4.5	Convergence speed of non-coherent detection of the differential Alamouti's STBC with Rate=1 (BPSK constellation),in $K=8$ users DS-CDMA system. . . . .	78
4.6	Performance of Non-coherent detection of the differential Alamouti's STBC with Rate=1 (BPSK constellation),in $K=8$ users DS-CDMA system. . . . .	79
4.7	Convergence speed of non-coherent detection of differential Quaternion STBC with Rate=1.5 (QPSK constellation), in $K=8$ users DS-CDMA system. . . . .	80
4.8	Performance of non-coherent detection of differential Quaternion STBC with Rate=1.5 (QPSK constellation), in $K=8$ users DS-CDMA system. . . . .	81

# Chapter 1

## Introduction

Wireless communication systems, which aim to allow people and machines to communicate with each other almost at anytime and anywhere, have greatly blossomed in last two decades. Nowadays, from wireless local networks for short range communications to cellular mobile networks for wide coverage, a variety of wireless applications have been successfully deployed. In return, this blossom and the rapid advance in technology explode the demands for wireless multimedia communications and better quality of service. To meet these demands, wireless communication systems continue to strive for higher data rates and higher reliability. However, for wireless communications, this goal is particularly challenging for several reasons. Firstly, the radio spectrum available for wireless services is extremely scarce and therefore the design of future high-rate wireless communication systems must be subject to the omnipresent bandwidth constraint. Secondly, increasing transmission power is also an undesirable approach since it will reduce the battery life of mobile unit and add interferences to other users. At last, very powerful coding and modulation schemes are not always blessings in wireless communications due to their high complexity.

A fundamental measure on reliable communication is channel capacity which was introduced by Shannon in his pioneering work on information theory in the 1940's. Channel capacity basically sets the ultimate upper bound of transmission rate for error-free communication. Since the spectrum is expensive and scarce, one needs to maximize the rate within a given bandwidth, i.e., to maximize *spectrum efficiency*. Therefore in

this dissertation, we consider the channel capacity within unit bandwidth. For additive white Gaussian noise(AWGN) channel, the channel capacity is given by the following well-known expression

$$C = \log \left( 1 + \frac{\Omega}{N_0} \right), \quad (1.0.1)$$

where  $\Omega$  denotes the transmit power and  $N_0$  denotes the noise power spectral density. In conventional single transmit and single receive antenna narrowband wireless system, the time-varying fading channel can be characterized by a channel coefficient  $\eta$ . Assume the channel is ergodic and the channel coefficient  $\eta$  is known to receiver, the capacity in this case can be written as

$$C = \mathcal{E}_\eta \left[ \log \left( 1 + \frac{\eta\Omega}{N_0} \right) \right], \quad (1.0.2)$$

where  $\mathcal{E}_\eta(\cdot)$  denotes the expectation operation with respect to random variable  $\eta$ . While the channel capacity can be improved by knowing the channel coefficient  $\eta$  at the transmitter, the improvement is negligible for most practical fading models [1]. Notice that for both AWGN channel and conventional narrowband fading channel, the channel capacity is limited by the transmit power. Therefore to achieve higher rate in bandwidth-limited and power-limited systems seems not just challenging, but impossible.

In recent years, systems equipped with multiple transmit antennas and receive antennas, which can be naturally modelled as a multiple-input-multiple-output (MIMO) channel, have been shown as breakthroughs in bandwidth-limited and power-limited wireless communications. In fact, the pioneer works by Foschini and Telatar [2] [3] shown that the capacity of a MIMO channel grows linearly with the minimum of transmit and receive antennas provided the environment is rich scattering and the channels can be well estimated at the receiver. The prophecy of the high capacity of MIMO channels, also known as *spatial multiplexing gain*, ignited huge research interest in developing efficient schemes to exploit this available high capacity, such as Bell Labs layered space-time (BLAST) architectures [4] and orthogonal spatio-temporal vector coding techniques [5].

Another challenge of reliable wireless communications is the issue of fading, which arises due to the existence of multiple paths between the transmitter and the receiver. For narrowband signals, a wireless link can be generally modelled as a Rayleigh

or a Rician fading channel if the doppler shift is not included [6]. Fading decreases the reliability of wireless communications unless some less-faded replica of the transmitted signal is provided to the receiver. This resource is called *diversity*. Time diversity and frequency diversity techniques have been already employed to combat fading for decades. However, these two diversity techniques can not be always available. For example, in slow fading channels, time diversity is not an option for delay-sensitive applications because time diversity is obtained by using channel coding and time interleaving. The efficiency of frequency diversity is limited when the delay spread is small. Besides, both time diversity and frequency diversity are acquired with sacrificing of spectral efficiency. When separated multiple antennas or different polarized antennas are employed at the transmitter and/or the receiver, multiple independent fading channels can be created and therefore diversity is obtained. This form of diversity is called as spatial diversity, which does not have the drawbacks associated with the aforementioned two forms of diversities. In parallel with research on exploiting high capacity of MIMO channels, how to utilize the spatial diversity of MIMO channels has also been extensively studied. A variety of space-time diversity techniques have been proposed, such as diversity combining [7], beamforming [8] and space-time coding [9] [10].

Most works on MIMO channels focus on designing schemes to maximize the spatial multiplexing gain or diversity gain. Recent works by Tse and Zheng shown that both gains can be simultaneously obtained but there exists a fundamental tradeoff between them [12]. In fact, it is shown that maximizing one gain will inevitably sacrifice the other. It is also realized that channel state information (CSI) plays an important role on exploiting the diversity and/or multiplexing gain. Based on how much the amount of CSI that transmitters and/or receivers have, MIMO systems can be classified into at least three cases: CSI available at neither the transmitter nor the receiver, CSI available only at the receiver, and CSI available both the transmitter and the receiver. For different cases, the achievable performance of MIMO channels and the corresponding signaling designs can be greatly different. For simplicity of future reference, we given the abbreviations on CSI in the following table.

Table 1.1: Table of some abbreviations.

CSI	Channel State Information
CSIT	Channel State Information at the Transmitter
CSIR	Channel State Information at the Receiver
NCSI	Channel State Information neither at the Transmitter nor at the Receiver

## 1.1 Contributions of the Dissertation

The contributions of this dissertation lie in two aspects: first, we design a multiple coding scheme for a point-to-point MIMO system which can closely approach the channel capacity; second, we develop blind decoders for space-time block codes in downlink DS-CDMA which can exploit the benefit of multiple antennas and efficiently suppress the multiple access interference (MAI) from other users.

For a point-to-point MIMO fading system, when the instantaneous CSI is available to both the transmitter and the receiver, the optimal power adaptation is known as the “water-filling” scheme if the MIMO system is subject to an average power constraint [3, 23]. A multiplexed coding scheme corresponding to “water-filling” power adaptation [25] can be applied to achieve the capacity. However, the multiplexed coding has high complexity since it requires in principle an infinite number of codes, or at least a very large number of codes, adapted to different SNR values, to implement the multiplexed coding and decoding. Biglieri et al. shown that the capacity of a MIMO system can also be archived by using one code with “water-filling” power adaptation [27]. However, Biglieri’s one code scheme needs a practical code operating on fading channels, therefore inter-block coding is required and the code might be very long, especially when deep fading happens. Therefore we focus on designing a more practical coding scheme to approach the capacity of a MIMO fading system. By applying proper channel transformations, we proposed a multiple coding scheme which can approach the capacity with a moderate coding/decoding complexity. The main idea is to transform the MIMO fading system into a set of parallel independent additive white Gaussian noise (AWGN) channels by exploiting the CSI at both the transmitter and the receiver. Therefore the code length and delay is determined solely by the length of codes chosen for the AWGN channel(s), not the fading dynamics.

We also shown that our proposed multiple coding scheme can achieve a very good tradeoff between the coding complexity and the performance. Besides, due to our proposed channel transformations, we show that capacity approaching practical coding designed for AWGN channels can be directly applied in MIMO fading channels.

For a multi-user system equipped multiple antennas at each unit, we consider the combination of existing MIMO space-time processing techniques and multi-user detection techniques. We consider the decoding of space-time block codes in the downlink DS-CDMA system. For the downlink transmission, since each mobile station typically has only the knowledge of its own spreading sequence, suppression of multiple access interference must be done blindly. Therefore blind joint decoders are studied. We firstly assume that the CSI is perfectly known at the each mobile station, and proposed joint blind decoders for a variety of space-time block codes by *borrowing* the structure of linear dispersion codes [47]. We apply the sphere decoder to improve the performance of blind decoder for the non-orthogonal space-time codes and propose a decimation-combining processing to reduce the complexity. We demonstrate that the proposed blind decoders significantly outperform the traditional method and decimation-combining processing can reduce the complexity with very slight performance loss. Then we assume that the CSI is known to neither the base station nor the mobile station and develop a non-coherent blind decoder by applying differential space-time block codes. We present the required structure of differential space-time block codes to suit the proposed blind non-coherent detection scheme and apply two popular differential space-time block codes, unitary group codes [57] and orthogonal codes [55][56]. We demonstrate that the proposed non-coherent blind decoders can approach closely the performance of a single user system and significantly outweighs the traditional method.

## 1.2 Organization of the Dissertation

The rest of the dissertation is organized as follows. Chapter 2 presents an overview on MIMO fading channels. Channel models and basic concepts on MIMO fading channels are introduced first. Then the recent advances on capacities of MIMO channels and transmi-

sion techniques under differential scenarios are briefly presented. In the end, a fundamental tradeoff between spatial multiplexing gain and diversity gain is reviewed.

In Chapter 3, we propose a capacity-approaching multiple coding scheme for MIMO uncorrelated fading channels with transmit CSI. We first build the system model and point out that multiple eigen-beamforming can be used by exploiting the CSI at both the transmitter and the receiver. Then we show that the marginal pdf's of unordered and ordered eigen-values of channel matrix can be obtained in closed-form. Using these preliminary results on marginal pdf, we investigate the achievable capacities of different power adaption and coding schemes. To reduce the complexity, we propose the truncated channel inversion and apply it on beamforming, unordered multiple eigen-beamforming and ordered multiple eigen-beamforming. we demonstrate that the proposed schemes can transform the MIMO fading channels into a set of independent AWGN channels and the sum capacity achieved by these AWGN channels closely approach the capacity of MIMO fading channels. We discuss the advantages of our multiple coding scheme over other existing coding schemes. In the end, we extend our schemes to correlated MIMO fading channels and evaluate the effect of correlation on the achievable rates of different transmission schemes. We show that transmit CSI is more crucial in highly correlated MIMO systems than in uncorrelated MIMO fading channels and beamforming combined with truncated channel inversion can closely approach the capacity in highly correlated case.

In Chapter 4, we study the combination of blind multi-user detection and space-time decoding in the downlink of a DS-CDMA system. We consider both the coherent decoding and the non-coherent decoding. In the previous case, we first introduce the linear dispersion codes. Then we stack the received signal into a form which allows us to implement the group-blind subspace detector. And we combine the sphere decoder for the non-orthogonal space-time codes and propose the decimation-combining method to reduce the complexity. in the last, we present a few simulation examples to demonstrate the performance of the proposed blind decoders. In the latter case, we first introduce the differential space-time block codes. Then we point out the required structure of differential space-time block codes to allow blind decoding. At last, we proposed blind linear MMSE decoders in Multi-Input-Single-Output (MISO) channels and MIMO channels respectively.

In Chapter 5, the conclusions are given.

### 1.3 Notations in the dissertation

The notation used in this dissertation is as follows. Bold letters denote matrices or column vectors. The symbol  $(\cdot)^\dagger$  denotes the operation of complex conjugate transpose and the symbol  $(\cdot)^T$  denotes the operation of transpose. The matrix  $I_P$  stands for a  $P \times P$  identity matrix,  $\mathcal{E}(\cdot)$  stands for expectation, and  $\text{tr}(\cdot)$  stands for the trace of a matrix.  $|\mathbf{A}|$  stands for the determinant of a square matrix  $\mathbf{A}$  and  $\mathbf{A}^\dagger$  stands for the pseudo-inverse of a matrix  $\mathbf{A}$ . All operations of logarithm are base 2.

## Chapter 2

# MIMO Fading Channels: An Overview

### 2.1 MIMO Fading Channel Model

Although a significant variety of situations can be modelled as a communication through a MIMO channel, we are only interested in a MIMO channel that models a wireless link equipped with multiple antennas at transmitter and/or receiver. Consider a wireless link comprising  $N_t$  transmit antennas and  $N_r$  receive antennas. For a narrow-band communication system, it can be assumed that there exists a frequency-flat fading channel between each pair of transmit antenna and the  $i$ -th receive antenna. Thus the fading channel gains can be described by a  $N_r \times N_t$  channel matrix  $\mathbf{H}$ , denoted by

$$\mathbf{H} = [H_{i,j}]_{i,j=1}^{N_r, N_t} = \begin{bmatrix} H_{1,1} & H_{1,2} & \cdots & H_{1,N_t} \\ H_{2,1} & H_{2,2} & \cdots & H_{2,N_t} \\ \vdots & \vdots & \ddots & \vdots \\ H_{N_r,1} & H_{N_r,2} & \cdots & H_{N_r,N_t} \end{bmatrix}, \quad (2.1.1)$$

where  $H_{i,j}$  is the complex channel gain factor between the  $j$ -th transmit antenna and the  $i$ -th receive antenna.

In a rich scattering environment with no line-of-sight (NLOS), the channel gains  $H_{i,j}$  are usually Rayleigh distributed. If all the transmit and receive antennas are separated far enough, we can assume that all the channels vary independently. Such a MIMO channel is referred to as an uncorrelated Rayleigh fading MIMO channel and each entry of channel

matrix  $\mathbf{H}$  can be modelled as an independent identically distributed (i.i.d) complex circular Gaussian random variable with zero-mean and unit variance. If there exists a LOS but still in a rich scattering environment, the channels are referred to as Rician fading channels, i.e., the channel gains  $H_{i,j}$  can be modelled as complex circular Gaussian random variables with non-zero mean.

When there are not enough scatters around the transmit and/or receive antennas (non-richness scattering environment) or when antenna elements are spaced closely, channel correlations are arisen. The correlation due to the lack of scatters is referred to as spatial correlation and the correlation introduced by nearness of antenna elements is referred to as mutual coupling [13]. When there exist channel correlations, which can be arisen by spatial correlation or mutual coupling or both, the channels are called correlated MIMO channels and the channel matrix can be modelled as [14][15]

$$\mathbf{H} = \mathbf{R}_r^{1/2} \mathcal{H} \mathbf{R}_t^{1/2}, \quad (2.1.2)$$

where  $\mathbf{R}_r \triangleq \mathbf{R}_r^{1/2} \mathbf{R}_r^{\dagger/2}$  denotes the receive correlation matrix,  $\mathbf{R}_t \triangleq \mathbf{R}_t^{1/2} \mathbf{R}_t^{\dagger/2}$  denotes the transmit correlation matrix, and  $\mathcal{H}$  is generally modelled as a random matrix with i.i.d entries. When channel correlations only exist at the transmitter side or at the receiver side but not at both, the channels are referred to as semi-correlated MIMO channels and the corresponding channel matrices are modelled as  $\mathbf{H} = \mathcal{H} \mathbf{R}_t^{1/2}$  and  $\mathbf{H} = \mathbf{R}_r^{1/2} \mathcal{H}$  respectively.

## 2.2 Ergodic Capacity of MIMO Fading Channels

Since a fading channel is usually described by a random variable, the channel capacity of the fading channel, which is a function of the given channel, should also be “random”. Assume fading channels considered in this dissertation are all ergodic, we can define two kinds of measurements on capacity of fading channels: *Outage capacity* and *Ergodic capacity*. Outage capacity for a value of  $p_0$  is defined as the maximum data rate at which outage probability is still below a target value  $p_0$ . Ergodic capacity is the mean of the “random” capacity. In this chapter, we only present the major results on ergodic capacity of MIMO fading channels.

### 2.2.1 Ergodic Capacity with NCSI

The capacity of a MIMO fading channel that CSI is unknown to both the transmitter and the receiver is firstly addressed in [5] by Marzetta and Hochwald. They model the channel as an uncorrelated Rayleigh fading MIMO channel and assume the channel is block-static, i.e., the channel matrix  $\mathbf{H}$  remains constant within  $T$  symbol intervals, then changes to a new independent value for  $T$  other symbols, and so on. It is shown that capacity with NCSI is achieved when the  $T \times N_t$  transmitted signal matrix is equal to the product of two statistically independent matrices: a  $T \times T$  isotropically distributed unitary matrix times a certain  $T \times N_t$  random matrix that is diagonal, real, and nonnegative. Marzetta and Hochwald also show that, for a fixed number of antennas, as the length of the coherence interval increases, the capacity approaches the capacity obtained as if the receiver knew the CSI. However, they proven that there is no point in making the number of transmitter antennas greater than the length of the coherence interval: the capacity for  $N_t > T$  is equal to the capacity for  $N_t = T$ . Marzetta and Hochwald point out that this is somewhat disappointing since it severely limits the ultimate capacity of a rapidly fading channel. For instance, in the extreme case where a fresh fade occurs every symbol period, only one transmitter antenna can be usefully employed. Strictly speaking, one still could increase capacity indefinitely by employing a very large number of receive antennas, but the capacity only increases logarithmically in this number.

Although Marzetta and Hochwald calculate the bounds of MIMO capacity with NCSI for quite a few non-trivial cases in [5], the general results on MIMO capacity with NCSI is accredited to Zheng and Tse [16]. They shown that at high Signal-to-Noise-Ratio (SNR) the capacity is achieved by using  $M^* = \min(N_t, N_r, \lfloor \frac{T}{2} \rfloor)$  transmit antennas. Therefore employing more transmit antennas than receive antennas provides no capacity gain at high SNR, while employing more receive antennas does yield a capacity gain that increases logarithmically in the number of receive antennas. Zheng and Tse also prove that for each 3-dB SNR increase, the capacity gain is  $M^*(1 - \frac{M^*}{T})$ . It can be seen that for a slowly fading channel, where coherent time interval  $T$  is quite large, the capacity gain is about  $\min(N_t, N_r)$  for each 3-dB SNR increase. We will see later that this result is agree with CSIR case.

## 2.2.2 Ergodic Capacity with CSIR

Foschini [2] and Telatar [3] are the pioneers who considered the capacity of MIMO channels. They show that the capacity of a point-to-point MIMO communication system characterized by channel matrix in (2.1.1) can be written as

$$C = \max_{\mathbf{Q}} \mathcal{E} \left[ \log \left| \mathbf{I}_{N_r} + \mathbf{H}\mathbf{Q}\mathbf{H}^\dagger \right| \right], \quad (2.2.1)$$

where  $\mathbf{Q}$  denotes the covariance matrix of the transmitted signal vector  $\mathbf{x}$ . Suppose the transmit power constraint is  $\Omega$ , we have  $\text{tr}(\mathbf{Q}) \leq \Omega$ . For uncorrelated Rayleigh fading MIMO channels, when the CSI is only perfectly known at the receiver, Telatar gives the following theorem on the MIMO capacity in [3].

**Theorem 1** *The capacity is achieved when  $\mathbf{x}$  is a circularly symmetric complex Gaussian with zero-mean and covariance  $\frac{\Omega}{N_t} \mathbf{I}_{N_t}$ . The capacity is given by*

$$C = \mathcal{E} \left[ \log \left| \mathbf{I}_{N_r} + \frac{\Omega}{N_t} \mathbf{H}\mathbf{H}^\dagger \right| \right] = \mathcal{E} \left[ \log \left| \mathbf{I}_{N_t} + \frac{\Omega}{N_t} \mathbf{H}^\dagger \mathbf{H} \right| \right]. \quad (2.2.2)$$

Furthermore, Foschini and Telatar show that the MIMO capacity with CSI grows linearly with  $\min(N_t, N_r)$ , i.e., the capacity gain is  $\min(N_t, N_r)$  for each 3-dB SNR increase. This is a significant improvement over a single antenna system which achieves one bit capacity gain for each 3-dB SNR increase.

## 2.2.3 Ergodic Capacity with CSIT and CSIR

When both transmitter and receiver have access to CSI, the transmitter can adjust its power and rate depending on the instantaneous value of the observed CSI and therefore higher capacity can be expected than the CSIR case. It is shown that the capacity with CSIT and CSIR can be achieved by “space-time waterfilling” scheme and the capacity is calculated by Jayaweera and Poor in [21, 22].<sup>1</sup> While the capacity gain of CSIT and CSIR over CSIR is negligible if fewer antennas are employed at the transmitter than at the receiver, the capacity gain is considerable if more fewer antennas are employed at

---

<sup>1</sup>After correspondence with the authors of [21, 22], it has been agreed that the numerical results presented in [21, 22] are too optimistic with respect to the effect of CSI. The numerical results in this dissertation are therefore different from those in [21, 22].

the transmitter than at the receiver. Specifically, based on the fact that the achieved rate of “constant power water-filling” approaches the capacity of “water-filling” [24], we can show that in the latter case, the capacity gain is  $N_r \log(\frac{N_t}{N_r})$  at high SNR. We compare the capacity with CSIT and CSIR to the capacity with CSIR in the  $(N_t = 8, N_r = 2)$  and the  $(N_t = 2, N_r = 2)$  uncorrelated Rayleigh fading MIMO channels. The results are shown in Figure 2.1. It can be seen that in the  $(N_t = 2, N_r = 2)$  case, having CSIT only provides very slight capacity gain. However, in the  $(N_t = 8, N_r = 2)$  case, the capacity gain is around  $2 \log(8/2) = 4$  bits/Sec/Hz. In other words, in the  $(N_t = 8, N_r = 2)$  case, by knowing CSI at the transmitter, we can gain about 7-dB in the given SNR region. In Chapter 3, we focus on designing a multiple coding scheme to exploit this capacity gain.

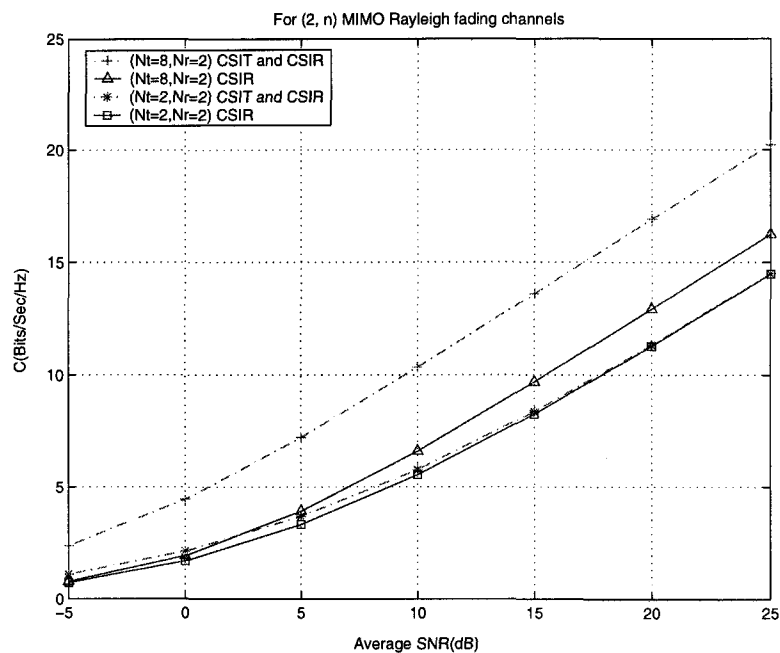


Figure 2.1: Capacity with CSIT and CSIR V.S Capacity with CSIR.

## 2.3 Transmission Techniques for MIMO Fading Channels

According to the availability of CSI at the transmitter and/or at the receiver, a variety of communication techniques have been proposed for efficient transmissions over

MIMO fading channels. Most of proposed transmission techniques are designed to maximize the spatial multiplexing gain or diversity gain, although some efforts have been made to achieve the tradeoff between two gains recently. Since the transmission techniques with CSIT and CSIR will be well described in Chapter 3, we only briefly review the transmission techniques when CSI is not available at the transmitter.

### 2.3.1 Space-time Coding

Space-time coding (STC) is proposed to exploit the gain provided by MIMO fading channels with CSIR only. Most space-time codes are designed to combat fading by introducing redundancy in the transmitted signal over both space and time. Space-time coding schemes, which were first studied by Alamouti [9] and then generalized by Tarokh et al. [10, 11], are essentially a joint design of coding, modulation, transmit and receive diversity. There are two main types of space-time coding techniques: space-time trellis coding (STTC) and space-time block coding (STBC).

#### A. Space-time Trellis Codes

A STTC codeword can be defined by an  $N_t \times T$  matrix, in which each column is transmitted during one symbol interval by mapping it onto  $N_t$  transmit antennas. Let  $\mathbf{C} = [c_1, c_2, \dots, c_T]$  and  $\mathbf{E} = [e_1, e_2, \dots, e_T]$  be two distinct codewords, where  $c_i$  and  $e_i$  are vectors with  $N_t$  entries. Obviously, the optimal code design criterion should be based on minimizing the average error probability. However, due to the difficulty of computing average error probability, most current criteria are based on analysis on the pairwise error probability (PEP), which is the probability that the maximum likelihood (ML) decoder selects  $\mathbf{E}$  as its estimate when in fact the codeword  $\mathbf{C}$  was transmitted. For an uncorrelated Rayleigh fading MIMO channel, an upper bound of PEP has been derived in [10]. Define  $\mathbf{A} \triangleq (\mathbf{C} - \mathbf{E})(\mathbf{C} - \mathbf{E})^\dagger$  and let  $r$  be the rank of matrix  $\mathbf{A}$ , the upper bound can be expressed as

$$P(\mathbf{C} \rightarrow \mathbf{E}) \leq \left( \prod_{i=1}^r \lambda_i^{1/r} \right)^{-rN_r} \left( \frac{SNR}{4} \right)^{-rN_r}, \quad (2.3.1)$$

where  $\lambda_i$  for  $i = 1, 2, \dots, r$  are the eigenvalues of matrix  $\mathbf{A}$ . Notice in the right hand of inequality (2.3.1),  $rN_r$  is the power of the SNR in the denominator and therefore  $rN_r$  is referred to as diversity gain.  $\left(\prod_{i=1}^r \lambda_i^{1/r}\right)$  is named as coding gain. The problem of minimizing the upper bound on PEP is equivalent to maximize the diversity gain and the coding gain. To obtain maximal diversity gain, one needs to maximize the minimum rank  $r$  of the matrix  $\mathbf{A}$  over all pairs of distinct codewords. To obtain maximal coding gain, one needs to maximize the minimum determinant of the matrix  $\mathbf{A}$  along the pairs of distinct codewords with minimum rank. These two criteria are referred to as *rank criterion* and *determinant criterion* respectively. Obviously, if the matrix  $\mathbf{A}$  over all pairs of distinct codewords is full rank, the maximum diversity gain is obtained.

The encoding for STTCs are similar to trellis coded modulation (TCM), except that at the beginning and the end of each frame, the encoder is required to be in the zero state. An example of STTC for  $N_t = 2$  transmit antennas and QPSK constellation is given in Figure 2.2, where each row beside the trellis represents the edge labels for transitions from the corresponding state. At each symbol interval, depending on the state of the encoder and the input bits, a transition branch is selected and the corresponding edge labels are parallel transmitted along  $N_t$  transmit antennas. Since one QPSK symbol is transmitted at each time interval, the bandwidth efficiency of the code is 2bits/s/Hz. It can be checked that the code has diversity gain of 2.

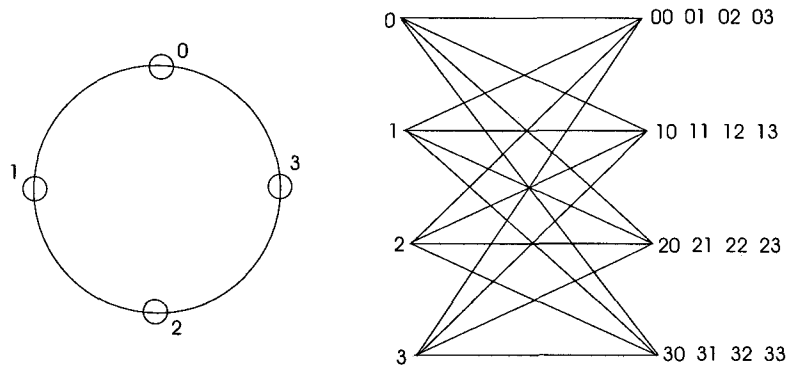


Figure 2.2: Space-time trellis code, QPSK, 2bits/s/Hz for  $N_t = 2$ .

Since the advent of STTC, there has been rapid progress in the field, targeted at finding better codes with full diversity advantage and with greater coding advantage than

original STTC presented in [10]. For example, a more accurate code design criteria by using a tighter bound on PEP is derived in [18] and a few codes with better performance are also presented. Hammons et al. propose a more structured method of code construction that ensures full diversity in [19] and they introduce several new construction methods that are quite general and open the door to more sophisticated and more powerful codes.

## B. Space-time Block Codes

Although the ML decoder for STTC can be implemented using the Viterbi algorithm, the decoding complexity of STTC still increases exponentially as a function of the diversity level and transmission rate [10]. Most space-time block codes aim to exploit the diversity gain and coding gain with a simple decoding. Among existing STBCs, Alamouti code [9] is the most popular STBC and later it is generalized into orthogonal STBCs in [11]. In this subsection, we only introduce the STBC with orthogonal design. More details on other STBCs can be found in Chapter 4.

Let  $c_i$  and  $c_{i+1}$  be two continuous complex symbols, an Alamouti code can be constructed as

$$\mathbf{C} = \begin{bmatrix} c_i & -c_{i+1}^* \\ c_{i+1} & c_i^* \end{bmatrix}. \quad (2.3.2)$$

At the  $i$ -th time interval, symbols  $c_i$  and  $c_{i+1}$  are transmitted simultaneously from antenna 1 and antenna 2 respectively. At the  $(i + 1)$ -th time interval, signals  $-c_{i+1}^*$  and  $c_i^*$  are transmitted simultaneously from antenna 1 and antenna 2 respectively. It is obvious that the rate of Alamouti code is 1. Consider an  $(N_t = 2, N_r = 1)$  system, the received signals at the  $i$ -th and the  $(i + 1)$ -th time intervals can be stacked as

$$\begin{bmatrix} y_i \\ y_{i+1} \end{bmatrix} = \underbrace{\begin{bmatrix} H_{1,1} & H_{1,2} \end{bmatrix}}_{\triangleq \mathbf{H}} \begin{bmatrix} c_i & -c_{i+1}^* \\ c_{i+1} & c_i^* \end{bmatrix} + \begin{bmatrix} z_i \\ z_{i+1} \end{bmatrix}, \quad (2.3.3)$$

where  $z_i$  and  $z_{i+1}$  are independent AWGN noise with zero mean and unit variance. Let us rewrite (2.3.3) as

$$\begin{bmatrix} y_i \\ y_{i+1}^* \end{bmatrix} = \underbrace{\begin{bmatrix} H_{1,1} & H_{1,2} \\ H_{1,2}^* & -H_{1,1}^* \end{bmatrix}}_{\triangleq \tilde{\mathbf{H}}} \begin{bmatrix} c_i \\ c_{i+1} \end{bmatrix} + \begin{bmatrix} z_i \\ z_{i+1}^* \end{bmatrix}. \quad (2.3.4)$$

Since  $\tilde{\mathbf{H}}^\dagger \tilde{\mathbf{H}} = \|\mathbf{H}\|_F^2 \mathbf{I}_2$ , where  $\|\cdot\|_F$  stands for the Frobenius norm,  $\tilde{\mathbf{H}}$  is referred to as *orthogonal matrix*. Due to the orthogonality of  $\tilde{\mathbf{H}}$ , the ML-decoding of  $c_i$  and  $c_{i+1}$  can be decoupled, i.e.,  $c_i$  and  $c_{i+1}$  can be decoded independently. Therefore, only simple linear processing is required to decode the Alamouti code. Alamouti code can be used in a system with 2 transmit antennas and an arbitrary number of receive antennas, and it provides a diversity gain of  $2N_r$  if  $N_r$  receive antennas are equipped.

General constructions of orthogonal STBC for an arbitrary number of transmit antennas have been studied in [11]. Similar to Alamouti code, all orthogonal STBCs achieve maximum-likelihood decoding through linear processing at the receiver, and exhibit maximum diversity. Although quite a few orthogonal STBCs with rate lower than 1 are proposed in [11], it is proven that Alamouti code is the only code with rate 1 for complex orthogonal STBCs.

### 2.3.2 Differential Space-time Coding

Decoding of the aforementioned STTC or STBC requires CSI available at the receiver. However, it is a very tough task to guarantee the accuracy of estimations of MIMO channels without exhausting computation, especially when the number of antennas is large. Besides, in some situations, we may want to forego channel estimation in order to reduce the cost and complexity of the handset, or perhaps fading conditions change so rapidly that channel estimation is difficult or requires too many training symbols. Differential space-time codes are designed to exploit the gain of MIMO channels without requiring the CSI either at the transmitter or at the receiver.

Differential space-time coding can be regarded as a natural extension of differential modulation for single antenna systems to multiple-antenna systems. One type of differential STBC is called unitary STBC, in which the signals transmitted by different antennas

are mutually orthogonal. It is proposed based on the information-theoretic arguments in [5] [16]. The design criteria and performance analysis for unitary codes are derived in [53] and a systematic construction of unitary codes is described in [54]. A general approach to differential modulation for multiple transmit antennas based on group codes is proposed by Hughes in [57]. A differential STBC for two transmit antennas based on orthogonal design is presented in [55] and later generalized for more transmit antennas in [56]. Like orthogonal STBC, differential STBC can also be decoded with linear processes at the receiver. The detail of encoding and decoding of differential STBC will be introduced in Chapter 4.

## 2.4 Diversity-Multiplexing Tradeoff

As shown in previous two sections, an MIMO channel can support a high data rate by improving the capacity and achieve a high reliability by providing diversity. In other words, we can obtain two types of gain, say, spatial multiplexing gain and diversity gain, from an MIMO channel. However, it is shown by Zheng and Tse in [12] that we can not maximize these two types of gain simultaneously. In fact, Zheng and Tse show that there is a fundamental tradeoff between two types of gain that any transmission scheme can achieve. They also present the optimal tradeoff curve achievable for any scheme.

Let us first introduce the specific definitions of spatial multiplexing gain and diversity gain given in [12]. A scheme  $C(SNR)$  is said to achieve spatial multiplexing gain  $r$  and diversity gain  $d$  if the data rate  $R(SNR)$  satisfies

$$\lim_{SNR \rightarrow \infty} \frac{R(SNR)}{\log SNR} = r, \quad (2.4.1)$$

and the average error probability  $P_e(SNR)$  satisfies

$$\lim_{SNR \rightarrow \infty} \frac{P_e(SNR)}{\log SNR} = d. \quad (2.4.2)$$

Define  $d_o(r)$  as the supremum of the diversity gain achieved by any scheme that achieves spatial multiplexing gain  $r$ . In the case that coherent time  $T$  is larger than  $N_t + N_r - 1$ , the optimal tradeoff curve is given in the following theorem [12].

**Theorem 2** Assume  $T \geq N_t + N_r - 1$ . The optimal tradeoff curve  $d_o(r)$  is given by a piecewise function connecting the points  $(r, d_o(r))$ , where  $r = 0, 1, \dots, \min(N_t, N_r)$  and  $d_o(r) = (N_t - r)(N_r - r)$ .

From the above theorem, we can immediately see that the maximum of achievable spatial multiplexing gain is  $r_{max} = \min(N_t, N_r)$  and the maximum of achievable diversity gain is  $d_{max} = N_t N_r$ . Obviously, if one scheme achieves the maximum of spatial multiplexing gain, the achievable diversity gain for this scheme is 0, and vice versa. In general, for a given MIMO channel, both gains can be obtained simultaneously. However, increasing one comes at the price of sacrificing the other. The only way to increase both gains simultaneously is to increase the number of transmit antennas and receiver antennas.

Although most existed transmission schemes aim to maximize the spatial multiplexing gain or the diversity gain, a variety of efforts have been made to simultaneously achieve low error probability and high rate. For example, a family of short structured space-time block codes that achieves the optimal tradeoff for the  $(N_t = 2, N_r = 2)$  system with minimum delay has been proposed in [17]. Linear dispersion code [47], which uses linear combinations of basis matrices to build codebooks, also aims to improve the rate and keep the low error probability.

# Chapter 3

## Multiple Coding for MIMO Rayleigh Fading Systems

### 3.1 Motivations

In chapter 2, we see that the capacity of a slowly changing block-static MIMO channel increases linearly with the minimum between the numbers of transmit and receive antennas provided the SNR is high. We also see that considerable capacity gain can be obtained by knowing the CSI at the transmitter when the number of transmit antennas is larger than the number of receive antennas, whereas the gain is limited when there are fewer transmit than receive antennas. Designing of the capacity-achieving signaling/coding for MIMO channels is closely related to how much the amount of channel state information (CSI) that transmitters and/or receivers have. When the CSI is known neither at the transmitter nor at the receiver, it is shown by Marzetta and Hochwald in [5] that the capacity achieving signal matrix can be written as  $S = \Phi V$ , where  $\Phi$  is an isotropically distributed unitary matrix, and  $V$  is an independent real, nonnegative, diagonal matrix. However, a practical coding scheme that can approach the capacity achieved by the random codes generated by the product of two statistically independent matrices is still unknown. In [3], the capacity of MIMO Rayleigh fading channels is calculated by assuming CSI at the receiver but no CSI at the transmitter, and it is shown that capacity is achieved by a Gaussian random coding. However, using a practical codes to approach this capacity is still a tough task because we

need a code operates well in fading channels. If the ergodic fading channel considered is changing reasonably slowly, the instantaneous CSI which is typically obtained by estimating unknown channel parameters at the receiver can be obtained at the transmitter through a dedicated feedback channel. In this case, we can expect that it can potentially reduce coding complexity considerably (cf. channel feedback in [23]). The aim of this chapter is to develop coding schemes that can both exploit the increase in capacity and reduce coding complexity.

When the instantaneous CSI is available to both the transmitter and the receiver, the optimal power adaptation is known as the “water-filling” scheme if the MIMO system is subject to an average power constraint [3, 22, 23]. It can be seen that a multiplexed coding scheme with “water-filling” power adaptation [25] can be applied to achieve the capacity. However, the multiplexed coding has high complexity since it requires in principle an infinite number of codes, or at least a very large number of codes, adapted to different SNR values, to implement the multiplexed coding and decoding. This is still true for constant power waterfilling though it simplifies the power adaptation [24]. It has been shown that in SISO system [26] and in MIMO system [27], capacity can in fact be achieved using a single code with a kind of “water-filling” power adaptation. However, this code in principle needs to span a whole ensemble of fading states, and the code length and decoding delay therefore could be very long in particular in slow fading. In other words, to overcome deep fades, the single coding scheme seems to require a very long code length to average fades over a sufficiently large number of channel realizations. A scheme to reduce complexity is the truncated channel inversion proposed in [25] (for SISO systems) [29] (for SIMO systems). With channel inversion, the fading channel is transformed into an AWGN channel, and any code designed for the AWGN channel can be used. Also, in slow fading the length of the code and coding delay can be chosen independently of the fading dynamics, only taking into account the AWGN properties. However, this simplification comes at the cost of capacity loss, which can be significant in particular when the scheme is generalized to MIMO systems. In [30], a channel partition method is proposed to approach the capacity in a SISO Rayleigh fading channel, allowing a tradeoff between complexity and performance. However, the channel inversion is not introduced. Therefore the codes still operate on fad-

ing channels and a relatively large number of partitions are required to closely approach the capacity.

Designing practical codes to approach the capacity of AWGN channels is relatively well researched. Capacity-approaching codes for AWGN channels have been already found, such as low-density parity-check codes (LDPC) and turbo codes. For example, a well-constructed rate 1/2 LDPC can approach 0.0045 dB away from the Shannon limit of the binary-input AWGN channel[28]. So we make efforts to approach the capacity of MIMO channels by taking advantage of the existed practical codes designed for AWGN channels. We investigate truncated channel inversion and channel partition for MIMO fading channels and propose simple schemes which achieve good tradeoff between coding/decoding complexity and capacity loss. The main idea is to transform the MIMO fading system into a set of parallel independent additive white Gaussian noise (AWGN) channels by exploiting the CSI at both the transmitter and the receiver. Therefore the code length and delay is determined solely by the length of codes chosen for the AWGN channel(s), not the fading dynamics. The focus of the paper is to develop simple, but powerful, methods for system transformation, and not on finding optimum coding. Transforming channel into a few sub-channels allows the use of a code of lower rate than that of the single code, better adapted to deep fades. The justification for the methods is that they can closely approach the channel capacity.

## 3.2 System Model with CSIT and CSIR

We consider a wireless link comprising  $N_t$  transmitter antennas and  $N_r$  receiver antennas that operates in a frequency-flat Rayleigh fading environment. Suppose that there is no correlations between any pair of channels, the channel can be modelled by the channel matrix defined in (2.1.1), where  $H_{i,j}$  is the complex channel gain factor between the  $j$ -th transmit antenna and the  $i$ -th receive antenna and it is modelled as an independent identically distributed (i.i.d) complex circular Gaussian random variable with zero-mean and unit variance. Furthermore, the channel is assumed to be block-static, i.e., the channel matrix  $H$  remains constant within  $L$  symbol intervals, then changes to a new independent value

for  $L$  other symbols, and so on. The received signal can be expressed as

$$\mathbf{y} = \mathbf{H}\mathbf{x} + \mathbf{z}, \quad (3.2.1)$$

where  $\mathbf{y}$  is a  $N_r \times 1$  vector of received signals,  $\mathbf{x}$  is a  $N_t \times 1$  vector of transmitted signals, and  $\mathbf{z}$  is a  $N_r \times 1$  vector of additive receiver noise values, which are independent, zero-mean circular complex Gaussian random variables with unit variance. For future reference, we define  $m = \min(N_t, N_r)$  and  $n = \max(N_t, N_r)$ , and we refer to such a system as an  $(n, m)$  MIMO system.

Let the singular value decomposition (SVD) of the channel matrix  $\mathbf{H}$  be  $\mathbf{H} = \mathbf{U}\mathbf{\Lambda}^{1/2}\mathbf{V}^\dagger$ , where  $\mathbf{U}$  and  $\mathbf{V}$  are unitary matrices and  $\mathbf{\Lambda}$  is a diagonal matrix with non-negative diagonal elements  $\{\lambda_1, \lambda_2, \dots, \lambda_m\}$ . Since the CSI is known at both the transmitter and the receiver, the transmitter can transmit  $\mathbf{x} = \mathbf{V}\mathbf{Q}^{1/2}\mathbf{s}$ , where  $\mathbf{s}$  is the coded source data with unit normalized power and  $\mathbf{Q}$  determines the transmit power of each symbol. By multiplying the received signal vector  $\mathbf{y}$  of (3.2.1) with the hermitian of  $\mathbf{U}$  and ignoring entries beyond  $m$  (only  $m$  eigenvalues are nonzero), we obtain

$$\begin{aligned} \tilde{\mathbf{y}} = \mathbf{U}^\dagger \mathbf{y} &= \mathbf{U}^\dagger \mathbf{H} \mathbf{V} \mathbf{Q}^{1/2} \mathbf{s} + \mathbf{U}^\dagger \mathbf{z} \\ &= \begin{bmatrix} \sqrt{\lambda_1} & & \\ & \ddots & \\ & & \sqrt{\lambda_m} \end{bmatrix} \mathbf{Q}^{1/2} \begin{bmatrix} s_1 \\ \vdots \\ s_m \end{bmatrix} + \tilde{\mathbf{z}}, \end{aligned} \quad (3.2.2)$$

where  $\tilde{\mathbf{z}} = \mathbf{U}^\dagger \mathbf{z}$  is still a complex additive Gaussian noise vector with zero mean and covariance matrix  $\mathbf{I}_m$ . It is well-known that  $\{\lambda_1, \lambda_2, \dots, \lambda_m\}$  are the eigenvalues of a Wishart matrix  $\mathbf{W}$ , defined by

$$\mathbf{W} \triangleq \begin{cases} \mathbf{H}\mathbf{H}^\dagger, & \text{for } N_r < N_t \\ \mathbf{H}^\dagger\mathbf{H}, & \text{for } N_r \geq N_t. \end{cases} \quad (3.2.3)$$

The joint pdf of the unordered eigenvalues  $\lambda_1, \lambda_2, \dots, \lambda_m$  is given in [31]

$$f_{\mathbf{\Lambda}}(\lambda_1, \lambda_2, \dots, \lambda_m) = K_{n,m} e^{-\sum_{i=1}^m \lambda_i} \prod_{i=1}^m \lambda_i^{n-m} \prod_{1 \leq i < j \leq m} (\lambda_i - \lambda_j)^2, \quad (3.2.4)$$

where  $K_{n,m}$  is defined by

$$K_{n,m} = \frac{1}{m! [\prod_{i=1}^m (m-i)! (n-i)!]}. \quad (3.2.5)$$

### 3.3 Marginal pdf of the Eigenvalues

In order to calculate capacities for the different MIMO signaling schemes, and for use in optimization, the marginal pdf's of the eigenvalues of the matrix  $\mathbf{W}$  in (3.2.3) are needed. In the following we will present explicit formulae both in the case when the eigenvalues are ordered and when they are unordered.

#### 3.3.1 Marginal pdf of the Unordered Eigenvalues

The marginal pdf of an unordered eigenvalue of the matrix  $\mathbf{W}$  was given in [3], and can be expressed as

$$f_{n,m}^u(\lambda) = \frac{e^{-\lambda} \lambda_i^{n-m}}{m} \sum_{j=0}^{m-1} \frac{j!}{(j+n-m)!} (L_j^{n-m}(\lambda))^2, \quad (3.3.1)$$

where  $L_j^{n-m}(\lambda)$  is the associated Laguerre polynomial of order  $j$ , which is defined as

$$L_j^{n-m}(\lambda) = \frac{1}{j!} e^{\lambda} \lambda^{m-n} \frac{d^j}{d\lambda^j} (e^{-\lambda} \lambda^{n-m+j}). \quad (3.3.2)$$

We state explicit formulae for the  $(n, 2)$  and  $(n, 3)$  MIMO systems (i.e., where the smaller of  $N_t$  and  $N_r$  is 2 or 3) as important special cases

$$f_{n,2}^u(\lambda) = K_{n,2} e^{-\lambda} \lambda^{n-2} \Phi(\lambda, n, 2), \quad (3.3.3)$$

$$f_{n,3}^u(\lambda) = K_{n,3} e^{-\lambda} \lambda^{n-3} \Phi(\lambda, n, 3), \quad (3.3.4)$$

where

$$\Phi(\lambda, n, 2) = (n-2)! \lambda^2 - 2(n-1)! \lambda + n! \quad (3.3.5)$$

$$\begin{aligned} \Phi(\lambda, n, 3) &= 2\lambda^4 [(n-1)! - ((n-2)!)^2] \\ &+ 4\lambda^3 [(n-1)!(n-2)! - n!] \\ &+ 2\lambda^2 [(n+1)! + 2n!(n-2)! - 3((n-1)!)^2] \\ &+ 4\lambda [n!(n-1)! - (n+1)!(n-2)!] \\ &+ 2 [(n+1)!(n-1)! - (n!)^2]. \end{aligned} \quad (3.3.6)$$

### 3.3.2 Marginal pdf of the Ordered Eigenvalues

We sort all the eigenvalues in non-increasing order and denote the  $k$ -th order statistic of  $\lambda_1, \lambda_2, \dots, \lambda_m$  by  $\eta_k$ . In the following, we find the marginal pdf of  $\eta_k$ . Notice that the probability that two eigenvalues are equal is zero, and we can therefore discard this case. Let  $\pi$  be defined by  $\pi(\Lambda, i) = k$  if  $\eta_k = \lambda_i$ , i.e., if  $\lambda_i$  is the  $k$ -th largest eigenvalue. Consider all  $\Lambda$  so that  $\pi(\Lambda, 1) = k$ . That means that among the remaining  $m - 1$  unordered eigenvalues,  $k - 1$  are larger than  $\lambda_1$  and  $m - k$  are smaller than  $\lambda_1$ . The  $k - 1$  larger eigenvalues can be selected in  $\binom{m-1}{k-1}$  ways, and each of these combinations has the same probability. We can then write

$$\begin{aligned} & Pr(\eta_k \leq \eta, \pi(\Lambda, 1) = k) \\ &= \binom{m-1}{k-1} Pr(\lambda_1 \leq \eta, \lambda_2, \dots, \lambda_k > \lambda_1, \lambda_{k+1}, \dots, \lambda_m < \lambda_1). \end{aligned} \quad (3.3.7)$$

Notice that because of the symmetry of the unordered eigenvalues,  $Pr(\eta_k \leq \eta, \pi(\Lambda, i) = k) = Pr(\eta_k \leq \eta, \pi(\Lambda, 1) = k)$ ,  $i = 2, \dots, m$ , and that these cases are mutually exclusive. The cumulative density function (cdf) of  $\eta_k$  therefore is

$$\begin{aligned} & Pr(\eta_k \leq \eta) \\ &= m \binom{m-1}{k-1} Pr(\lambda_1 \leq \eta, \lambda_2, \dots, \lambda_k > \lambda_1, \lambda_{k+1}, \dots, \lambda_m < \lambda_1). \end{aligned} \quad (3.3.8)$$

By applying the joint pdf of the unordered eigenvalues (3.2.4) and differentiating with respect to  $\eta$ , the marginal pdf of  $\eta_k$  can be obtained as

$$f_{n,m}^k(\eta) = m \binom{m-1}{k-1} \underbrace{\int_{\eta}^{\infty} \dots \int_{\eta}^{\infty}}_{k-1} \underbrace{\int_0^{\eta} \dots \int_0^{\eta}}_{m-k} f_{\Lambda}(\eta, \lambda_2, \dots, \lambda_m) d\lambda_2 \dots d\lambda_m. \quad (3.3.9)$$

Notice that  $f_{\Lambda}$  given in (3.2.4) is a linear combination of terms of the form  $\lambda_1^{i_1} e^{-\lambda_1} \lambda_2^{i_2} e^{-\lambda_2} \dots \lambda_m^{i_m} e^{-\lambda_m}$ . The multi-dimensional integration in (3.3.9) can therefore be written as a sum of products of integrals of the following form

$$\int_x^{\infty} e^{-t} t^m dt = m! e^{-x} \sum_{i=0}^m \frac{x^i}{i!}, \quad (3.3.10)$$

$$\int_0^x e^{-t^m} dt = m! \left( 1 - e^{-x} \sum_{i=0}^m \frac{x^i}{i!} \right). \quad (3.3.11)$$

A closed-form expression of (3.3.9) can straightforwardly be obtained for any  $(n, m)$  MIMO system. This is used to obtain the results in the following sections. However, for  $m$  large, the expressions get very complex, so we will only list the case  $m = 2$  here,

$$\begin{aligned} f_{n,2}^1(\eta) &= 2 \int_0^\eta f_\Lambda(\eta, \lambda_2) d\lambda_2 \\ &= 2K_{n,2} (\varphi_1(n, n-2, \eta_1) - 2\varphi_1(n-1, n-1, \eta_1) + \varphi_1(n-2, n, \eta_1)), \end{aligned}$$

and

$$\begin{aligned} f_{n,2}^2(\eta) &= 2 \int_\eta^\infty f_\Lambda(\eta, \lambda_2) d\lambda_2 \\ &= 2K_{n,2} (\varphi_2(n, n-2, \eta_2) - 2\varphi_2(n-1, n-1, \eta_2) + \varphi_2(n-2, n, \eta_2)), \end{aligned}$$

where

$$\varphi_1(l, k, \eta) = e^{-\eta} \eta^l k! \left( 1 - e^{-\eta} \sum_{i=0}^k \frac{\eta^i}{i!} \right), \quad (3.3.12)$$

$$\varphi_2(l, k, \eta) = e^{-2\eta} \eta^l k! \sum_{i=0}^k \frac{\eta^i}{i!}. \quad (3.3.13)$$

### 3.4 The Beamforming Case

Beamforming, which always transmits the signal along the direction corresponding to the largest eigenvalue, has recently received considerable attention since it can maximize the received SNR and exploit the diversity gain of MIMO channels [32]. In [33], it is shown that beamforming with proper power control can achieve significant average transmit power saving compared to the systems with constant transmit power. Therefore we first consider power adaption and coding/decoding for beamforming. Based on [26], splitting the problem into power adaptation and coding does not introduce any capacity loss. With the transmit power constraint  $\Omega$ , the system model for beamforming with power adaption can therefore be written as

$$\tilde{y} = \sqrt{q(\eta_1, \Omega)\eta_1} s + \tilde{z}, \quad (3.4.1)$$

where  $\eta_1$  is the largest eigenvalue defined in Section 3.3.2,  $\tilde{z}$  is a zero mean additive complex Gaussian noise with unit variance,  $s$  is the transmitted symbols satisfying  $E[|s|^2] = 1$ , and  $q(\eta_1, \Omega)$  denotes the power control function. The optimal power control scheme can be obtained by solving the following optimization problem

$$\begin{aligned} C &= \max_{q(\eta_1, \Omega)} \int_{\eta_1} \log(1 + q(\eta_1, \Omega)\eta_1) f_{n,m}^1(\eta_1) d\eta_1 \\ \text{s.t. } &\int_{\eta_1} q(\eta_1, \Omega) f_{n,m}^1(\eta_1) d\eta_1 = \Omega, \quad q(\eta_1, \Omega) \geq 0, \end{aligned} \quad (3.4.2)$$

where  $f_1(\eta_1)$  is the marginal p.d.f of the largest eigenvalue  $\eta_1$ . It can be shown that the optimal power adaption is the “water-filling” method

$$q(\eta_1, \Omega) = \begin{cases} \frac{1}{\eta'_0} - \frac{1}{\eta_1}, & \eta_1 \geq \eta'_0 \\ 0, & \eta_1 < \eta'_0 \end{cases} \quad (3.4.3)$$

where  $\eta'_0$  is some cutoff value and can be obtained by solving the average power constraint equation (3.4.2). In [25], a truncated channel inversion scheme was proposed as a sub-optimal power adaption scheme. Since the truncated channel inversion scheme converts the fading channel into one AWGN channel, it has a much lower coding complexity. However, the truncated channel inversion scheme suffers a large capacity penalty relative to the optimal power adaption in some cases.

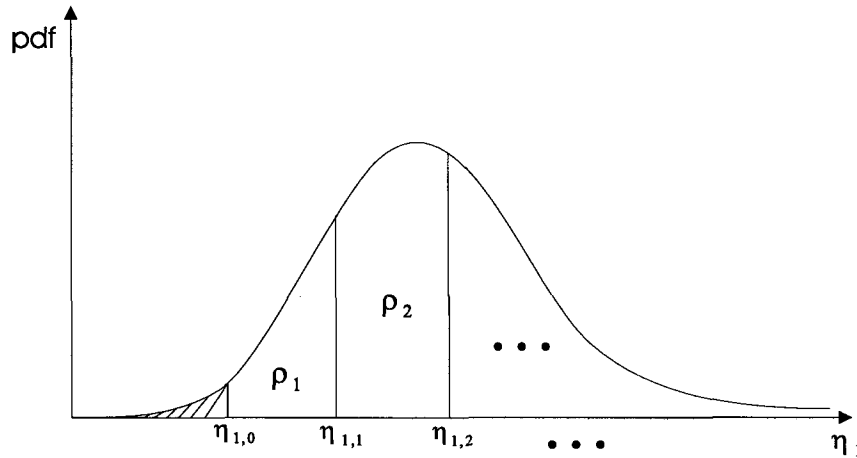


Figure 3.1: The illustration of truncated partitioned channel inversion.

In order to obtain a tradeoff between coding/decoding complexity and capacity loss, we applied a partitioned channel inversion scheme to convert the beamforming fading channel into a few exclusive AWGN channels. It uses a finite number of codes to approximate the channel capacity instead of using only one code. The general partitioned channel inversion scheme is illustrated in Fig. 3.1, where we first partition the value of channel gain into two regions. The first region, from 0 to  $\eta_{1,0}$ , is called the truncated region because no signal will be transmitted if  $\eta_1$  falls into this region; the second region, which begins at  $\eta_{1,0}$ , is partitioned into  $N$  sub-regions, each of which can be regarded as a fading sub-channel; it is referred to as the un-truncated region. Let  $\rho_i$  be the average power allocated to the  $i$ -th sub-channel. By applying channel inversion at the transmitter for each fading sub-channel, we obtain the following power adaption scheme in the  $i$ -th sub-channel as

$$q_i(\eta_1, \Omega) = \frac{\rho_i}{a_i \eta_1}, \quad (3.4.4)$$

where  $a_i$  is a normalizing factor given by

$$a_i \triangleq \int_{\eta_{1,i-1}}^{\eta_{1,i}} \frac{1}{\eta_1} f_{n,m}^1(\eta_1) d\eta_1. \quad (3.4.5)$$

Substituting the power adaption scheme into (3.4.1), we obtain the following channel model when  $\eta_1$  falls into the  $i$ -th sub-region

$$\tilde{y} = \sqrt{\frac{\rho_i}{a_i}} s + \tilde{z}. \quad (3.4.6)$$

Obviously, the scheme converts the fading sub-channels into  $N$  AWGN sub-channels with different SNR values. It is readily seen that these  $N$  AWGN sub-channels are independent, and therefore only  $N$  codes are required to approach the capacity of the beamforming. The problem left is to find the channel partition points  $\eta_i$ ,  $i = 0 \dots N$ , and the power allocation  $\rho_i$ ,  $i = 1 \dots N$ . As will be seen below, the values  $\rho_i$  can be found explicitly, given the values  $\eta_{1,i}$ . However, searching the values  $\eta_{1,i}$  results in a multi-dimensional optimization problem that can only be solved numerically. Instead, we suggest a heuristic solution. The simplest possible solution is to divide the probability space (for  $\eta_1$  above cutoff) into  $N$  equal partitions. Although this is a simple solution it can be readily seen that for  $N \rightarrow \infty$  it converges toward optimum water filling; and as we will see later, even for small  $N$  it

gives performance close to optimum. Let  $P_i$  be the probability that  $\eta_1$  falls into the  $i$ -th sub-region given by

$$P_i \triangleq \int_{\eta_{1,i-1}}^{\eta_{1,i}} f_{n,m}^1(\eta_1) d\eta_1 = \frac{\int_{\eta_{1,0}}^{\infty} f_{n,m}^1(\eta_1) d\eta_1}{N} \triangleq P_a, \quad i = 1, \dots, N. \quad (3.4.7)$$

where we denote  $\eta_{1,N} \triangleq \infty$  for convenience. It is clear that if the cutoff value  $\eta_{1,0}$  is fixed, all the other partition positions  $\eta_{1,i}$  for  $i = 1, 2, \dots, N - 1$  are also fixed. Therefore the multi-dimensional optimization problem can be avoided. The achievable capacity  $C_e$  of the beamforming with the proposed scheme can be obtained by solving the following optimization problem

$$C_e = \max_{\eta_{1,0}, \rho_i} \sum_{i=1}^N P_a \left\{ \log \left( 1 + \frac{\rho_i}{a_i} \right) \right\}, \quad (3.4.8)$$

$$\text{s.t. } \sum_{i=1}^N \rho_i = \Omega, \quad \rho_i \geq 0. \quad (3.4.9)$$

For a given set of  $\eta_{1,i}, i = 0, 1, \dots, N - 1$ , this is a standard optimization problem and can be solved by applying Lagrange multiplier and Kuhn-Tucker conditions [23]. It is shown that the best power adaption scheme in this case can be acquired from the following equations

$$\rho_{i,o} = [P_i \mu - a_i]^+, \quad \sum_{i=1}^N \rho_{i,o} = \Omega, \quad (3.4.10)$$

where  $[x]^+ = \max\{x, 0\}$ , and  $\mu$  is some constant ("water filling level") that is chosen so that the power constraint (3.4.10) is satisfied. Solving the above equations and substituting the solution of  $\rho_{i,o}$  into (3.4.8), the achievable capacity can be expressed as

$$C_e = \max_{\eta_{1,0}} P_a \sum_{i=1}^N \left[ \log \left( 1 + \frac{\rho_{i,o}}{a_i} \right) \right]. \quad (3.4.11)$$

From Section 3.3.2, we notice that each term in  $f_{n,m}^1(\eta_1)$  or  $\frac{1}{\eta_1} f_{n,m}^1(\eta_1)$  can be written as  $c_1 e^{-c_2 \eta_1} \eta_1^l$ , where  $c_1$  is some constant coefficient,  $c_2$  is a positive scalar and  $l$  is an integer which is no less than  $-1$ . By applying the following identities

$$\int_x^{\infty} c_1 e^{-c_2 \eta_1} \eta_1^l d\eta_1 = \frac{c_1 l!}{c_2^{l+1}} e^{-c_2 x} \sum_{i=0}^l \frac{(c_2 x)^i}{i!}, \quad l \geq 0, \quad (3.4.12)$$

$$\int_x^{\infty} e^{-\eta} \eta^{-1} d\eta = E_1(x), \quad (3.4.13)$$

where  $E_1(x)$  is the exponential integral of order 1, it can be shown that  $P_a$  and  $a_i$  for any  $(n, m)$  MIMO system can be expressed in closed-form. We demonstrate the results explicitly for the  $(n, 2)$  system. The integral of  $\varphi_1(l, k, \eta)$  defined in (3.3.12) for  $l \geq -1, k \geq 0$  can be found to be

$$\begin{aligned}\bar{\varphi}_1(l, k, x) &\triangleq \int_x^\infty \varphi_1(l, k, \eta) d\eta \\ &= \begin{cases} k!l!e^{-x} \sum_{j=0}^l \frac{x^j}{j!} - k! \sum_{i=0}^k \frac{(l+i)!}{i!2^{l+i+1}} e^{-2x} \sum_{j=0}^{l+i} \frac{(2x)^j}{j!}, & l \geq 0 \\ k!E_1(x) - k!E_1(2x) - k! \sum_{i=1}^k \frac{(i-1)!}{i!2^i} e^{-2x} \sum_{j=0}^{i-1} \frac{(2x)^j}{j!}, & l = -1. \end{cases} \end{aligned} \quad (3.4.14)$$

Then  $P_a$  and  $a_i$  can be expressed as

$$P_a = \frac{\mathcal{P}(\eta_{1,0})}{N}, \quad (3.4.15)$$

$$a_i = \mathcal{A}(\eta_{1,i-1}) - \mathcal{A}(\eta_{1,i}), \quad (3.4.16)$$

respectively, where  $\mathcal{P}(x)$  and  $\mathcal{A}(x)$  are given by

$$\begin{aligned}\mathcal{P}(x) &\triangleq \int_x^\infty f_{n,m}^1(\eta_1) d\eta_1 \\ &= 2K_{n,2} [\bar{\varphi}_1(n, n-2, x) - 2\bar{\varphi}_1(n-1, n-1, x) + \bar{\varphi}_1(n-2, n, x)] \end{aligned} \quad (3.4.17)$$

$$\begin{aligned}\mathcal{A}(x) &\triangleq \int_x^\infty \frac{1}{\eta_1} f_{n,m}^1(\eta_1) d\eta_1 \\ &= 2K_{n,2} [\bar{\varphi}_1(n-1, n-2, x) - 2\bar{\varphi}_1(n-2, n-1, x) + \bar{\varphi}_1(n-3, n, x)] \end{aligned} \quad (3.4.18)$$

respectively. When  $\eta_{1,0}$  is given,  $\eta_{1,i}$  for  $i = 1, 2, \dots, N-1$  can be obtained by recursively solving

$$P_a = \int_{\eta_{1,i-1}}^{\eta_{1,i}} f_{n,m}^1(\eta_1) d\eta_1 = \mathcal{P}(\eta_{1,i-1}) - \mathcal{P}(\eta_{1,i}), \quad (3.4.19)$$

i.e., given  $\eta_{1,0}$ ,  $\eta_{1,1}$  is found, then with  $\eta_{1,1}$  found,  $\eta_{1,2}$  can be found and so on. The achievable capacity  $C_e$  now can be numerically calculated by following the algorithm in Table I. We illustrate the achievable capacity  $C_e$  with a few examples in Fig 3.2 and 3.3, and discuss the results next.

Fig. 3.2 depicts the achievable capacity of beamforming with the proposed scheme in SISO (1, 1) and SIMO (2, 1) Rayleigh fading channels. Truncated channel inversion [25], which corresponds to the our scheme with  $N = 1$ , has the smallest coding/decoding complexity as it requires only one code designed for a AWGN channel. However, from the

Table 3.1: Algorithm for numerically calculating  $C_e$ .

[Initial step]
1. Given $N$ , set $C_e = 0$ .
2. Choose initial value $\eta_{1,0}$ , step $\Delta$ , and terminate value $\bar{\eta}$ .
3. Compute $P_a$ using (3.4.15).
4. Recursively solve $\eta_{1,i}$ for $i = 1, 2, \dots, N - 1$ using (3.4.19).
5. Compute $a_i$ for $i = 1, 2, \dots, N - 1$ using (3.4.16).
6. Solve (3.4.10) to compute $\rho_{i,o}$ .
7. Compute $C = P_a \sum_{i=1}^N \left[ \log\left(1 + \frac{\rho_{i,o}}{a_i}\right) \right]$ .
8. If $C > C_e$ , $C_e = C$ ; $\eta_{1,0} = \eta_{1,0} + \Delta$ .
9. If $\eta_{1,0} > \bar{\eta}$ , exit; Else go to 3.

figure it can be seen that it suffers a consequent capacity penalty, especially at high SNR. By using two or three codes designed for AWGN channels, i.e. channel partitioning with  $N = 2$  or  $N = 3$ , the capacity penalty can be greatly decreased. Since both the transmitter and the receiver know which code is used and all the sub-channels are exclusive, even if more than one code can be applied, still only one pair of code/decoder is needed. It can be seen that the sub-optimality introduced by equally partitioning of the un-truncated region is not significant, and as  $N \rightarrow \infty$ , this sub-optimality vanishes since it can be readily argued that the capacity with equally truncated channel partitioning will converge towards the optimal water-filling scheme asymptotically. It is more interesting that for even small  $N$  the achievable capacity is very close to the optimum water-filling. Fig. 3.3 depicts the achievable capacity of beamforming with channel partitioning in (2, 2) and (4, 4) MIMO Rayleigh fading channels. It is worth mentioning that the capacity penalty of truncated channel inversion (channel partitioning with  $N = 1$ ) diminishes remarkably as the number of antennas increases. This observation extends the conclusion made on SIMO fading channels with diversity-combining [29] to MIMO fading channels with beamforming.

### 3.5 The Multiple Eigen-Beamforming Case

If CSI is available at both the transmitter and the receiver, (3.2.2) indicates that an  $(n, m)$  MIMO fading channel can be decomposed into  $m$  parallel channels and these par-

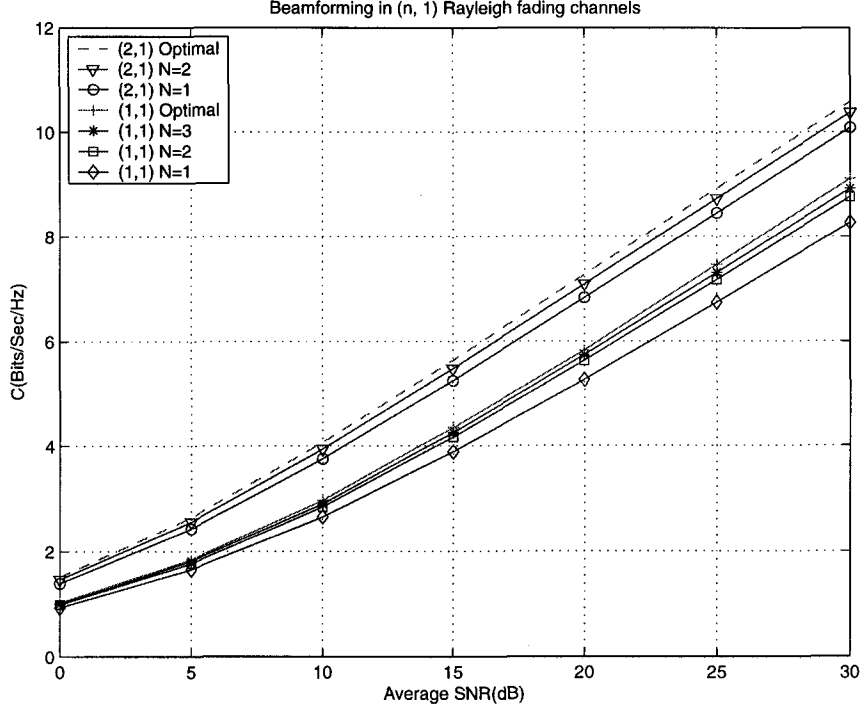


Figure 3.2: Capacity of beamforming in SISO and SIMO Rayleigh fading channels.

allel channels are characterized by an eigenvalue matrix  $\Lambda$ . When the SNR is high, instead of just using the best channel among the  $m$  channels as in beamforming, multiple parallel channels could be utilized to support high transmission rates. With an average transmit power constraint, the transmit power also should be dynamically allocated according to the instantaneous CSI. Consequently, the transmit power should be a function of  $\Lambda$  and the average power constraint  $\Omega$ . Again, the power adaptation and coding can be separated without introducing any capacity loss [27]. Therefore the multiple eigen-beamforming model with power control can be modelled by

$$\tilde{\mathbf{y}} = \Lambda^{1/2} \mathbf{Q}(\Lambda, \Omega)^{1/2} \mathbf{s} + \tilde{\mathbf{z}}, \quad (3.5.1)$$

where  $\mathbf{s}$  is the transmitted symbol satisfying  $E[\mathbf{s}^\dagger \mathbf{s}] = 1$ , and  $\mathbf{Q}(\Lambda, \Omega)$  features the transmit power control scheme. It is readily seen that  $\mathbf{Q}(\Lambda, \Omega)$  should be a diagonal matrix and satisfy the following average power constraint

$$\mathcal{E} \{ \text{tr} [\mathbf{Q}(\Lambda, \Omega)] \} = \Omega. \quad (3.5.2)$$

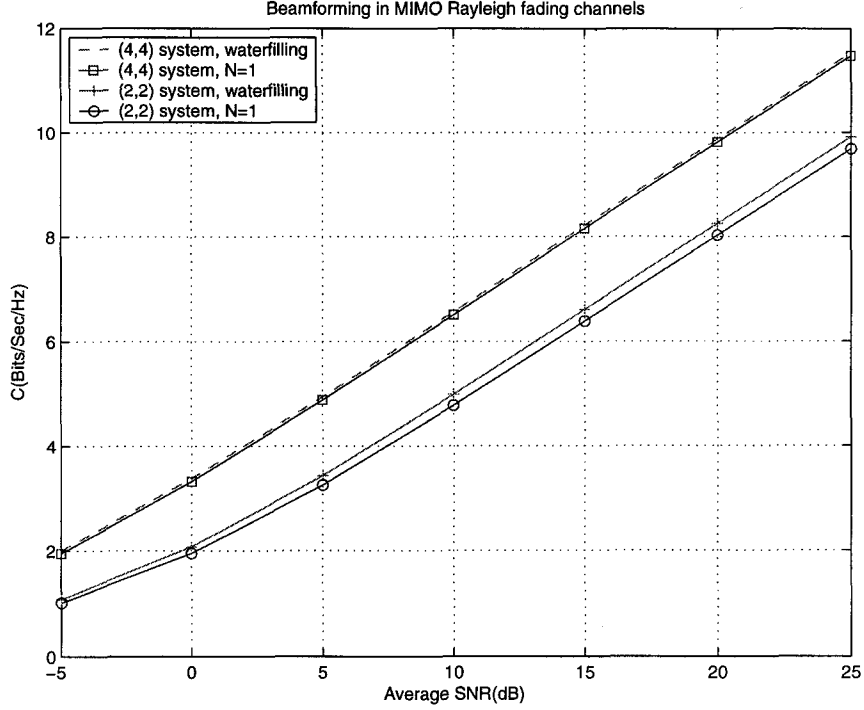


Figure 3.3: Capacity of beamforming in MIMO Rayleigh fading channels.

It is shown in [21] that optimal power adaption in multiple eigen-beamforming technique is still the “water-filling” method with

$$Q_{i,i} = \begin{cases} \frac{1}{\lambda'_0} - \frac{1}{\lambda_i}, & \lambda_i \geq \lambda'_0 \\ 0, & \lambda_i < \lambda'_0 \end{cases} \quad (3.5.3)$$

where  $\lambda'_0$  is a unique cutoff value for all eigenvalues and can be obtained by solving the following average power constraint equation

$$\int_{\lambda'_0}^{\infty} \left( \frac{1}{\lambda'_0} - \frac{1}{\lambda} \right) f_{n,m}^u(\lambda) d\lambda = \frac{\Omega}{m}, \quad (3.5.4)$$

where  $f(\lambda)$  is the marginal pdf of the un-ordered eigenvalue for a  $(n, m)$  MIMO system. The capacity with the optimal power control scheme is

$$C = m \int_{\lambda'_0}^{\infty} \log \left( \frac{\lambda}{\lambda'_0} \right) f_{n,m}^u(\lambda) d\lambda. \quad (3.5.5)$$

Again, there are two methods to achieve the capacity: multiple coding with optimal power adaptation [25] and single coding with optimal power adaptation [27]. The former method requires an infinite number of codes in principle and joint multiplexed coding/decoding among  $m$  parallel channels. The latter method requires inter-block coding and therefore might need quite long codes to compensate the fading, especially when deep fading appears. To obtain a better tradeoff, we propose a capacity approaching scheme that converts the dependent fading parallel channels into independent AWGN parallel channels. It turns out that the truncated channel inversion method is a straightforward method to achieve this goal.

### 3.5.1 Unordered Multiple Eigen-Beamforming

Let us first consider applying the truncated channel partition among the  $m$  *unordered parallel* channels defined by SVD. Notice that in unordered case all channels have the same fading characteristic. Therefore each channel should be truncated and partitioned in the same way, and the equal power should be allocated to each channel, namely  $\Omega/m$ . We partition each truncated channel into  $N$  sub-channels as in Section 3.4. After channel inversion on each sub-channel, if the value of  $k$ -th channel falls into the  $i$ -th sub-region, the input-output relation can be expressed as

$$\tilde{y}_k = \sqrt{\frac{\rho_i}{a_i}} s_k + \tilde{z}_k, \quad (3.5.6)$$

where  $\rho_i$  is the average power allocated to the  $i$ -th sub-channel and  $a_i$  is defined as

$$a_i \triangleq \int_{\lambda_{i-1}}^{\lambda_i} \frac{1}{\lambda} f_{n,m}^u(\lambda) d\lambda, \quad (3.5.7)$$

where  $\lambda_i$  for  $i = 1, 2, \dots, N-1$  stands for the  $i$ -th partition position,  $\lambda_0$  is the truncated value, and  $\lambda_N$  is defined as  $\lambda_N \triangleq \infty$ . From (3.5.6), we can see that the  $N$  sub-channels of the  $k$ -th channel are exclusive and any sub-channel of the  $k$ -th channel is independent of any sub-channel of the  $k'$ -th channel if  $k \neq k'$ . Thus, we convert the  $m$  dependent parallel channels into independent parallel AWGN channels. The achievable capacity  $C_e$  in this case can now be found by solving the following optimization problem

$$C_e = \max_{\lambda_0, \rho_i} m P_a \sum_{i=1}^N \left\{ \log \left( 1 + \frac{\rho_i}{a_i} \right) \right\},$$

$$\text{s.t. } \sum_{i=1}^N \rho_i = \frac{\Omega}{m}, \rho_i \geq 0, \quad (3.5.8)$$

where we define

$$P_a \triangleq \frac{\int_{\lambda_0}^{\infty} f_{n,m}^u(\lambda) d\lambda}{N}. \quad (3.5.9)$$

As in Section 3.4, the optimal values of  $\rho_i$  can be found given  $\lambda_0$ , and we get the achievable capacity as

$$C_e = \max_{\lambda_0} \left\{ m P_a \sum_{i=1}^N \left[ \log \left( 1 + \frac{\rho_{i,o}}{a_i} \right) \right] \right\} \quad (3.5.10)$$

$$\rho_{i,o} = [m P_a \mu - a_i]^+, \sum_{i=1}^m \rho_{i,o} = \frac{\Omega}{m} \quad (3.5.11)$$

where  $\mu$  is a "water-filling level" chosen so that (3.5.11) is satisfied. With a similar argument as in Section 3.4, we can show that  $P_a$  and  $a_i$  can be expressed in closed form. We will give the expressions for the  $(n, 2)$  system. Define

$$\tilde{\psi}(l, x) \triangleq \int_x^{\infty} e^{-\eta} \eta^l d\eta = \begin{cases} l! e^{-x} \sum_{i=0}^l \frac{x^i}{i!}, & l \geq 0 \\ E_1(x), & l = -1, \end{cases} \quad (3.5.12)$$

and using  $f_{n,m}^u(\lambda)$  derived in Section 3.3.1, we can write  $P_a$  and  $a_i$  in closed form as

$$P_a = \frac{\mathcal{P}_u(\lambda_0)}{N}, \quad (3.5.13)$$

$$a_i = \mathcal{B}(\lambda_{i-1}) - \mathcal{B}(\lambda_i), \quad (3.5.14)$$

respectively, where  $\mathcal{P}_u(x)$  and  $\mathcal{B}(x)$  are given by

$$\mathcal{P}_u(x) \triangleq K_{n,2} \left[ (n-2)! \tilde{\psi}(n, \lambda_0) - 2(n-1)! \tilde{\psi}(n-1, \lambda_0) + n! \tilde{\psi}(n-2, \lambda_0) \right] \quad (3.5.15)$$

$$\mathcal{B}(x) \triangleq K_{n,2} \left[ (n-2)! \tilde{\psi}(n-1, x) - 2(n-1)! \tilde{\psi}(n-2, x) + n! \tilde{\psi}(n-3, x) \right] \quad (3.5.16)$$

The achievable capacity of the unordered multiple eigen-beamforming with the proposed scheme can therefore easily be found numerically by following the same procedure as in Table I.

When  $N \rightarrow \infty$  it can be easily seen that truncated channel partitioning approaches channel capacity. What is more interesting is that we can come close to channel capacity with even moderate  $N$ , as the following numerical examples will show.

In Fig. 3.4 and 3.5, we present the achievable capacities of the unordered multiple eigen-beamforming with channel partitioning in MIMO Rayleigh fading channels. It can be seen that there exists a considerable capacity penalty for simple truncated channel inversion, especially at high SNR. Unlike the conclusion for beamforming, where the capacity penalty diminishes as the number of antennas increases, we notice that the capacity penalty for (4, 4) MIMO channels is actually bigger than the capacity penalties for (3, 3) and (2, 2) MIMO channels. However, from Fig. 3.4, we observe that the capacity penalty in  $(n, 2)$  MIMO channels decreases as  $n$  increases. Therefore in the unordered multiple eigen-beamforming system, we can only say that the capacity penalty diminishes as the maximum between the number of transmit and receive antennas increases while the minimum between the number of transmit and receive antennas is fixed. It can be seen that the capacity penalty can be greatly decreased by applying channel partitioning. For instance, when  $N = 4$ , the capacity penalty becomes very small in all our examples.

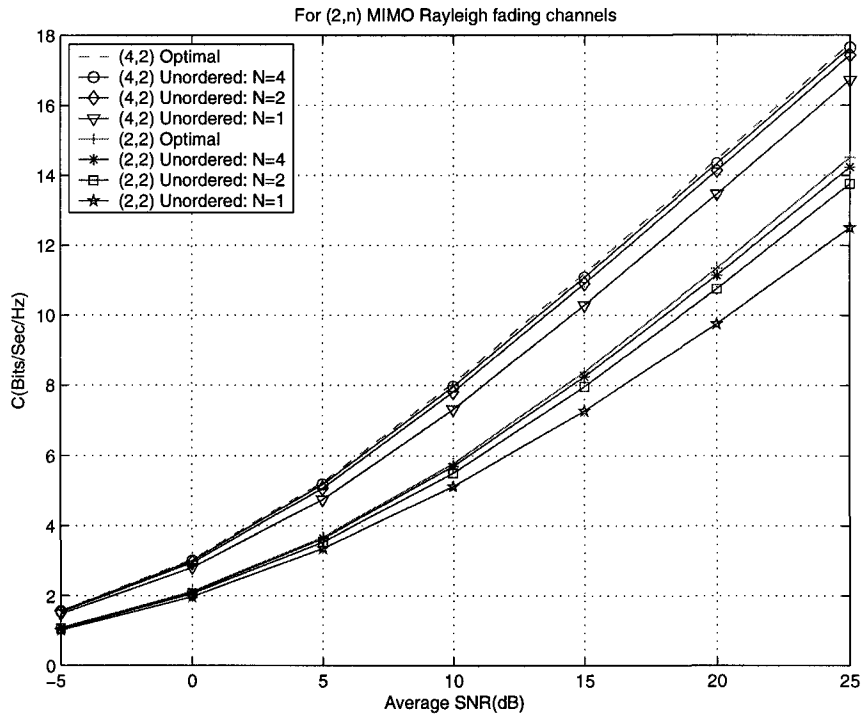


Figure 3.4: Capacity of unordered multiple eigen-beamforming for  $(n, 2)$  MIMO Rayleigh fading channels.

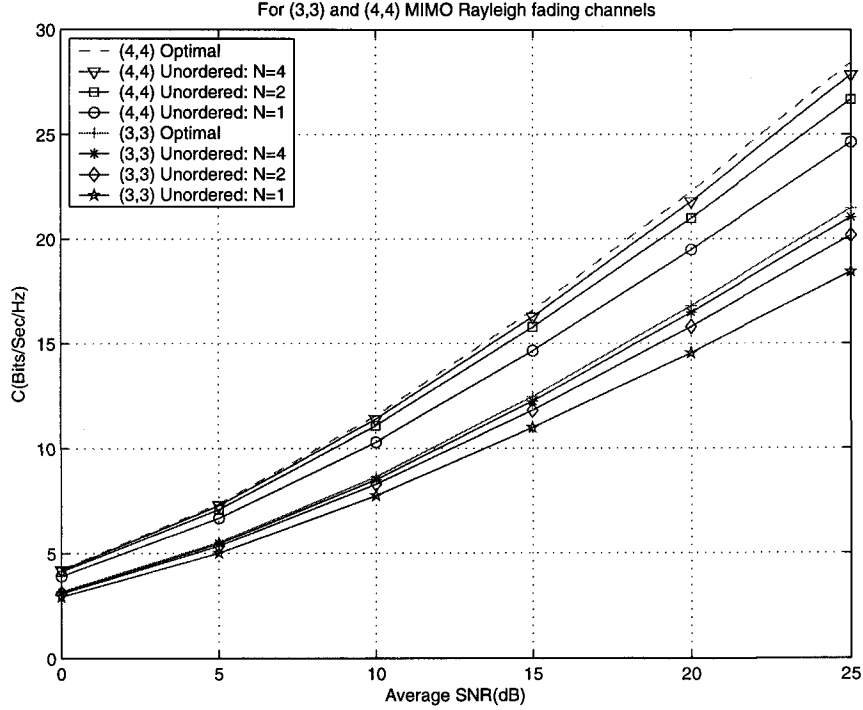


Figure 3.5: Capacity of unordered multiple eigen-beamforming for (3, 3) and (4, 4) MIMO Rayleigh fading channels.

Although our heuristic solution that partitions channel according to equal probability already approaches very closely to the capacity by using a few codes, we still want to know how far it from the optimal partition. Therefore we numerically calculated the rate achieved by optimal partition for  $N = 2$  in the  $(m = 2, n = 2)$  system and the results are shown in Fig. 3.6. From Fig. 3.6, we can observe that the optimal method has negligible gain over the heuristic method.

### 3.5.2 Ordered Multiple Eigen-Beamforming

The unordered multiple eigen-beamforming scheme emphasizes power control and coding/decoding in *time*, and it always needs  $m$  pairs of coder/decoders. In this section, we consider the ordered channels which can provide more efficient power allocation and coding/decoding in both *time and space*. We assume that the eigenvalues have been ordered, and that the  $K$  ( $1 \leq K \leq m$ ) best eigen-modes are used in the communication

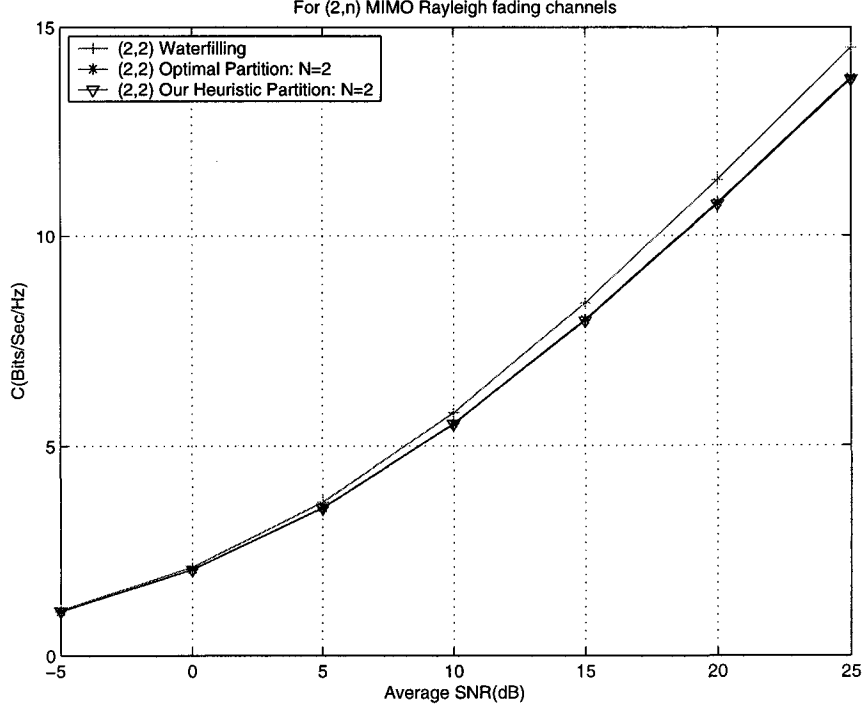


Figure 3.6: Comparison between the method with optimal partition and our heuristic partition method.

system. In this case only  $K$  pairs of coder/decoders are required. We still apply the truncated channel partition on each ordered channel. Let  $\rho_{k,i}$  be the average power allocated to the  $i$ -th sub-channel of the  $k$ -th channel, if the value of  $k$ -th channel falls into the  $i$ -th sub-region, the input-output relation can be expressed as

$$\tilde{y}_k = \sqrt{\frac{\rho_{k,i}}{a_{k,i}}} s_k + \tilde{z}_k, \quad (3.5.17)$$

where we define

$$a_{k,i} \triangleq \int_{\eta_{k,i-1}}^{\eta_{k,i}} \frac{1}{\eta_k} f_{n,m}^k(\eta_k) d\eta_k, \quad (3.5.18)$$

where  $f_{n,m}^k(\eta_k)$  is the marginal p.d.f of the  $k$ -th largest eigenvalue defined in Section 3.3.2,  $\eta_{k,i}$  for  $i = 1, 2, \dots, N - 1$  stands for the  $i$ -th partition position of the  $k$ -th channel,  $\eta_{k,0}$  is the truncated value of the  $k$ -th channel, and  $\lambda_{k,N}$  is defined as  $\lambda_{k,N} \triangleq \infty$ . The sub-channels resulting from the truncated channel partition are still independent AWGN channels. We

therefore get the following achievable capacity

$$C_g = \max_{\eta_{k,i-1}, \rho_{k,i}} \sum_{k=1}^K \sum_{i=1}^N \left\{ P_{k,i} \log \left( 1 + \frac{\rho_{k,i}}{a_{k,i}} \right) \right\}, \quad (3.5.19)$$

$$\text{s.t. } \sum_{k=1}^K \sum_{i=1}^N \rho_{k,i} = \Omega, \quad \rho_{k,i} \geq 0, \quad (3.5.20)$$

where  $P_{k,i}$  denotes the probability that  $\eta_k$  falls into the sub-region between  $\eta_{k,i-1}$  and  $\eta_{k,i}$ , given as

$$P_{k,i} \triangleq \int_{\eta_{k,i-1}}^{\eta_{k,i}} f_{n,m}^k(\eta_k) d\eta_k. \quad (3.5.21)$$

Unfortunately, the optimization of (3.5.19) is a  $KN$ -dimensional optimization problem, which can only be solved numerically. For simplicity, we consider a special case in which we use the same cut-off value for all the channels, and then apply channel inversion ( $N = 1$ ) to the region of each channel above this cutoff value. Let  $\eta_0$  denote the universal cut-off value. The achievable capacity by ordered multiple eigen-beamforming is

$$C_e = \max_{\eta_0} \sum_{k=1}^K \left[ P_{k,a} \log \left( 1 + \frac{\rho_{k,o}}{a_k} \right) \right], \quad (3.5.22)$$

where  $a_k$  and  $P_{k,a}$  are given by

$$a_k = \int_{\eta_0}^{\infty} \frac{1}{\eta_k} f_{n,m}^k(\eta_k) d\eta_k, \quad P_{k,a} = \int_{\eta_0}^{\infty} f_{n,m}^k(\eta_k) d\eta_k, \quad (3.5.23)$$

and  $\rho_{k,o}$  can be obtained by solving the following equations

$$\rho_{k,o} = [P_{k,a} \mu - a_k]^+, \quad \sum_{k=1}^K \rho_{k,o} = \Omega. \quad (3.5.24)$$

Again, closed form expressions for  $P_{k,a}$  and  $a_k$  are obtainable for any MIMO system. For the  $(n, 2)$  system, it is readily seen that  $P_{1,a} = \mathcal{P}(\eta_0)$  and  $a_1 = \mathcal{A}(\eta_0)$  where  $\mathcal{P}(x)$  and  $\mathcal{A}(x)$  are given in (3.4.17) and (3.4.18) respectively. To calculate  $P_{2,a}$  and  $a_2$ , we define

$$\begin{aligned} \tilde{\varphi}_2(l, k, x) &\triangleq \int_x^{\infty} \varphi_2(l, k, \eta) d\eta \\ &= \begin{cases} k! \sum_{i=0}^k \frac{(l+i)!}{i! 2^{l+i+1}} e^{-2x} \sum_{j=0}^{l+i} \frac{(2x)^j}{j!}, & l \geq 0 \\ k! E_1(2x) + k! \sum_{i=1}^k \frac{(i-1)!}{i! 2^i} e^{-2x} \sum_{j=0}^{i-1} \frac{(2x)^j}{j!}, & l = -1. \end{cases} \end{aligned} \quad (3.5.25)$$

Noticing the similarity between the forms of  $f_{n,2}^1(\eta_1)$  and  $f_{n,2}^2(\eta_2)$ , we can still obtain  $P_{2,a} = \mathcal{P}(\eta_0)$  and  $a_2 = \mathcal{A}(\eta_0)$  through (3.4.17) and (3.4.18) respectively, except that we need to replace  $\tilde{\varphi}_1(l, k, x)$  with  $\tilde{\varphi}_2(l, k, x)$ . The achievable capacity  $C_e$  of ordered multiple eigen-beamforming can be evaluated from (3.5.22) through a similar numerical search algorithm as in Table I. Notice that only  $\eta_0$  has to be optimized numerically, and it is therefore a one-dimensional numerical optimization problem.

Fig. 3.7 and 3.8 illustrate the capacities achieved by ordered multiple eigen-beamforming in MIMO Rayleigh fading channels. As expected, the more eigen-modes are used, the higher the achievable capacities are, with the differences increasing with SNR values. It is worth pointing out that the achievable capacity by the ordered multiple eigen-beamforming ( $K = m$ ) is clearly superior to that of beamforming, which corresponds to the ordered multiple eigen-beamforming with  $K = 1$ . It is shown that if  $K < m$ , increasing  $K$  provides significant improvement, and if  $K = m$ , the choice ( $N = 1$ ) is sufficient to closely approach the channel capacity. In that case, the influence of the suboptimality introduced by simplified optimization is not noticeable. In Fig. 3.7, it is shown that the capacity penalty diminishes as the maximum of the number of antenna increases while the minimum of number of antennas is fixed.

### 3.5.3 Discussions

In Fig. 3.9, we compare the achievable capacity of the proposed schemes in ordered and unordered multiple eigen-beamforming for (3, 3) and (4, 4) MIMO systems. We first compare the achievable capacity by truncated channel inversion. For the (3,3) MIMO system, we observe that the ordered multiple eigen-beamforming ( $K = 2$ ) attains higher capacity than the unordered multiple eigen-beamforming ( $N = 1$ ) if the SNR is below 20dB. For the (4,4) MIMO system, the ordered multiple eigen-beamforming ( $K = 3$ ) attains higher capacity than the unordered multiple eigen-beamforming ( $N = 1$ ) in the considered SNR region. Remember that unordered eigen-beamforming always uses  $m$  parallel coders/decoders, while ordered eigen-beamforming uses  $K$ . Therefore for the truncated channel inversion, the ordered case can use less number of coder/decoders than unordered case but still achieve higher capacity in a certain SNR region.

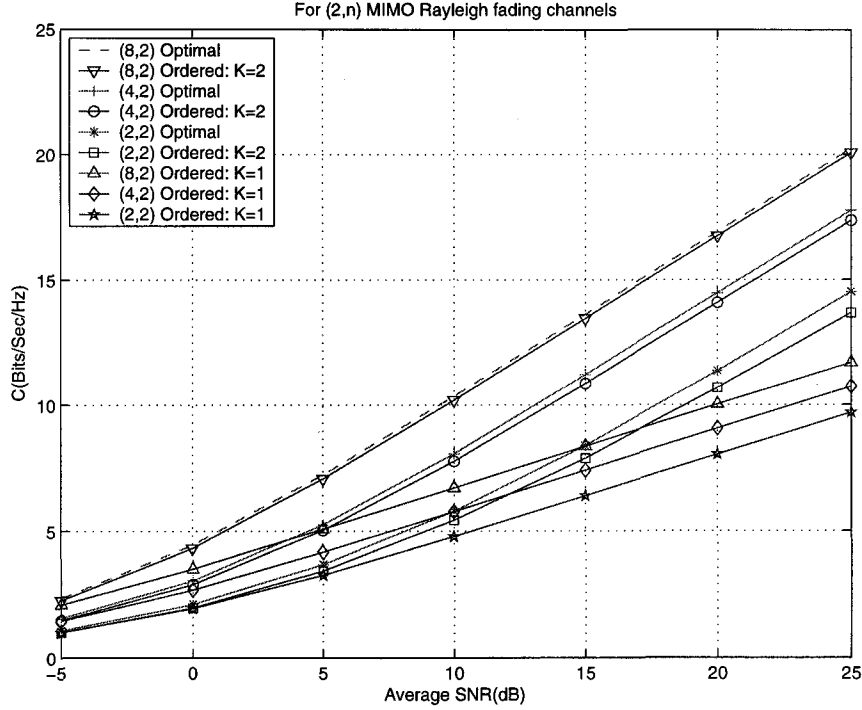


Figure 3.7: Capacity of ordered multiple eigen-beamforming for  $(n, 2)$  MIMO Rayleigh fading channels.

In Fig. 3.9, we also observe that both the unordered and ordered cases closely approach the capacity when the same number ( $K = N = m$ ) codes are used. However, for the unordered case, the code selection among the  $N$  candidates depends on the channel realization, while for the ordered case, the same  $K$  codes are always used (unless the channel is in outage). In the other words, for the unordered case, there are  $N$  candidate codes can be used by each eigen-channel. Based on the channel realization, each eigen-channel selects one code among these  $N$  candidate codes. For the ordered case,  $K$  ordered eigen-channel are used and each ordered eigen-channel uses one fixed code.

In Fig. 3.10, we compare the capacities achieved by knowing the CSI at the transmitter with the MIMO capacities in the case when the CSI is available only at the receiver. It is shown that, for the case the CSI only available at receiver and  $N_r \leq N_t$ , only increasing the number of transmit antennas  $N_t$  can not provide major capacity gain. However, when the CSI is also known at the transmitter, only increasing the number of

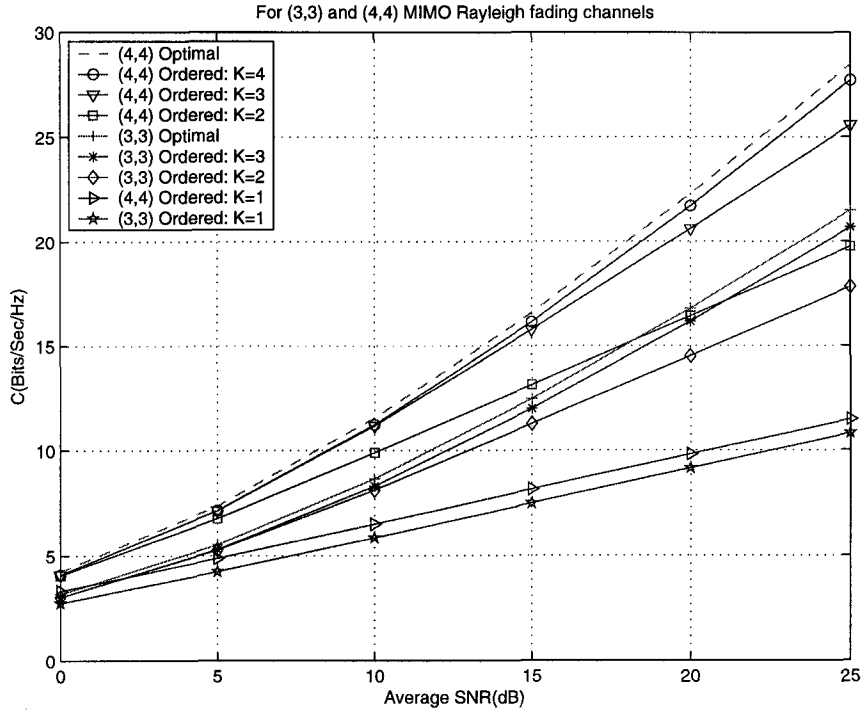


Figure 3.8: Capacity of ordered multiple eigen-beamforming for (3, 3) and (4, 4) MIMO Rayleigh fading channels.

transmit antennas  $N_t$  can provide considerable capacity gain. It is also shown that our proposed schemes allow to closely approach the capacity values.

The main advantage of the proposed schemes is that they can approach channel capacity for MIMO systems with a moderate coding/decoding complexity. Beamforming with channel partitioning requires only  $N$  different codes, matched to  $N$  different SNR values, where  $N$  need be only in the order of 2 or 3. Unordered multiple eigen-beamforming uses  $m$  coders/decoders in parallel, but these  $m$  coders use the same selection of  $N$  codes, i.e., also here only  $N$  different codes are needed. Ordered multiple eigen-beamforming uses  $K$  coders/decoders in parallel, and each coder/decoder uses a different code, so  $K$  codes are used. Notice that in our multiple coding scheme, all channels have been converted to Gaussian channels, and many code design methods for the Gaussian channel can therefore be used to design practical coding schemes. Compared to the scheme using one code with CSI-dependent power control [26, 27], our multiple-coding scheme has the fol-

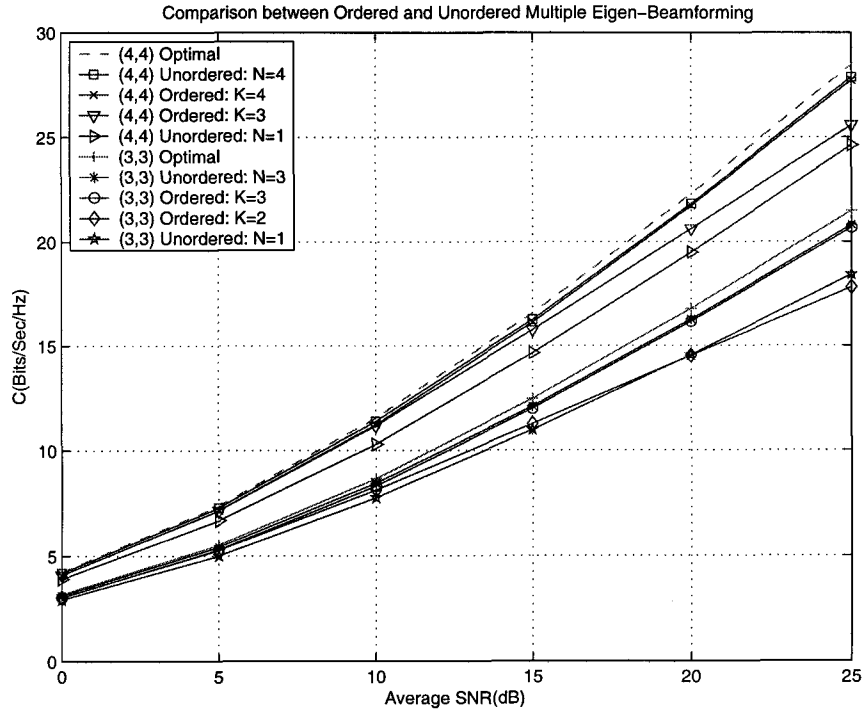


Figure 3.9: Comparison between ordered and unordered multiple eigen-beamforming for (3, 3) and (4, 4) MIMO Rayleigh fading channels.

lowing advantages. First, the coding problem of our scheme is coding on AWGN channel while the coding problem in [26, 27] is still coding on fading channel. Coding on AWGN channel is well researched and capacity-approaching practical coding methods already existed in AWGN channel. Also, it is shown that using linear binary codes in AWGN channel only introduces negligible loss compared to using random codes. Second, since our multiple-coding scheme can adaptive the rates to the channel besides the power adaptation, our scheme potentially need a shorter code than scheme in [26, 27], especially when deep fading appears. By applying puncture, actually only one code (with different puncture) can actually be used in our multiple-coding scheme and therefore the complexity does not increase much. It is also worth to mentioning that our scheme can be coded in one block while scheme in [26, 27] requires inter block coding. To the end, capacity-approaching iteratively decodable codes seem particularly promising [34]-[37].

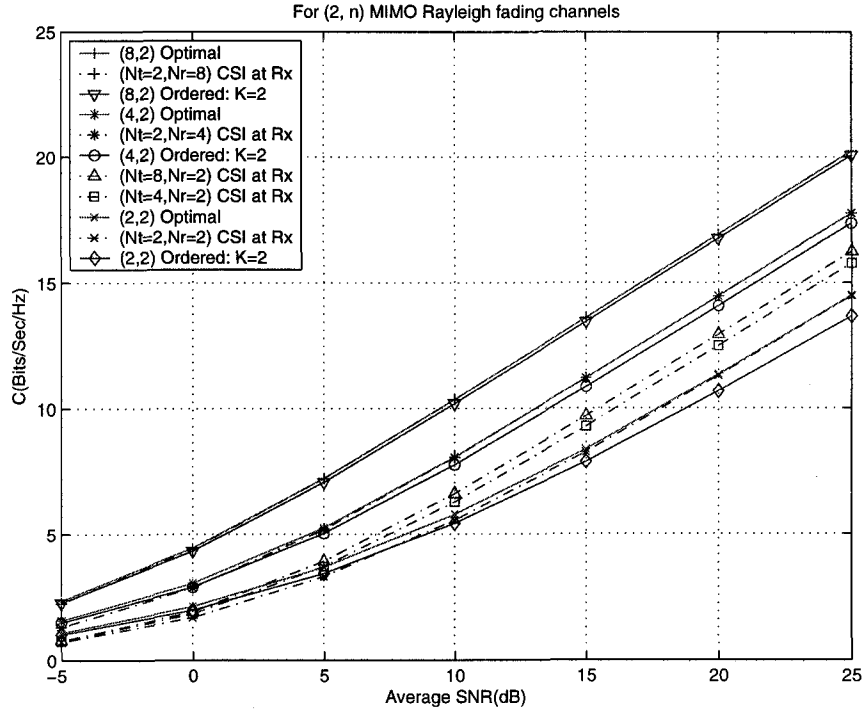


Figure 3.10: Comparison with the capacity of CSI at receiver only in MIMO Rayleigh fading channels.

### 3.6 Extended to Correlated MIMO Rayleigh Fading Systems

It is shown that the capacity of the uncorrelated MIMO Rayleigh fading channels grows linearly with the minimum of transmit and receive antennas [2][3]. In many practical situations, when there are not enough scatters around the transmit and/or receive antennas (non-richness scattering environment) or when antenna elements are spaced closely, correlations among the MIMO channels are introduced. As shown in Chapter 2, a correlated MIMO channel can be modelled by the channel matrix in (2.1.2). The asymptotic growth rate of capacity of certain correlated MIMO fading channels was studied in [38]. It is shown that in the given patterns, the capacity of  $N \times N$  correlated MIMO channels still grows linearly with  $N$  as  $N \rightarrow \infty$ , even though it is smaller than the capacity of  $N \times N$  uncorrelated MIMO channels. However, Shiu *et al* [14] showed that in other patterns, the

capacity is very sensitive to the presence of correlations. In fact, they shown that the capacity of an  $N \times N$  correlated MIMO system decreases and approaches the capacity of a  $1 \times N$  single-input-multiple-output (SIMO) system. The impact of correlations on the capacity of MIMO channels with finite number of antennas has been recently considered in [39] [40]. In these papers, it is again demonstrated that the presence of correlations results in capacity loss. However, it is also demonstrated that the capacity loss is negligible even with a correlation coefficient between two adjacent antennas as large as 0.5 for an exponential correlation model.

We have shown that considerable capacity gain and reduced coding complexity can be obtained by knowing CSIR and CSIT in uncorrelated MIMO Rayleigh fading channels. In [41], it is illustrated that the transmit side information plays an important part in correlated MIMO channels. However, the exact results of the impact of correlations on MIMO fading channels with transmit CSI are still not clear. How to exploit the transmit CSI in correlated MIMO fading channels also needs to add extra knowledge. Therefore we evaluate the capacity of the correlated MIMO channels with CSIT and CSIR. We also make efforts to exploit the high capacity with simple transmission schemes. We calculate the achievable rate by using simple beamforming when the MIMO channel is highly correlated. To further simplify the coding/decoding, we apply truncated channel inversion (TCI) [25] in MIMO correlated channels and evaluate the achievable rates.

### 3.6.1 System Description

We consider a wireless link comprising  $N_t$  transmitter antennas and  $N_r$  receiver antennas that operates in a semi-correlated Rayleigh flat-fading environment, which means correlation exists either at the transmitter or at the receiver but not both. Due to the duality between correlation at the transmitter and correlation at the receiver, only the case of correlation at the receiver is considered in this paper. Denote the correlation matrix as  $\mathbf{R}$ . From chapter 2, we can see that the channels can be characterized by a matrix defined as  $\mathbf{H} \triangleq \mathbf{R}^{1/2} \mathcal{H}$ , where  $\mathcal{H}$  is an  $N_r \times N_t$  matrix, of which the entries are modelled as independent complex circular symmetric Gaussian random variables with zero-mean and unit

variance. Again, the discrete-time baseband received signal can be expressed as

$$\mathbf{y} = \mathbf{H}\mathbf{x} + \mathbf{z}. \quad (3.6.1)$$

Assume there is an average transmit power constraint  $\Omega$ ; then we have  $\mathcal{E}[\mathbf{x}^\dagger\mathbf{x}] = \Omega$ . Let the singular value decomposition (SVD) of the channel matrix  $\mathbf{H}$  be  $\mathbf{H} = \mathbf{U}\mathbf{\Lambda}^{1/2}\mathbf{V}^\dagger$ . With the similar processing as we did in the uncorrelated cases, we obtain

$$\begin{aligned} \tilde{\mathbf{y}} = \mathbf{U}^\dagger\mathbf{y} &= \mathbf{U}^\dagger\mathbf{H}\mathbf{V}\mathbf{Q}^{\frac{1}{2}}\mathbf{s} + \mathbf{U}^\dagger\mathbf{z} \\ &= \mathbf{\Lambda}^{1/2}\mathbf{Q}^{\frac{1}{2}} \begin{bmatrix} s_1 \\ \vdots \\ s_m \end{bmatrix} + \tilde{\mathbf{z}}, \end{aligned} \quad (3.6.2)$$

where  $\tilde{\mathbf{z}} = \mathbf{U}^\dagger\mathbf{z}$  is still a complex additive Gaussian noise vector with zero mean and covariance matrix  $\mathbf{I}_m$ . Define a Wishart matrix  $\mathbf{W}$  as in (3.2.3). It can be shown that the eigenvalues of  $\mathbf{W}$  play the key roles in the capacity calculation. If the number of receive antennas is no less than the number of transmit antennas, the correlation matrix  $\mathbf{R}$  is an  $n \times n$  matrix; otherwise, it is an  $m \times m$  matrix. For these two cases, the probability density functions (pdf's) of the eigenvalues of  $\mathbf{W}$  have different forms. In the former case, the joint pdf of the unordered eigenvalues has been given by equation (29) in [39]; in the latter case, the joint pdf of the ordered eigenvalues are given in [40]. We consider correlations are present at the receiver and in general more capacity gain can be obtained by having the transmit CSI in a MIMO system which equips more antennas at the transmitter than those at the receiver. Hence we have an  $m \times m$  correlation matrix as modelled. Denote the joint pdf of unordered eigenvalues as  $g_{\mathbf{\Lambda}}(\lambda_1, \dots, \lambda_m)$ , where we denote  $\lambda_1, \lambda_2, \dots, \lambda_m$  as the eigenvalues of  $\mathbf{W}$ . We can derive  $g_{\mathbf{\Lambda}}(\lambda_1, \dots, \lambda_m)$  from the joint pdf of the ordered eigenvalues [40]. Denote  $\gamma_1 \geq \gamma_2 \geq \dots \geq \gamma_m$  as the ordered eigenvalues of correlation matrix  $\mathbf{R}$ , then  $g_{\mathbf{\Lambda}}(\lambda_1, \dots, \lambda_m)$  can be expressed as

$$g_{\mathbf{\Lambda}}(\lambda_1, \dots, \lambda_m) = \frac{\prod_{i=1}^m \lambda_i^{n-m}}{\prod_{i=1}^m (n-i)! \gamma_i^n} \frac{|\mathbf{E}(\boldsymbol{\lambda}, \boldsymbol{\gamma})| |\boldsymbol{\Psi}(\boldsymbol{\lambda})|}{m! |\boldsymbol{\Psi}(\boldsymbol{\gamma})|}, \quad (3.6.3)$$

where we define

$$\boldsymbol{\lambda} = \begin{bmatrix} \lambda_1 & \lambda_2 & \dots & \lambda_m \end{bmatrix},$$

$$\gamma = \begin{bmatrix} -\gamma_1^{-1} & -\gamma_2^{-1} & \cdots & -\gamma_m^{-1} \end{bmatrix},$$

$$E(\lambda, \gamma) \triangleq \begin{bmatrix} e^{-\frac{\lambda_1}{\gamma_1}} & e^{-\frac{\lambda_2}{\gamma_1}} & \cdots & e^{-\frac{\lambda_m}{\gamma_1}} \\ e^{-\frac{\lambda_1}{\gamma_2}} & e^{-\frac{\lambda_2}{\gamma_2}} & \cdots & e^{-\frac{\lambda_m}{\gamma_2}} \\ \vdots & \vdots & \ddots & \vdots \\ e^{-\frac{\lambda_1}{\gamma_m}} & e^{-\frac{\lambda_2}{\gamma_m}} & \cdots & e^{-\frac{\lambda_m}{\gamma_m}} \end{bmatrix}, \quad (3.6.4)$$

$$\Psi(\lambda) \triangleq \begin{bmatrix} 1 & 1 & \cdots & 1 \\ \lambda_1 & \lambda_2 & \cdots & \lambda_m \\ \vdots & \vdots & \ddots & \vdots \\ \lambda_1^{m-1} & \lambda_2^{m-1} & \cdots & \lambda_m^{m-1} \end{bmatrix}, \quad (3.6.5)$$

and we define  $\Psi(\gamma)$  just by replacing  $\lambda$  in  $\Psi(\lambda)$  with  $\gamma$ . Again, in order to calculate capacities for the different MIMO signaling schemes, and for use in optimization, the marginal pdf's of both the unordered and ordered eigenvalues of the matrix  $W$  are needed. Due to the complete symmetry among all unordered eigenvalues in (3.6.3), the marginal pdf's of all the unordered eigenvalues should have exactly the same expression, and it can be obtained by

$$g_{n,m}(x) = \underbrace{\int_0^\infty \cdots \int_0^\infty}_{m-1} g_\Lambda(x, \lambda_2, \dots, \lambda_m) d\lambda_2 \cdots d\lambda_m. \quad (3.6.6)$$

We sort all the eigenvalues in non-decreasing order and denote the  $k$ -th order statistic of  $\lambda_1, \lambda_2, \dots, \lambda_m$  by  $\eta_k$ . Notice that the probability that two eigenvalues are equal is zero, and we can therefore discard this case. Following the same procedure as in the uncorrelated case, it can be shown that the marginal pdf of  $\eta_k$  can be obtained by

$$g_{n,m}^k(x) = m \binom{m-1}{k-1} \underbrace{\int_x^\infty \cdots \int_x^\infty}_{k-1} \underbrace{\int_0^x \cdots \int_0^x}_{m-k} g_\Lambda(x, \lambda_2, \dots, \lambda_m) d\lambda_2 \cdots d\lambda_m. \quad (3.6.7)$$

Notice that  $g_\Lambda(\lambda_1, \dots, \lambda_m)$  is composed of a sum of terms which have the following forms

$$\prod_{i=1}^m c_{1,i} e^{-c_{2,i} \lambda_i^{l_i}},$$

where  $l_i$  is some non-negative integer,  $c_{1,i}$  and  $c_{2,i}$  are some constant scalars. By applying the following identity

$$\int_x^\infty c_{1,i} e^{-c_{2,i} \lambda_i} \lambda_i^{l_i} d\lambda_i = \frac{c_{1,i} l_i!}{c_{2,i}^{l_i+1}} e^{-c_{2,i} x} \sum_{k=0}^{l_i} \frac{(c_{2,i} x)^k}{k!}, \quad (3.6.8)$$

it can be shown that the close-form expressions of (3.6.6) and (3.6.7) can be obtained for any MIMO system (with the use of symbolic computation software when  $m$  is large).

### 3.6.2 Capacity and Achievable Rate with Different Signaling Schemes

As shown in Chapter 2, the ergodic capacity of the correlated MIMO channels with CSIR only can be also given as

$$C_1 = \mathcal{E} \left[ \log_2 \left| \mathbf{I}_{N_r} + \frac{\Omega}{N_t} \mathbf{H} \mathbf{H}^\dagger \right| \right]. \quad (3.6.9)$$

Since we already obtained the marginal pdf of the unordered eigenvalues and all of them have the same expressions, (3.6.9) can be simplified as

$$C_1 = m \int_0^\infty \log_2 \left( 1 + \frac{\Omega}{N_t} x \right) g_{n,m}(x) dx. \quad (3.6.10)$$

When the CSI is available at both the transmitter and the receiver, (3.6.2) indicates that a MIMO fading channel can be decomposed into  $m$  parallel channels and these parallel channels are characterized by an eigenvalue matrix  $\Lambda$ . With an average transmit power constraint, the transmit power also should be dynamically allocated according to the instantaneous CSI. It can be shown that optimal power adaption in multiple eigen-beamforming scheme is the “water-filling” method with

$$Q_{i,i} = \begin{cases} \frac{1}{\lambda_0} - \frac{1}{\lambda_i}, & \lambda_i \geq \lambda_0 \\ 0, & \lambda_i < \lambda_0 \end{cases} \quad (3.6.11)$$

where  $\lambda_0$  is a unique cutoff value for all eigenvalues and it can be obtained by solving the following average power constraint equation

$$\int_{\lambda_0}^\infty \left( \frac{1}{\lambda_0} - \frac{1}{x} \right) g_{n,m}(x) dx = \frac{\Omega}{m}. \quad (3.6.12)$$

The capacity of the MIMO fading channel with both transmit and receive CSI can therefore be calculated as

$$C_2 = m \int_{\lambda_0}^{\infty} \log_2 \left( \frac{x}{\lambda_0} \right) g_{n,m}(x) dx. \quad (3.6.13)$$

A beamforming scheme maximizes the received SNR and its achievable rate approaches the capacity of a MIMO fading channel provided the SNR is low. However, the achievable rate of beamforming in highly correlated MIMO fading channels is still not clear. Therefore we also evaluate the achievable rate of beamforming in correlated MIMO fading channels. It turns out that the optimal power adaption scheme in beamforming case is still the “water-filling” method and the achievable rate in this case can be calculated by

$$C_3 = \int_{\lambda'_0}^{\infty} \log_2 \left( \frac{x}{\lambda'_0} \right) g_{n,m}^1(x) dx, \quad (3.6.14)$$

where  $\lambda'_0$  is again some cutoff value obtained by solving an average power constraint equation as follows

$$\int_{\lambda'_0}^{\infty} \left( \frac{1}{\lambda'_0} - \frac{1}{x} \right) g_{n,m}^1(x) dx = \Omega. \quad (3.6.15)$$

However, to achieve capacity of correlated MIMO systems  $C_2$  or the beamforming achievable rate  $C_3$  with water-filling method, an infinite number of codes is required in principle. Furthermore, achieving  $C_2$  also requires joint multiplexed coding/decoding among  $m$  parallel dependent eigen-channels. Therefore the water-filling scheme introduces high coding/decoding complexity. Another scheme to achieve the capacity of MIMO fading channels is using one CSI-independent code with separate CSI-dependent power control [27]. This scheme requires inter block coding and may require long code, especially when deep fading occurs. To reduce the coding/decoding complexity and avoid complicated power adaption, yet still approach the capacity  $C_2$ , we apply the TCI [25] to each un-ordered eigen-channel (multi-TCI). To calculate the achievable rate  $C_{2,e}$  by using multi-TCI, we realize that we should allocate the same power to each of the  $m$  eigen-channels and truncate all  $m$  eigen-channels in the same way due to the complete symmetry among the unordered eigen-values. It turns out that  $C_{2,e}$  can be found by maximizing the following integral over all possible cutoff values  $\mu_0$

$$C_{2,e} = \max_{\mu_0} m \left\{ \log_2 \left( 1 + \frac{\Omega}{m\alpha} \right) \int_{\mu_0}^{\infty} g_{n,m}(x) dx \right\}, \quad (3.6.16)$$

where  $a$  is defined as

$$a \triangleq \int_{\mu_0}^{\infty} \frac{1}{x} f_{n,m}(x) dx. \quad (3.6.17)$$

Similarly,  $C_{3,e}$ , which is the rate achieved by applying the TCI to the beamforming (BF-TCI), can be acquired by maximizing over all  $\mu'_0$ , so that

$$C_{3,e} = \max_{\mu'_0} \left\{ \log_2 \left( 1 + \frac{\Omega}{\int_{\mu'_0}^{\infty} \frac{1}{x} g_{n,m}^1(x) dx} \right) \int_{\mu'_0}^{\infty} g_{n,m}^1(x) dx \right\}.$$

Notice that to achieve  $C_{2,e}$  or  $C_{3,e}$ , only one code designed for an AWGN channel is needed since each eigen-channel becomes an AWGN channel after TCI. Also notice that BF-TCI requires only one pair of coder/decoder, but Multi-TCI requires  $m$  pairs of coder/decoders.

### 3.6.3 Examples and Discussion

In this section, we illustrate the capacities and the achievable rates of the aforementioned schemes in the  $(N_t = n, N_r = 2)$  and the  $(N_t = 3, N_r = 3)$  correlated MIMO systems. We apply an exponential decaying correlation model [42] in our calculations. Therefore the  $i, j$ -th entry of correlation matrix  $\mathbf{R}$  is  $r^{|i-j|}$  with  $0 \leq r \leq 1$ , where  $r$  is referred to as the exponential correlation parameter.

In Figure 3.11, we compare the capacities achieved by knowing the CSI at the transmitter with the capacities when the CSI is available only at the receiver in the highly correlated MIMO systems. It is shown that knowing CSI at the transmitter can provide considerable capacity gain in the highly correlated MIMO systems when the number of transmit antennas is larger than the number of receive antennas.

In Figures 3.12 and 3.13, we evaluate the effects of correlation on capacities and the achievable rates of the proposed schemes in  $(N_t = 4, N_r = 2)$  and  $(N_t = 3, N_r = 3)$  MIMO systems. First, we observe that, when the correlation is small (say,  $r \leq 0.3$ ), the effects of correlation on capacities are negligible. In the  $(N_t = 3, N_r = 3)$  MIMO system, we can also observe that the capacity achieved by knowing the CSI at the transmitter and the capacity of only knowing the CSI at the receiver decrease as the correlation increases. However, the larger the correlation, the more capacity gain can be obtained by knowing the CSI at the transmitter. Therefore in highly correlated MIMO systems, transmit CSI is more

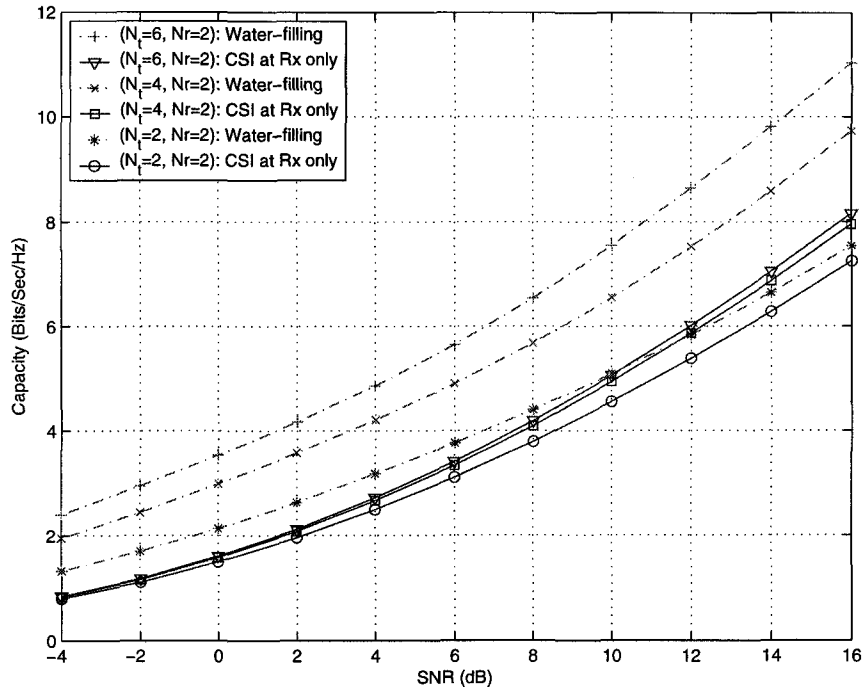


Figure 3.11: Capacities of  $(N_t = n, N_r = 2)$  highly correlated ( $r = 0.9$ ) MIMO fading channels at different SNR.

crucial than in uncorrelated MIMO fading channels. At last, it is interesting to notice that the achievable rate by using beamforming slightly increases as the correlation increases. When the correlation is high, the achievable rate by using beamforming approaches very closely to the capacity achieved by knowing the CSI at the transmitter.

In Figures 3.14 and 3.15, we depict the capacities and the achievable rates of the proposed schemes at different SNR in the  $(N_t = 3, N_r = 3)$  MIMO system. It is shown that the achievable rate by using multi-TCI scheme, which requires one code designed for an AWGN channel and three pairs of coder/decoders, approaches the capacity achieved by knowing the CSI at the transmitter. Although the achievable rate by using multi-TCI scheme outweighs the capacity of only knowing the CSI at the receiver in the very low SNR region when correlation is low, it outweighs the capacity of only knowing the CSI at the receiver in the relatively large SNR region when the correlation is high. In the highly correlated case, it is shown that the BF-TCI scheme, which requires one code designed for

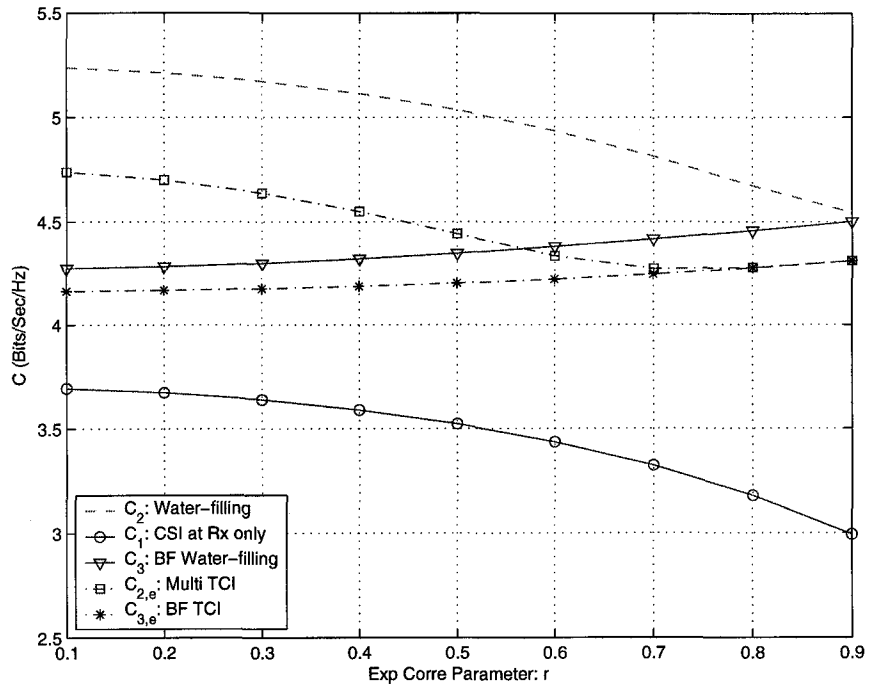


Figure 3.12: Effect of exponential correlation parameter on capacities and achievable rates of the  $(N_t = 4, N_r = 2)$  correlated MIMO fading channels at  $SNR = 5dB$ .

an AWGN channel and one pair of coder/decoder, achieves the same rate as the multi-TCI scheme in the considered SNR region.

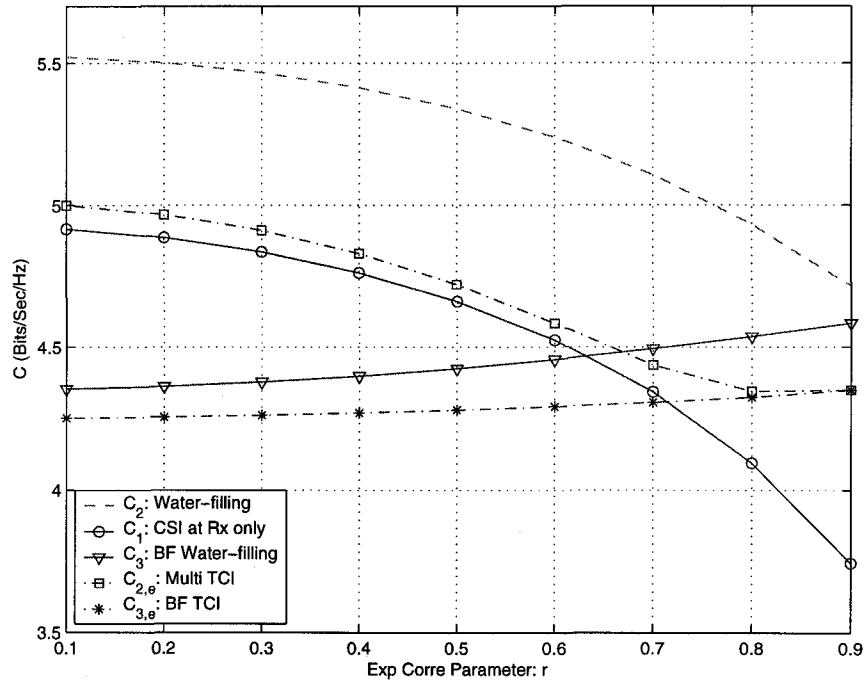


Figure 3.13: Effect of exponential correlation parameter on capacities and achievable rates of the  $(N_t = 3, N_r = 3)$  correlated MIMO fading channels at  $SNR = 5dB$ .

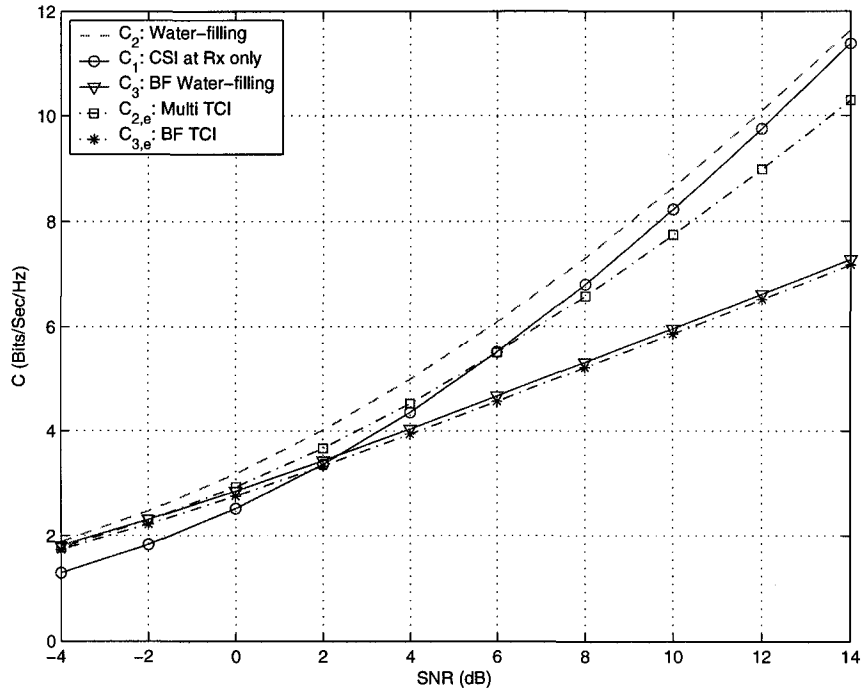


Figure 3.14: Capacities and achievable rates of the  $(N_t = 3, N_r = 3)$  slightly correlated ( $r = 0.1$ ) MIMO fading channels at different SNR.

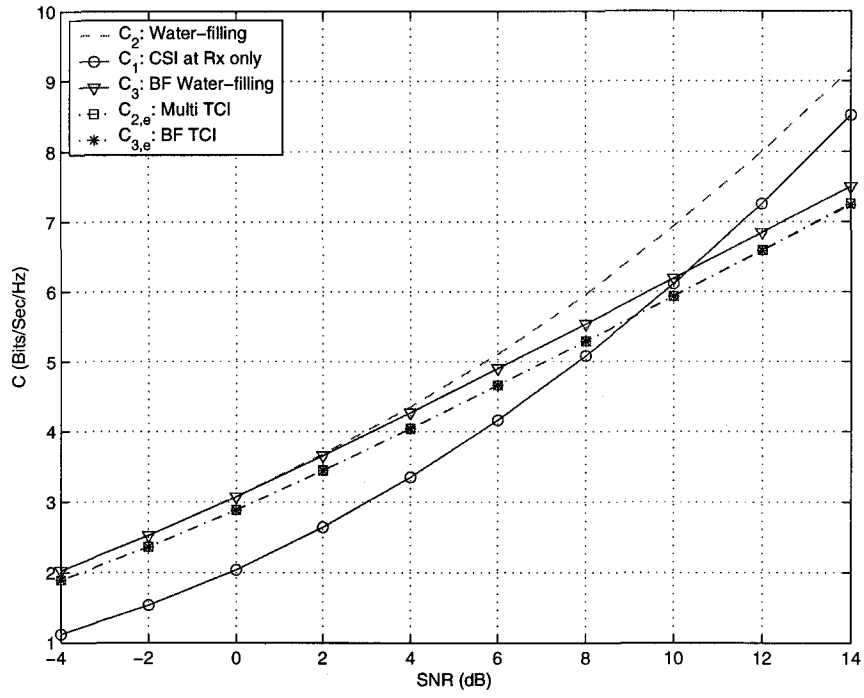


Figure 3.15: Capacities and achievable rates of the ( $N_t = 3, N_r = 3$ ) highly correlated ( $r = 0.9$ ) MIMO fading channels at different SNR.

## Chapter 4

# Blind Decoders of Space-time Block Codes in Downlink DS-CDMA Systems

### 4.1 Introduction

It has been shown that the performance of a wireless communication system can be greatly improved by applying multiple antennas and numerous efficient communication schemes have been proposed, such as beamforming in MIMO fading channels with CSIT and CSIR [32], space-time coding in MIMO fading channels with CSIR only [10][11], differential space-time coding in MIMO fading channels with NCSI [57] [56]. Unfortunately, most of these schemes are designed for a point-to-point communication system, i.e., a single user system. However, most practical communication systems are with multiple users.

Direct-sequence code-division multiple access (DS-CDMA) is a promising radio access technique for the third-generation mobile (3G) communication system due to its flexibility to support a variety of services. A major impediment to the performance of a DS-CDMA system is multiple-access interference (MAI), which is inherent to any nonorthogonal CDMA system. It has been demonstrated that multiuser detection techniques are powerful for MAI suppression in CDMA systems, especially in uplinks, where the base station has the knowledge of all users' spreading sequences [43]. However, in downlinks, each mobile station typically has only the knowledge of its own spreading sequence. Therefore suppression of MAI in the downlink is more challenging because it must

be done blindly. Since wireless Internet, video-on-demand and multimedia services are required in the next-generation wireless communication systems, the downlink performance is more important than the uplink and how to improve the downlink performance becomes a key problem.

Multiple antennas are typically equipped at the base station instead at the mobile station due to its limited size. For a system with large number of users, it is more realistic to assume that the CSI is only known at mobile stations. In this scenario, space-time coding seems a promising transmission technique to improve the downlink performance because it can provide diversity gain and coding gain without knowing the CSI at the transmitter. A variety of space-time codes have been proposed based on different design criteria some of them have already been adopted as industry standards, such as Alamouti code in IEEE 802.16. Among the existed space-time codes, space-time block codes can provide quite good performance with reasonable decoding complexity and therefore be more practical. Both space-time coding and multiuser detection can be applied to improve the performance of the downlinks of DS-SS systems. How to combine these two techniques to obtain higher performance becomes an interesting task.

There has been a line of work studying the combination of space-time coding and multiuser detection. The design of good space-time codes in multipath CDMA systems has been studied in [44][45]. It is shown that the multiuser coding problem decouples to multiple single user coding problem in the uplink, however, a true multiple user coding problem exists in the downlink. G.Khang and A.Naguib firstly combined the blind multiuser detection and decoding of space-time block code in DS-SS system in [46]. However, only a non-joint approach has been proposed. A linear blind multiuser receiver, referred to as the Capon receiver, for space-time block codes has been presented in [48]. However, the paper focused on joint decoding with blind channel estimation and only Alamouti's code was considered. Our works on this topic lie in two aspects: first, we propose a joint blind space-time decoders which is suitable for most existing space-time block codes; second, we study the blind non-coherent decoder for differential space-time block codes.

## 4.2 Blind Decoders of Linear Dispersion Codes

### 4.2.1 Linear Dispersion Codes

Linear Dispersion (LD) [47] code has been proposed as a high-rate space-time coding scheme that retains the decoding simplicity as of V-BLAST [4]. Unlike V-BLAST, which requires more antennas at the receiver than at the transmitter, LD codes can be applied with any configuration of transmit and receive antennas. Since LD codes are designed to maximize the mutual information between the transmit and receive signals, they generally outperforms V-BLAST and orthogonal designed space-time codes [11] in high SNR region. Besides the aforementioned coding/decoding advantages, LD codes subsume both VBLAST and orthogonal designed space-time block codes as special cases. Therefore LD codes can be taken to express the general structure of many existing space-time block codes, and decoding algorithms of LD codes will be suitable for many types of space-time block codes. Therefore we consider the application of LD codes in the downlink of a DS-CDMA system.

Let us briefly introduce the general structure of the LD codes. For a block-static wireless link with  $N_t$  transmit antennas, assume that the coherent time interval spans  $T$  symbols, an LD code is defined by a  $T \times N_t$  matrix  $\mathbf{C}$  that governs the transmission over  $N_t$  transmit antennas during the interval. Each entry of the codeword  $\mathbf{C}$  is linear combination of  $Q$  complex symbols ( $d_1, d_2, \dots, d_Q$ ) chosen from an arbitrary constellation of the  $Q$  data substreams. It can be seen that the rate of the corresponding LD code is  $R = \frac{Q}{T} \log r$  if  $d_q$  is chosen from a  $r$ -PSK or a  $r$ -QAM constellation. With the definition of  $d_q = \alpha_q + j\beta_q$ , where  $\alpha_q$  and  $\beta_q$  are real scalars, the general structure of linear dispersion codeword  $\mathbf{C}$  is

$$\mathbf{C} = \sum_{q=1}^Q (\alpha_q \mathbf{A}_q + j\beta_q \mathbf{B}_q). \quad (4.2.1)$$

where  $\{\mathbf{A}_q, \mathbf{B}_q\}$  are referred to as the dispersion matrices and they are chosen such that the mutual information between the transmitted signals  $\{\alpha_q, \beta_q\}$  and the received signals is maximized. Obviously the design of LD codes depends crucially on the choices of the dispersion matrices. By selecting dispersion matrices, both V-BLAST and orthogonal designed space-time block codes can be written in the forms of LD codes. For example,

Alamouti code corresponds to an  $N_t = Q = T = 2$  LD code with

$$\mathbf{A}_1 = \begin{bmatrix} 1 & 0 \\ 0 & 1 \end{bmatrix}, \quad \mathbf{A}_2 = \begin{bmatrix} 0 & 1 \\ -1 & 0 \end{bmatrix}, \quad \mathbf{B}_1 = \begin{bmatrix} 1 & 0 \\ 0 & -1 \end{bmatrix}, \quad \mathbf{B}_2 = \begin{bmatrix} 0 & 1 \\ 1 & 0 \end{bmatrix}. \quad (4.2.2)$$

## 4.2.2 System Model

Consider a downlink transmission of a  $K$ -user synchronous DS-SS-CDMA system equipped with  $N_t$  transmit antennas at the base station and  $N_r$  receive antennas at each mobile station. We assume that the channels are quasi-static frequency flat Rayleigh fading and the CSI is known perfectly at the mobile station. Denote the LD codeword transmitted to the  $k$ -th user as  $\mathbf{C}_k$ . The  $(t, n)$ -th entry in  $\mathbf{C}_k$  is transmitted in the  $t$ -th symbol interval on the  $n$ -th transmit antenna and it can be written as

$$C_k(t, n) = \sum_{q=1}^Q (\alpha_{k,q} A_{k,q}(t, n) + j\beta_{k,q} B_{k,q}(t, n)). \quad (4.2.3)$$

We suppose that all  $N_t$  transmit antennas of a specific user are assigned the same signature waveform. Then  $\mathbf{s}_k$ , the signature waveform applied to the  $k$ -th user, is of form

$$\mathbf{s}_k = \frac{1}{\sqrt{P}} \begin{bmatrix} s_k(1) & s_k(2) & \cdots & s_k(P) \end{bmatrix}^T, \quad (4.2.4)$$

where  $P$  is the spreading gain and  $s_k(i)$  for  $i = 1, 2, \dots, P$  is of  $\pm 1$ . Without loss of generality, let us focus on the decoding of user 1. Denote the complex path gain between transmit antenna  $n$  and receive antenna  $m$  of user 1 as  $h_{1,m,n}$ , which is modelled as a complex circular Gaussian random variable with zero-mean and unit variance. Then the received signal of  $m$ -th receive antenna at the  $t$ -th symbol interval, sampled at the chip-rate, is given by

$$\begin{aligned} \mathbf{r}_m(t) &= \sum_{k=1}^K \sum_{n=1}^{N_t} h_{1,m,n}(t) \mathbf{s}_k(t) \mathbf{C}_k(t, n) + \mathbf{v}_m(t) \\ &= \sum_{k=1}^K \sum_{n=1}^{N_t} \sum_{q=1}^Q h_{1,m,n}(t) \mathbf{s}_k(t) (\alpha_{k,q} A_{k,q}(t, n) + j\beta_{k,q} B_{k,q}(t, n)) + \mathbf{v}_m(t) \end{aligned} \quad (4.2.5)$$

where  $\mathbf{r}_m(t)$  is the  $P$ -dimensional vector of chip-samples during one symbol interval and  $\mathbf{v}_m(t)$  is a  $P$ -dimensional noise vector with i.i.d entries modelled as complex Gaussian

random variable with zero-mean and variance  $\sigma^2$ . To design the joint decoder, we define

$$\mathbf{s}_{k,m,q}^\alpha(t) = \sum_{n=1}^{N_t} h_{1,m,n}(t) \mathbf{s}_k(t) A_{k,q}(t, n), \quad (4.2.6)$$

$$\mathbf{s}_{k,m,q}^\beta(t) = \sum_{n=1}^{N_t} j h_{1,m,n}(t) \mathbf{s}_k(t) B_{k,q}(t, n), \quad (4.2.7)$$

where  $\mathbf{s}_{k,m,q}^\alpha(t)$ ,  $\mathbf{s}_{k,m,q}^\beta(t)$  are referred to as *LD-waveforms*. (4.2.5) can be rewritten as

$$\mathbf{r}_m(t) = \sum_{k=1}^K \sum_{q=1}^Q (\alpha_{k,q} \mathbf{s}_{k,m,q}^\alpha(t) + \beta_{k,q} \mathbf{s}_{k,m,q}^\beta(t)) + \mathbf{v}_m(t). \quad (4.2.8)$$

Keep in mind that  $\alpha_{k,q}$  and  $\beta_{k,q}$  are the information data sent to user  $k$ . Therefore the following vector is required to be decoded at  $k$ -th mobile receiver

$$\boldsymbol{\theta}_k = \left[ \alpha_{k,1} \ \cdots \ \alpha_{k,Q}, \beta_{k,1} \ \cdots \ \beta_{k,Q} \right]^T. \quad (4.2.9)$$

It can be seen that there are  $2Q$  *LD-waveforms* for each user. We stack the  $2Q$  *LD-waveforms* as follows

$$\begin{aligned} \mathbf{S}_{k,m}^\alpha(t) &= \begin{bmatrix} \mathbf{s}_{k,m,1}^\alpha(t) & \mathbf{s}_{k,m,2}^\alpha(t) & \cdots & \mathbf{s}_{k,m,Q}^\alpha(t) \end{bmatrix}, \\ \mathbf{S}_{k,m}^\beta(t) &= \begin{bmatrix} \mathbf{s}_{k,m,1}^\beta(t) & \mathbf{s}_{k,m,2}^\beta(t) & \cdots & \mathbf{s}_{k,m,Q}^\beta(t) \end{bmatrix}, \\ \mathbf{S}_{k,m}(t) &= \begin{bmatrix} \Re \left( \begin{bmatrix} \mathbf{S}_{k,m}^\alpha(t) & \mathbf{S}_{k,m}^\beta(t) \end{bmatrix} \right) \\ \Im \left( \begin{bmatrix} \mathbf{S}_{k,m}^\alpha(t) & \mathbf{S}_{k,m}^\beta(t) \end{bmatrix} \right) \end{bmatrix}. \end{aligned}$$

Given the following definitions

$$\begin{aligned} \mathbf{r}_m^V(t) &= \begin{bmatrix} \Re(\mathbf{r}_m(t)) \\ \Im(\mathbf{r}_m(t)) \end{bmatrix}, \quad \mathbf{v}_m^V(t) = \begin{bmatrix} \Re(\mathbf{v}_m(t)) \\ \Im(\mathbf{v}_m(t)) \end{bmatrix}, \\ \boldsymbol{\theta} &= \left[ \boldsymbol{\theta}_1^T \ \boldsymbol{\theta}_2^T \ \cdots \ \boldsymbol{\theta}_K^T \right]^T, \end{aligned}$$

the received signal of  $m$ -th receive antenna at the  $t$ -th symbol for the first user can be rewritten as

$$\mathbf{r}_m^V(t) = \left[ \mathbf{S}_{1,m}(t) \ \tilde{\mathbf{S}}_m(t) \right] \boldsymbol{\theta} + \mathbf{v}_m^V(t), \quad (4.2.10)$$

where  $\tilde{\mathbf{S}}_m(t)$  is given by

$$\tilde{\mathbf{S}}_m(t) = \begin{bmatrix} \mathbf{S}_{2,m}(t) & \mathbf{S}_{3,m}(t) & \cdots & \mathbf{S}_{K,m}(t) \end{bmatrix}.$$

Since there are  $N_r$  receive antennas at each mobile station and each LD codeword spans  $T$  symbol intervals, decoding of LD code requires us to stack the received signals from all the receive antennas and  $T$  symbol intervals. The overall observations of user 1 for the whole duration of  $l$ -th codeword can be formed as

$$\underbrace{\begin{bmatrix} \mathbf{r}_1^V(1) \\ \vdots \\ \mathbf{r}_{N_r}^V(1) \\ \vdots \\ \mathbf{r}_1^V(T) \\ \vdots \\ \mathbf{r}_{N_r}^V(T) \end{bmatrix}}_{\triangleq \mathbf{r}^{(l)}} = \underbrace{\begin{bmatrix} \mathbf{S}_{1,1}(1) & \tilde{\mathbf{S}}_1(1) \\ \vdots & \vdots \\ \mathbf{S}_{1,N_r}(1) & \tilde{\mathbf{S}}_{N_r}(1) \\ \vdots & \vdots \\ \vdots & \vdots \\ \mathbf{S}_{1,1}(T) & \tilde{\mathbf{S}}_1(T) \\ \vdots & \vdots \\ \mathbf{S}_{1,N_r}(T) & \tilde{\mathbf{S}}_{N_r}(T) \end{bmatrix}}_{\triangleq \begin{bmatrix} \mathbf{S}_1 & \tilde{\mathbf{S}} \end{bmatrix}} \boldsymbol{\theta} + \underbrace{\begin{bmatrix} \mathbf{v}_1^V(1) \\ \vdots \\ \mathbf{v}_{N_r}^V(1) \\ \vdots \\ \vdots \\ \mathbf{v}_1^V(T) \\ \vdots \\ \mathbf{v}_{N_r}^V(T) \end{bmatrix}}_{\triangleq \mathbf{v}} \quad (4.2.11)$$

For convenience, we ignore the index  $l$  when there is no confusion and rewrite (4.2.11) as

$$\mathbf{r} = \mathbf{S}_1 \boldsymbol{\theta}_1 + \tilde{\mathbf{S}} \tilde{\boldsymbol{\theta}} + \mathbf{v} = \mathbf{S} \boldsymbol{\theta} + \mathbf{v}, \quad (4.2.12)$$

where we define

$$\mathbf{S} \triangleq \begin{bmatrix} \mathbf{S}_1 & \tilde{\mathbf{S}} \end{bmatrix}, \quad \boldsymbol{\theta} \triangleq \begin{bmatrix} \boldsymbol{\theta}_1 & \tilde{\boldsymbol{\theta}} \end{bmatrix}. \quad (4.2.13)$$

### 4.2.3 Direct Subspace-based Blind Decoder

Notice that  $\mathbf{S}_1$  is a  $2PN_r T \times 2Q$  matrix and  $\tilde{\mathbf{S}}$  is a  $2PN_r T \times 2Q(K-1)$  matrix. Under the assumption that the receiver of user 1 knows the CSI of its own channel and the original signature waveform of itself, but nothing about other users, only the matrix  $\mathbf{S}_1$  is known at the receiver of user 1. Regard each column of matrices  $\mathbf{S}_1$  and  $\tilde{\mathbf{S}}$  as one long LD waveform, therefore the number of known long LD-waveforms is  $2Q$  and the

number of unknown long LD-waveforms is  $2Q(K - 1)$ . Denote  $\theta_{1,i}$  as the  $i$ -th entry of  $\theta_1$ . To decode  $\theta_{1,i}$ , we need to suppress both the interference from other symbols of user 1 and the interference from other users. This is similar to a group-blind multiuser detection problem considered in [49] which requires to suppress the interference from the known users based on the spreading sequences of these users and to suppress the interference from other unknown users using subspace-based blind methods. Therefore we develop the joint decoder based on the group-blind detection [49].

We consider a linear zero-forcing detector given by optimizing the following problem

$$\mathbf{w}_i = \arg \min_{\mathbf{w}_i \in \text{range}(\mathbf{S})} \|\mathbf{w}_i^T \mathbf{S}\|^2 \quad \text{s.t.} \quad \mathbf{w}_i^T \mathbf{S}_1 = \mathbf{1}_i^T, \quad (4.2.14)$$

where  $\mathbf{1}_i$  is a  $2Q$  dimensional column vector with all-zero entries except for the  $i$ -th entry. Using the method of Lagrange multiplier to solve the constrained optimization problem (4.2.14), we obtain

$$\begin{aligned} \mathbf{w}_i &= \arg \min_{\mathbf{w}_i \in \text{range}(\mathbf{S})} \mathbf{w}_i^T \mathbf{S} \mathbf{S}^T \mathbf{w}_i + \boldsymbol{\lambda}^T (\mathbf{w}_i^T \mathbf{S}_1 - \mathbf{1}_i^T) \\ &= (\mathbf{S} \mathbf{S}^T)^\dagger \mathbf{S}_1 \boldsymbol{\lambda}. \end{aligned} \quad (4.2.15)$$

Substituting (4.2.15) into the constraint  $\mathbf{w}_i^T \mathbf{S}_1 = \mathbf{1}_i^T$ , we have

$$\boldsymbol{\lambda} = [\mathbf{S}_1^T (\mathbf{S} \mathbf{S}^T)^\dagger \mathbf{S}_1]^{-1} \mathbf{1}_i. \quad (4.2.16)$$

There the solution for linear zero-forcing detector  $\mathbf{w}_i$  has the form of

$$\mathbf{w}_i = (\mathbf{S} \mathbf{S}^T)^\dagger \mathbf{S}_1 \boldsymbol{\lambda} [\mathbf{S}_1^T (\mathbf{S} \mathbf{S}^T)^\dagger \mathbf{S}_1]^{-1} \mathbf{1}_i. \quad (4.2.17)$$

It should be noticed that above detector can not be applied because  $\mathbf{S}$  is not known at the receiver of user 1 due to unavailability of  $\tilde{\mathbf{S}}$ . However, the subspace spanned by  $\mathbf{S}$  can be estimated at the receiver of user 1 blindly. Suppose that LD codes are selected from QPSK modulation, the subspace parameters are obtained from an eigenvalue decomposition of the correlation matrix  $\mathbf{R}$

$$\begin{aligned} \mathbf{R} &= \mathbf{E} [\mathbf{r} \mathbf{r}^T] = \mathbf{S} \mathbf{S}^T + \sigma^2 \mathbf{I}_{2QK} \\ &= \mathbf{U}_s \boldsymbol{\Lambda}_s \mathbf{U}_s^T + \sigma^2 \mathbf{U}_v \mathbf{U}_v^T. \end{aligned} \quad (4.2.18)$$

where  $\Lambda_s$  is a diagonal matrix of the  $2QK$  eigenvalues larger than  $\sigma^2$ , and  $U_s$  and  $U_v$  are matrices with columns of the corresponding eigenvectors. Therefore  $(SS^T)^\dagger$  can be replaced by

$$(SS^T)^+ = U_s(\Lambda_s - \sigma^2\mathbf{I})^{-1}U_s^T. \quad (4.2.19)$$

Substituting (4.2.19) into (4.2.17), the subspace-base linear-forcing detector is obtained as

$$\mathbf{w}_i = U_s(\Lambda_s - \sigma^2\mathbf{I})^{-1}U_s^T\mathbf{S}_1 [\mathbf{S}_1^T U_s(\Lambda_s - \sigma^2\mathbf{I})^{-1}U_s^T\mathbf{S}_1]^{-1} \mathbf{1}_i. \quad (4.2.20)$$

Notice that the detector can be implemented blindly by replacing subspace parameters with their estimates. Say,  $\hat{\mathbf{R}}$ , which is the estimate of  $\mathbf{R}$ , is given by

$$\hat{\mathbf{R}} = \frac{1}{L} \sum_{l=1}^L \{\mathbf{r}(l)\mathbf{r}(l)^T\}. \quad (4.2.21)$$

where we suppose the channel keeps unchange for  $L$  LD codewords. And the estimated subspace parameters can be obtained by decomposing  $\hat{\mathbf{R}}$ . Applying  $\mathbf{w}_i$  in (4.2.17), we can define the direct subspace blind decoder by

$$\hat{\theta}_{1,i} = \arg \min_{\theta_{1,i}} (\theta_{1,i} - \mathbf{w}_i^T \mathbf{r})^2. \quad (4.2.22)$$

#### 4.2.4 Subspace-based Blind Sphere Decoder

Let us consider decoding of a whole LD codeword. It can be easily shown that the zero-forcing detector for one whole codeword  $\theta_1$  has the form of

$$\mathbf{W} = U_s(\Lambda_s - \sigma^2\mathbf{I})^{-1}U_s^T\mathbf{S}_1 [\mathbf{S}_1^T U_s(\Lambda_s - \sigma^2\mathbf{I})^{-1}U_s^T\mathbf{S}_1]^{-1}.$$

Apply the subspace-based blind detector  $\mathbf{W}$  to  $\mathbf{r}$ , we obtain

$$\mathbf{y}_z = \mathbf{W}^T \mathbf{r} = \theta_1 + \mathbf{W}^T \mathbf{v}, \quad (4.2.23)$$

where  $\mathbf{W}^T \mathbf{v}$  is gaussian noise with zero mean and covariance matrix  $\sigma^2(\mathbf{W}^T \mathbf{W})$ . Since typically  $\sigma^2(\mathbf{W}^T \mathbf{W})$  is not a diagonal matrix, decoupled decoding as direct subspace blind decoder in (4.2.22) is not optimum. However, for LD codes with orthogonal structure, this direct subspace blind decoder is optimum because  $\sigma^2(\mathbf{W}^T \mathbf{W})$  is a diagonal matrix.

But for LD codes which do not have orthogonal structure, the optimal decoder is given by the maximum likelihood solution. Whitening the noise with a matrix defined  $\mathbf{G}_z = (\sigma^2 \mathbf{W}^T \mathbf{W})^{-\frac{1}{2}}$ , we obtain

$$\mathbf{y} = \mathbf{G}_z \mathbf{y}_z = \mathbf{G}_z \boldsymbol{\theta}_1 + \mathbf{G}_z \mathbf{W}^T \mathbf{v}, \quad (4.2.24)$$

where  $\mathbf{G}_z \mathbf{W}^T \mathbf{v}$  is zero-mean Gaussian noise with covariance matrix identity. The maximum likelihood solution is given by solving the following integer least-square problem

$$\hat{\boldsymbol{\theta}}_1 = \arg \min_{\boldsymbol{\theta}_1} \|\mathbf{y} - \mathbf{G}_z \boldsymbol{\theta}_1\|^2. \quad (4.2.25)$$

It is well-known that the problem in (4.2.25) is NP hard for general  $\mathbf{G}_z$ . For LD codes with large size, the complexity of the problem in (4.2.25) can be formidable. Therefore we feed the output of the subspace blind detector to a sphere decoder in order to approach the maximum likelihood solution with reasonable complexity.

The above integer least-square problem has a simple geometric interpretation. It can be regarded that  $\boldsymbol{\theta}_1$  spans a  $2Q$  dimensional *rectangle* lattice due to its discrete uniform entries. For any given matrix  $\mathbf{G}_z$ ,  $\mathbf{G}_z \boldsymbol{\theta}_1$  stands for a *skewed* lattice. Therefore the above integer least-square problem is to find a closest lattice point for a given vector  $\mathbf{y}$  in the *skewed* lattice  $\mathbf{G}_z \boldsymbol{\theta}_1$ . Sphere decoder reduces the computations by restricting its computation to the points which are found inside a sphere of radius  $\varepsilon$  centered at the received point instead of the whole lattice. Obviously the choice of  $\varepsilon$  is vital to sphere decoding because too larger radius brings exponentially increased complexity and too small radius fails the decoding. In fact, it is shown that the choice of  $\varepsilon$  to cover given number of points in a given lattice is still a NP hard problem [50]. Sphere decoder does not solve the problem how to wisely choose  $\varepsilon$ . However, sphere decoder does present an efficient algorithm to determine which lattice points are inside the given sphere of radius  $\varepsilon$ . It is demonstrated in [51] that the expected complexity of sphere decoding is typically polynomial, in fact often roughly cubic, in most cases. In this dissertation, we apply the sphere decoding algorithm proposed in [52].

## 4.2.5 Decimation-combining Processing

The major computational effort of the subspace-method blind decoders discussed so far involves estimating the autocorrelation matrix  $\mathbf{R}$ , computing the eigen-decomposition of  $\mathbf{R}$ , and sphere decoding of  $\theta_1$ . Since  $\theta_1$  has much lower dimension than  $\mathbf{R}$ , the complexity of sphere decoding of  $\theta_1$  is minor compared to the complexity of the other two. Specifically, estimating the autocorrelation matrix  $\mathbf{R}$  and computing the eigen-decomposition of  $\mathbf{R}$  have computational complexity of  $O(LP^2N_r^2T^2)$  and  $O(P^3N_r^3T^3)$  respectively, where  $L$  is the number of LD codewords used to estimate the autocorrelation matrix. To decrease the complexity of subspace-based blind sphere decoder, we propose the following decimation-combining processing.

By down sampling the received signal sample vector  $\mathbf{r}$  by a factor  $J$ , where we suppose  $J$  divides  $2PMT$ , and using the  $J$  interleaved signals, we can reduce the problem to  $J$  parallel calculations in  $(2PN_rT/J)$ -dimensional spaces instead of the original  $(2PN_rT)$ -dimensional space. Let the  $j^{\text{th}}$  decimated received signal sample vector be defined by

$$\mathbf{r}^j = \left[ \mathbf{r}[j] \quad \mathbf{r}[J+j] \quad \cdots \quad \mathbf{r}[2PN_rT - J + j] \right]^T, \quad (4.2.26)$$

where  $\mathbf{r}[j]$  is the  $j^{\text{th}}$  entry of  $\mathbf{r}$ . For each  $\mathbf{r}^j$ ,  $j = 1, 2, \dots, J$ , we find a blind decoder  $\mathbf{W}^j$  (notice that the problem is completely equivalent to the problem considered before, just with a dimension  $2PN_rT/J$ ). After applying the decimated detector to its corresponding decimated received signal sample vector, the  $J$  outputs are then combined to yield the decision statistics

$$\mathbf{y}_z = \frac{1}{J} \sum_{j=1}^J \mathbf{W}^{jT} \mathbf{r}^j = \theta_1 + \frac{1}{J} \sum_{j=1}^J \mathbf{W}^{jT} \mathbf{v}^j, \quad (4.2.27)$$

where  $\mathbf{v}^j$  is defined as

$$\mathbf{v}^j = \left[ \mathbf{v}[j] \quad \mathbf{v}[J+j] \quad \cdots \quad \mathbf{v}[2PN_rT - J + j] \right]^T. \quad (4.2.28)$$

It is easily to see that  $\frac{1}{J} \sum_{j=1}^J \mathbf{W}_z^{jT} \mathbf{v}^j$  is still gaussian noise with zero mean and covariance matrix  $\frac{\sigma^2}{J^2} \sum_{j=1}^J \mathbf{W}^{jT} \mathbf{W}^j$ . Therefore a sphere decoder can be applied for non-orthogonal LD codes in the same way as discussed above. It is obvious that the complexity of estimating and eigen-decomposing the autocorrelation matrix  $\mathbf{R}$  are decreased to

$O(LP^2M^2T^2/J)$  and  $O(P^3M^3T^3/J^2)$  respectively after the decimation-combining processing.

#### 4.2.6 Simulation Examples

In this section, we present simulation results to demonstrate the performance of the proposed subspace-based blind decoders for different kinds of LD codes. In our simulations, QPSK constellation is applied and the original signature waveforms are generated as random sequences with spreading gain  $P = 32$ .

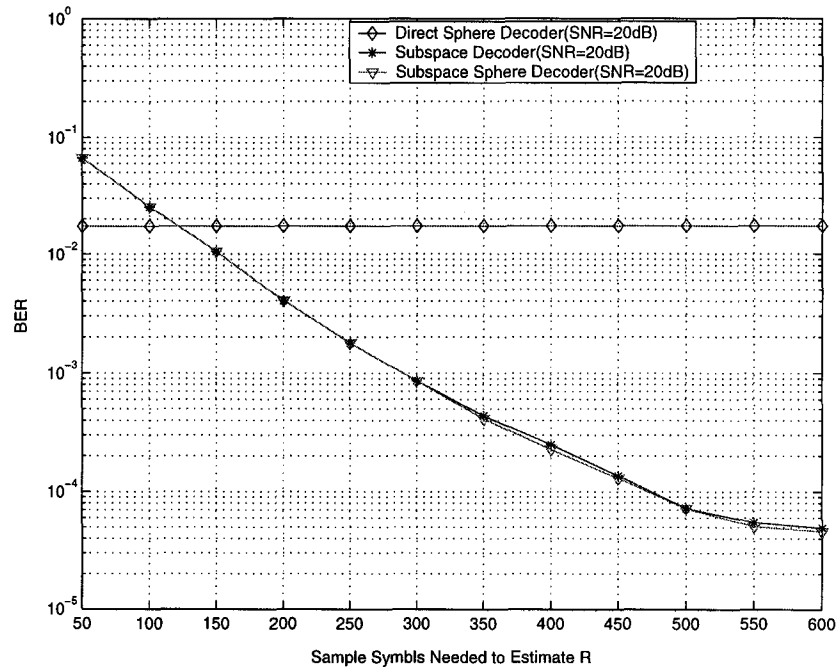


Figure 4.1: Convergence speed of subspace-method blind decoders for  $N_t = 2, N_r = 1, T = Q = 2$  in  $K = 8$  users DS-CDMA system.

As shown in (4.2.2), Alamouti code can be regarded as a  $T = N_t = Q = 2$  LD code. Since it achieves full channel capacity of the  $(N_t = 2, N_r = 1)$  system and can be simply decoded, it is very likely to be applied in the future wireless communication system. Fig. 4.1 presents the convergence speed of the subspace-based blind decoders at  $SNR = 20dB$  for Alamouti code. It is worth mentioning that after a frame length of

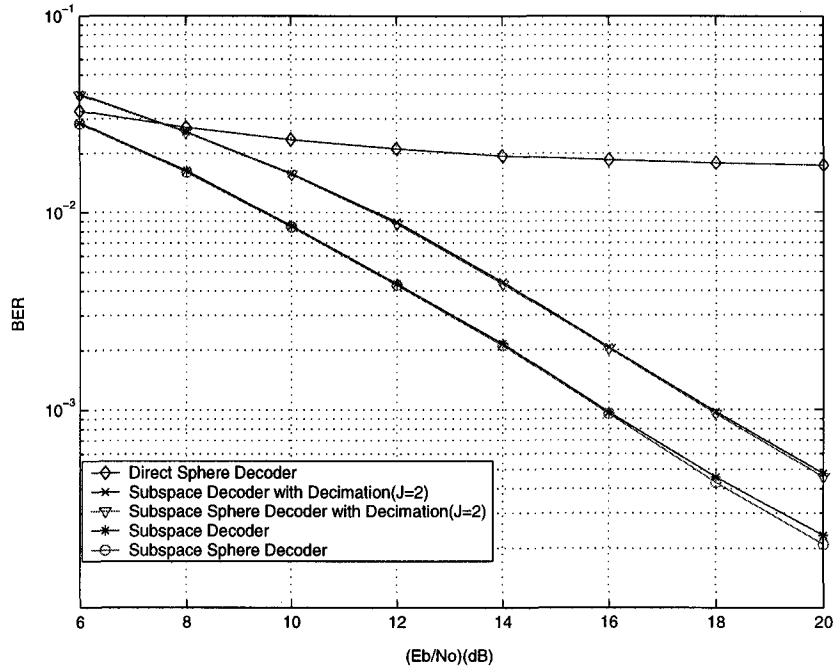


Figure 4.2: Performance of different decoders for LD code with  $N_t = 2, N_r = 1, T = Q = 2$  in  $K = 8$  users DS-CDMA system.

120 blocks the subspace-based decoders have better performance than the direct sphere decoder, which uses conventional matched filter to suppress the interferences. Because of the orthogonality of Alamouti code, as expected there is no difference between the direct subspace-based blind decoder and subspace-based blind sphere decoder. It can be also observed that the subspace method requires about  $L = 550$  codewords to approach its best performance.

Fig. 4.2 shows the performance of proposed subspace-based blind decoders by using  $L = 400$  codewords to estimate the autocorrelation matrix  $R$ . A bit error rate (BER) of  $2 \times 10^{-4}$  is attained at  $SNR = 20\text{dB}$  for the subspace-method decoders but only  $2 \times 10^{-2}$  for the direct sphere decoder. It can be seen that the decimation-combining processing with decimation factor ( $J = 2$ ) only degrades the BER performance in the 2dB range.

VBLAST codes [4] are designed to exploit the multiplexing gain of MIMO systems. Therefore we select a VBLAST code as an example of non-orthogonal LD code. In [47], it is shown that VBLAST code is also a special case of LD codes. For a ( $N_t = 2, N_r =$

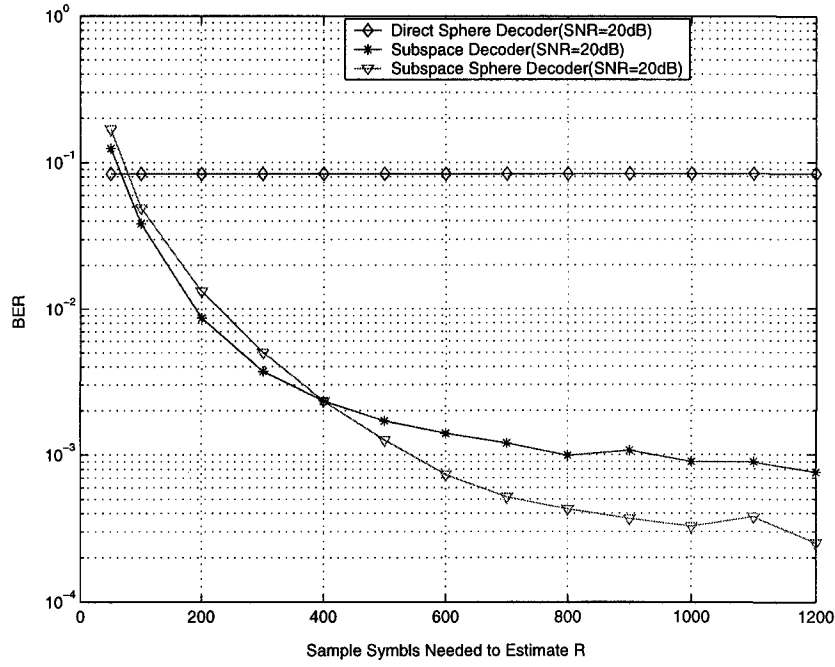


Figure 4.3: Convergence speed of subspace-method blind Decoders for  $N_t = 2, N_r = 2, T = 2, Q = 4$  LD code in K=4 users DS-CDMA system.

2) system, the dispersion matrices of a  $(T = 2, Q = 4)$  LD code can be constructed with the following transformations of a VBLAST code

$$\begin{aligned} \mathbf{A}_1 &= \frac{\mathbf{A}'_1 + \mathbf{A}'_4}{\sqrt{2}}, & \mathbf{A}_2 &= \frac{\mathbf{A}'_2 + \mathbf{A}'_3}{\sqrt{2}}, \\ \mathbf{A}_3 &= \frac{\mathbf{A}'_1 - \mathbf{A}'_4}{\sqrt{2}}, & \mathbf{A}_4 &= \frac{\mathbf{A}'_2 - \mathbf{A}'_3}{\sqrt{2}}, \end{aligned}$$

where  $\mathbf{A}'_q$  for  $q = 1, 2, 3, 4$  is the VBLAST codeword. The dispersion matrices  $\mathbf{B}_q$  can be constructed by similar transformations. Fig. 4.3 and Fig. 4.4 present the convergence speed and BER performance for this  $N_t = 2, T = 2, Q = 4$  non-orthogonal LD code respectively. It is shown that VBLAST code requires more LD codes to approach its best performance because in this case there are more channels and the code rate is high. It is also demonstrated that the subspace sphere decoder has worse performance than the direct subspace decoder for a small number of LD codewords (here less than 400), but has better performance for a large number of codewords. The reason is that when  $\mathbf{R}$  is

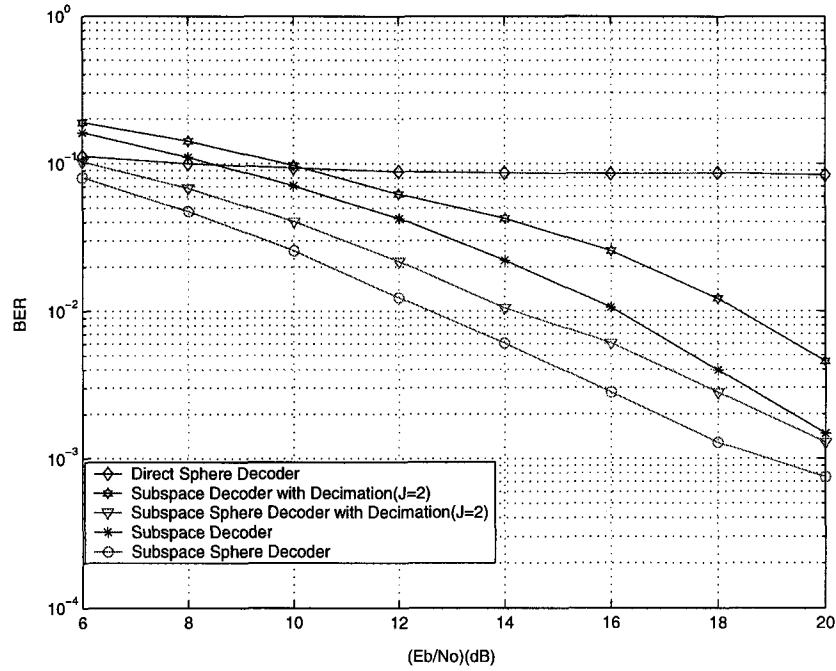


Figure 4.4: Performance of different decoders for  $N_t = 2, N_r = 2, T = 2, Q = 4$  LD code in K=4 users DS-CDMA system.

inexactly estimated, the subspace detector is far from being decorrelating among symbols of the same user, an assumption that was used in applying the sphere decoder. In Fig. 4.4,  $L = 600$  symbols are used to estimate the autocorrelation matrix  $\mathbf{R}$ . It is shown that performance of the subspace sphere decoder is more than 2dB better than the direct subspace decoder and even the performance of subspace sphere decoder with decimation-combining processing(J=2) is better than the direct subspace decoder.

### 4.3 Non-coherent Blind Decoders for Differential STBC

We have proposed the subspace-based blind decoders that can exploit the diversity of MIMO systems and suppress the MAI blindly. However, the proposed decoders are based on knowing the CSI at the receiver. The CSI of MIMO channels can only be known to the receiver by channel estimation through training-based methods or blind methods.

Although lots of works have been done in this area, it is still a very tough task to guarantee the accuracy of MIMO channel estimation without exhausting computation, especially when the number of antennas is large. And in some situations, we may want to forego channel estimation in order to reduce the cost and complexity of the handset, or perhaps fading channels change so rapidly that channel estimation is difficult or requires too many training symbols. Therefore the differential space-time block codes have been proposed to achieve the diversity and coding gains when neither the transmitter nor the receiver has the channel state information [55]-[58].

Most current papers on differential space-time codes are constricted in point-to-point communication. [59] discussed the application of differential space-time block codes in DS-CDMA system under the assumption that the spreading sequences of the different users are absolute orthogonal. The assumption is very unrealistic and with this assumption the multiple user system indeed becomes a point-to-point communication system. In this part, we consider the non-coherent decoding of differential space-time codes in downlink DS-CDMA system with random sgenerated spreading sequences because the downlink transmission is more challenging than the uplink transmission.

### 4.3.1 System Model

We consider a  $K$ -user synchronous DS-CDMA system with  $N_t$  transmit antennas at the base station and  $N_r$  receive antennas at each mobile station. The channel between each antenna pair is assumed to be quasi-static flat Rayleigh fading so that the channel coefficients remain constant over a frame of  $(LT)$  length and vary from one frame to another independently. The  $l$ -th differential space-time codeword of the  $k$ -th user is denoted as an  $N_t \times T$  matrix  $\mathbf{C}_k(l)$

$$\mathbf{C}_k(l) = \begin{bmatrix} \mathbf{c}_k(lT + 1) & \cdots & \mathbf{c}_k(lT + T) \end{bmatrix},$$

where  $\mathbf{c}_k(lT + t)$  is an  $N$ -dimensional column vector which denotes the  $t$ -th column in  $\mathbf{C}_k(l)$  for  $t = 1, 2, \dots, T$ . For downlink transmission, the entries of  $\mathbf{c}_k(lT + t)$  are transmitted simultaneously from the  $N$  transmit antennas at time slot  $lT + t$ . Suppose we always focus on the detection for the  $q$ -th user, the received signal of the  $m$ -th receive antenna at

the  $q$ -th user, sampled at the time slot  $lT + t$ , is

$$\mathbf{y}_{qm}(lT + t) = \sum_{k=1}^K \sum_{n=1}^{N_t} s_k h_{qmn} c_{kn}(lT + t) + \mathbf{v}_{qm}(lT + t), \quad (4.3.1)$$

where  $s_k$  is the spreading code of the  $k$ -th user with spreading gain  $P$ ;  $\mathbf{v}_{qm}(lT + t)$  is the noise vector whose entries are independent samples of a zero-mean complex Gaussian random variable with variance  $\sigma_{qm}^2/2$  per real dimension;  $h_{qmn}$  is channel coefficient between  $n$ -th transmit antenna at the base station and the  $m$ -th receive antenna at the user  $q$ , and  $h_{qmn}$  is modeled as samples of independent complex Gaussian random variable with variance 0.5 per real dimension. Denote  $\tau \triangleq lT + t$  and give the following definitions

$$\mathbf{S} \triangleq \begin{bmatrix} \mathbf{s}_1 & \mathbf{s}_2 & \cdots & \mathbf{s}_K \end{bmatrix}; \mathbf{c}(\tau) \triangleq \begin{bmatrix} c_1(\tau) \\ c_2(\tau) \\ \vdots \\ c_K(\tau) \end{bmatrix};$$

$$\mathbf{h}_{qm} \triangleq \begin{bmatrix} h_{qm1} & h_{qm2} & \cdots & h_{qmN_t} \end{bmatrix};$$

$$\mathbf{H}_{qm} \triangleq \begin{bmatrix} \mathbf{h}_{qm} & & & \\ & \mathbf{h}_{qm} & & \\ & & \ddots & \\ & & & \mathbf{h}_{qm} \end{bmatrix},$$

the equation (4.3.1) can be rewritten as

$$\begin{aligned} \mathbf{y}_{qm}(\tau) &= \mathbf{S}\mathbf{H}_{qm}\mathbf{c}(\tau) + \mathbf{v}_{qm}(\tau) \\ &= \mathbf{S}\mathbf{x}_{qm}(\tau) + \mathbf{v}_{qm}(\tau), \end{aligned} \quad (4.3.2)$$

where  $\mathbf{x}_{qm}(\tau) = \mathbf{H}_{qm}\mathbf{c}(\tau)$ . The received signal for the whole  $l$ -th codeword can be constructed by stacking the received signal at each time slot  $\tau$  into a matrix

$$\begin{aligned} \mathbf{Y}_{qm}(l) &\triangleq \begin{bmatrix} \mathbf{y}_{qm}(lT + 1) & \cdots & \mathbf{y}_{qm}(lT + T) \end{bmatrix} \\ &= \mathbf{S}\mathbf{X}_{qm}(l) + \mathbf{V}_{qm}(l), \end{aligned} \quad (4.3.3)$$

where  $\mathbf{X}_{qm}(l) \triangleq \mathbf{H}_{qm}\mathbf{C}(l)$  and  $\mathbf{C}(l)$  is defined as

$$\mathbf{C}(l) = \begin{bmatrix} \mathbf{C}_1^T(l) & \mathbf{C}_2^T(l) & \cdots & \mathbf{C}_K^T(l) \end{bmatrix}^T. \quad (4.3.4)$$

### 4.3.2 Encoding and Decoding of Differential STBC

Differential STBC based on unitary group codes [57] is regarded as the typical differential STBC because it holds the general structure of differential modulation for a rich class of space-time block codes. Differential STBC based on orthogonal designs [55][56] is very important in practical sense due to its simple encoding/decoding algorithm. With the considerations of both generality and practicality, these two kinds of differential STBC are discussed in this paper. Furthermore, we select the differential Alamouti STBC as the typical differential STBC based on general orthogonal design since the generalization is straightforward.

#### Encoding

Let  $\mathcal{G}$  be any group of unitary matrix, to send signal  $\mathbf{G}_k(l) \in \mathcal{G}$  in block  $l$ , the differential STBC based on unitary group codes are denoted as

$$\mathbf{C}_k(l) = \mathbf{C}_k(l-1)\mathbf{G}_k(l), \quad l = 1, 2, \dots, L. \quad (4.3.5)$$

For the differential Alamouti STBC (T=2), the codeword send in block  $l$  can be denoted as

$$\mathbf{C}_k(l) = \begin{bmatrix} c_{k1}(2l+1) & -c_{k2}(2l+2)^* \\ c_{k2}(2l+2) & c_{k1}(2l+1)^* \end{bmatrix}, \quad (4.3.6)$$

with

$$\begin{bmatrix} c_{k1}(2l+1) \\ c_{k2}(2l+2) \end{bmatrix} = \theta_k(l) \begin{bmatrix} c_{k1}(2l-1) \\ c_{k2}(2l) \end{bmatrix} + \phi_k(l) \begin{bmatrix} -c_{k2}(2l)^* \\ c_{k1}(2l-1)^* \end{bmatrix},$$

where  $\theta_k(l)$  and  $\phi_k(l)$  are mapped from source data sending in block  $l$  under a certain mapping pattern  $\mathcal{Q}$ . Subject to the transmit power constraint, it is easily seen that  $\|\theta_k(l)\|^2 + \|\phi_k(l)\|^2 = 1$ .

#### Decoding

Still Consider the decoding of the  $q$ -th user, we suppose that  $x_m^q(\tau) = \mathbf{h}_{qm}\mathbf{c}_q(\tau)$  is known somehow by estimation, which is the first entry in  $\mathbf{x}_{qm}(\tau)$ . To avoid confusion

with the previously defined matrix  $\mathbf{X}_{qm}(l)$ , we can stack  $x_m^q(\tau)$  into a matrix as

$$\mathbf{X}^q(l) \triangleq \begin{bmatrix} \mathbf{x}_1^q(l) \\ \vdots \\ \mathbf{x}_{N_r}^q(l) \end{bmatrix},$$

where we define

$$\mathbf{x}_m^q(l) \triangleq \left[ x_m^q(lT+1) \ \cdots \ x_m^q(lT+T) \right].$$

The decoding scheme for the differential STBC based on unitary group codes is

$$\hat{\mathbf{G}}_q(l) = \arg \max_{\mathbf{G}_q(l) \in \mathcal{G}} \text{Tr} \left( \bar{\mathbf{X}}^q(l) \bar{\mathbf{C}}_q(l) \bar{\mathbf{C}}_q^\dagger(l) (\bar{\mathbf{X}}^q(l))^\dagger \right),$$

where  $\text{Tr}(\cdot)$  denotes the trace and we define

$$\begin{aligned} \bar{\mathbf{X}}^q(l) &\triangleq \begin{bmatrix} \mathbf{X}^q(l-1) & \mathbf{X}^q(l) \end{bmatrix}, \\ \bar{\mathbf{C}}_q(l) &\triangleq \begin{bmatrix} \mathbf{C}_q(l-1) & \mathbf{C}_q(l) \end{bmatrix}. \end{aligned}$$

If the mapping pattern  $\mathcal{Q}$  of the differential Alamouti STBC is BPSK, the decoding scheme of the differential Alamouti STBC is

$$\begin{aligned} \hat{\theta}_q(l) &= \text{sign} \left( (\boldsymbol{\alpha}^q(l-1))^\dagger \boldsymbol{\alpha}^q(l) \right), \\ \hat{\phi}_q(l) &= \text{sign} \left( (\boldsymbol{\beta}^q(l-1))^\dagger \boldsymbol{\alpha}^q(l) \right), \end{aligned}$$

where we define

$$\begin{aligned} \boldsymbol{\alpha}_m^q(l) &= \begin{bmatrix} x_m^q(2l+1) & (x_m^q(2l+2))^* \end{bmatrix}, \\ \boldsymbol{\beta}_m^q(l) &= \begin{bmatrix} x_m^q(2l+2) & -(x_m^q(2l+1))^* \end{bmatrix}, \\ \boldsymbol{\alpha}^q(l) &= \begin{bmatrix} \boldsymbol{\alpha}_1^q(l) & \boldsymbol{\alpha}_2^q(l) & \cdots & \boldsymbol{\alpha}_{N_r}^q(l) \end{bmatrix}^T, \\ \boldsymbol{\beta}^q(l) &= \begin{bmatrix} \boldsymbol{\beta}_1^q(l) & \boldsymbol{\beta}_2^q(l) & \cdots & \boldsymbol{\beta}_{N_r}^q(l) \end{bmatrix}^T. \end{aligned}$$

### 4.3.3 Non-coherent Detection with Blind Linear Multiuser Estimator

From the aforementioned differential STBC decoding scheme, we can see that the key part of non-coherent detecting the differential STBC in MIMO DS-CDMA system

is to estimate  $x_m^q(\tau)$ , and the performance of this non-coherent detecting scheme largely depends on how accurately we could estimate  $x_m^q(\tau)$ . Since the mobile station only knows its own spreading code in the downlink, we also need to suppress the MAI blindly as we estimate  $x_m^q(\tau)$ . Of course a simple and direct method to estimate  $x_m^q(\tau)$  does exist, which is the well-known conventional matched filter. Because the conventional matched filter simply treats the interferences from other users as noise, it is natural that the performance of this "direct" method would not be good. To suppress the MAI efficiently, we define the linear MMSE estimator  $\mathbf{w}_{qm}$  for  $x_m^q(\tau)$

$$\mathbf{w}_{qm} = \arg \min \mathcal{E} [\|x_m^q(\tau) - \mathbf{w}_{qm}^\dagger \mathbf{y}_{qm}(\tau)\|^2]. \quad (4.3.7)$$

The well-known solution of  $\mathbf{w}_{qm}$  is

$$\mathbf{w}_{qm} = \mathbf{R}_{qm}^{-1} \mathcal{E} [\mathbf{y}_{qm}(\tau)(x_m^q(\tau))^*], \quad (4.3.8)$$

where  $\mathbf{R}_{qm}$  is the autocorrelation matrix of the received signal at the  $m$ -th receive antenna, which is denoted as

$$\mathbf{R}_{qm} = \mathcal{E} [\mathbf{Y}_{qm}(l)\mathbf{Y}_{qm}^\dagger(l)]. \quad (4.3.9)$$

To obtain a practical solution to equation (4.3.8), we require that the differential STBC possess the following structure:

- *Property A.* For any PSK constellation, there is

$$\mathcal{E} [\mathbf{C}(l)\mathbf{C}^\dagger(l)] = \mathbf{I}_{KN_t}. \quad (4.3.10)$$

For the two kinds of differential STBC mentioned above, it is obvious that  $\mathbf{C}_q(l)\mathbf{C}_q^\dagger(l) = \mathbf{I}_N$  due to the orthogonality of unitary group codes and STBC with orthogonal design. Furthermore, by selecting  $\mathcal{G}$  and  $\mathcal{Q}$ , we can easily show that *Property A* can hold water for most of the existing differential STBC. Apply *Property A* in equation (4.3.8), we obtain

$$\mathbf{w}_{qm} = \|\mathbf{h}_{qm}\|^2 \mathbf{R}_{qm}^{-1} \mathbf{s}_q, \quad (4.3.11)$$

and the autocorrelation matrix  $\mathbf{R}_{qm}$  can be written as

$$\mathbf{R}_{qm} = \mathbf{S}\mathbf{A}_{qm}\mathbf{S}^\dagger + \sigma_{qm}^2 \mathbf{I}_P, \quad (4.3.12)$$

where  $\mathbf{A}_{qm}$  is a diagonal matrix defined as

$$\mathbf{A}_{qm} \triangleq \begin{bmatrix} \|\mathbf{h}_{qm}\|^2 & & & \\ & \|\mathbf{h}_{qm}\|^2 & & \\ & & \ddots & \\ & & & \|\mathbf{h}_{qm}\|^2 \end{bmatrix}.$$

The correlation matrix  $\mathbf{R}_{qm}$  can be decomposed into a signal subspace and a noise subspace as

$$\mathbf{R}_{qm} = \mathbf{U}_{S,qm} \mathbf{\Lambda}_{S,qm} \mathbf{U}_{S,qm}^\dagger + \sigma^2 \mathbf{U}_{V,qm} \mathbf{U}_{V,qm}^\dagger, \quad (4.3.13)$$

where  $\mathbf{U}_{S,qm}$  is the signal subspace eigenvector matrix,  $\mathbf{U}_{V,qm}$  is the noise subspace eigenvector matrix,  $\mathbf{\Lambda}_{S,qm}$  is the signal subspace eigenvalue matrix. Because  $\mathbf{s}_q$  is orthogonal to the noise subspace, we can define the subspace-based linear MMSE estimator as in [60]

$$\mathbf{w}_{S,qm} = \|\mathbf{h}_{qm}\|^2 \mathbf{U}_{S,qm} \mathbf{\Lambda}_{S,qm}^{-1} \mathbf{U}_{S,qm}^\dagger \mathbf{s}_q. \quad (4.3.14)$$

It is interesting to notice that the above estimator can be a blind estimator if  $\|\mathbf{h}_{qm}\|^2$  can be blindly estimated or omitted because  $\mathbf{s}_q$  is known to the  $q^{th}$  user and  $\mathbf{R}_{qm}$  can be blindly estimated by  $\hat{\mathbf{R}}_{qm} = \frac{1}{L} \sum_{l=1}^L [\mathbf{Y}_{qm}(l) \mathbf{Y}_{qm}^\dagger(l)]$ .

#### 4.3.4 For MISO DS-CDMA System

Since only one receive antenna is equipped at the mobile station in an MISO DS-CDMA system, we have  $M = 1$  and therefore  $m = 1$ . However, we still keep sub-index  $m$  instead of 1 in this part for consistency. By exploiting the non-coherent detection algorithms of two kinds of differential STBC mentioned above, we can prove the following property:

- *Property B.* In MISO DS-CDMA system which applies the differential STBC based on unitary group codes or orthogonal designs, multiplying an arbitrary real positive scalar to the linear estimator  $\mathbf{w}_{qm}$  does not affect the performance.

(*Proof of Property B:*) Define a linear estimator  $\check{\mathbf{w}}_{qm} \triangleq a_{qm} \mathbf{w}_{qm}$ , where  $a_{qm}$  is an arbitrary real positive scalar, we can denote the estimations of  $x_m^q(\tau)$  as

$$\begin{aligned}\hat{x}_m^q(\tau) &= \mathbf{w}_{qm}^\dagger \mathbf{y}_{qm}(\tau), \\ \check{x}_m^q(\tau) &= \check{\mathbf{w}}_{qm}^\dagger \mathbf{y}_{qm}(\tau) = a_{qm} (\mathbf{w}_{qm}^\dagger \mathbf{y}_{qm}(\tau)).\end{aligned}$$

As in subsection 4.3.2, we can stack them as

$$\begin{aligned}\hat{\mathbf{x}}_m^q(l) &\triangleq \begin{bmatrix} \hat{x}_m^q(lT+1) & \cdots & \hat{x}_m^q(lT+T) \end{bmatrix}, \\ \check{\mathbf{x}}_m^q(l) &\triangleq \begin{bmatrix} \check{x}_m^q(lT+1) & \cdots & \check{x}_m^q(lT+T) \end{bmatrix}, \\ \hat{\mathbf{x}}^q(l) &\triangleq \begin{bmatrix} \hat{\mathbf{x}}_m^q(l-1) & \hat{\mathbf{x}}_m^q(l) \end{bmatrix}, \\ \check{\mathbf{x}}^q(l) &\triangleq \begin{bmatrix} \check{\mathbf{x}}_m^q(l-1) & \check{\mathbf{x}}_m^q(l) \end{bmatrix}.\end{aligned}$$

Obviously, we have  $\check{\mathbf{x}}^q(l) = a_{qm} \hat{\mathbf{x}}^q(l)$ . For differential STBC based on unitary group codes, the non-coherent detection algorithm is

$$\begin{aligned}\hat{\mathbf{G}}_q(l) &= \arg \max_{\mathbf{G}_q(l) \in \mathcal{G}} \text{Tr} \left( \check{\mathbf{x}}^q(l) \bar{\mathbf{C}}_q(l) \bar{\mathbf{C}}_q^\dagger(l) (\check{\mathbf{x}}^q(l))^\dagger \right) \\ &= \arg \max_{\mathbf{G}_q(l) \in \mathcal{G}} \|a_{qm}\|^2 \left( \hat{\mathbf{x}}^q(l) \bar{\mathbf{C}}_q(l) \bar{\mathbf{C}}_q^\dagger(l) (\hat{\mathbf{x}}^q(l))^\dagger \right) \\ &= \arg \max_{\mathbf{G}_q(l) \in \mathcal{G}} \left( \hat{\mathbf{x}}^q(l) \bar{\mathbf{C}}_q(l) \bar{\mathbf{C}}_q^\dagger(l) (\hat{\mathbf{x}}^q(l))^\dagger \right).\end{aligned}$$

For differential Alamouti's STBC with BPSK constellation, the non-coherent detection algorithm is

$$\begin{aligned}\hat{\theta}_q(l) &= \text{sign} \left\{ \begin{bmatrix} \check{x}_m^q(lT-1) \\ (\check{x}_m^q(lT))^* \end{bmatrix}^\dagger \begin{bmatrix} \check{x}_m^q(lT+1) \\ (\check{x}_m^q(lT+2))^* \end{bmatrix} \right\} \\ &= \text{sign} \left\{ a_{qm}^2 \begin{bmatrix} \hat{x}_m^q(lT-1) \\ (\hat{x}_m^q(lT))^* \end{bmatrix}^\dagger \begin{bmatrix} \hat{x}_m^q(lT+1) \\ (\hat{x}_m^q(lT+2))^* \end{bmatrix} \right\} \\ &= \text{sign} \left\{ \begin{bmatrix} \hat{x}_m^q(lT-1) \\ (\hat{x}_m^q(lT))^* \end{bmatrix}^\dagger \begin{bmatrix} \hat{x}_m^q(lT+1) \\ (\hat{x}_m^q(lT+2))^* \end{bmatrix} \right\}.\end{aligned}$$

Similarly, we can show the same conclusion for the detection of  $\phi_q(l)$ . Furthermore, the proof can be generalized to all differential STBC based on orthogonal designs. (*End of Proof*)

From *Property B*, we can omit the scalar  $\|\mathbf{h}_{qm}\|^2$  since it does not affect the performance of our detection scheme. Therefore in MISO DS-CDMA system, the linear MMSE estimator can be a blind linear MMSE estimator, which is redefined as  $\tilde{\mathbf{w}}_{qm} \triangleq \mathbf{R}_{qm}^{-1} \mathbf{s}_q$ , and the subspace-based blind linear MMSE estimator can be redefined as

$$\tilde{\mathbf{w}}_{S,qm} \triangleq \mathbf{U}_{S,qm} \mathbf{\Lambda}_{S,qm}^{-1} \mathbf{U}_{S,qm}^\dagger \mathbf{s}_q. \quad (4.3.15)$$

### 4.3.5 For MIMO DS-CDMA System

Unlike the MISO DS-CDMA system, for the non-coherent detection of user  $q$  in MIMO DS-CDMA system, we can't just omit  $\|\mathbf{h}_{qm}\|^2$  and stack the detected signals directly for differential decoding since that is similar to the ratio combining of  $x_m^q$  for  $m = 1, 2, \dots, M$  in a negative way. Therefore we need to blindly estimate  $\|\mathbf{h}_{qm}\|^2$  at each receive antenna. Obviously this kind of estimation is much easier than the multiple channels identification in coherent detection since only a positive scalar needs to be estimated. Let us first apply the  $\tilde{\mathbf{w}}_{S,qm}$  defined in MISO DS-CDMA system to the received signal  $\mathbf{y}_{qm}(\tau)$

$$\tilde{x}_m^q(\tau) = \tilde{\mathbf{w}}_{qm}^\dagger \mathbf{y}_{qm}(\tau).$$

Note  $\tilde{x}_m^q(\tau)$  is not the estimation  $x_m^q(\tau)$ , but the estimation of  $z_{qm}^{-1} x_m^q(\tau)$  instead, where  $z_{qm}$  is defined as  $z_{qm} \triangleq \|\mathbf{h}_{qm}\|^2$ . We stack  $\tilde{x}_m^q(\tau)$  into a vector as

$$\tilde{\mathbf{x}}_m^q(l) \triangleq \begin{bmatrix} \tilde{x}_m^q(lT+1) & \dots & \tilde{x}_m^q(lT+T) \end{bmatrix}.$$

Since  $\mathcal{E}[\mathbf{C}_q(l)\mathbf{C}_q^\dagger(l)] = \mathbf{I}_N$  for the two kinds of differential STBC considered in this paper, we can estimate  $z_{qm}$  as

$$\hat{z}_{qm} = \frac{1}{\frac{1}{L} \sum_{l=1}^L [\tilde{\mathbf{x}}_m^q(l)(\tilde{\mathbf{x}}_m^q(l))^\dagger]}. \quad (4.3.16)$$

Therefore the subspace-based blind linear MMSE estimator for MIMO DS-CDMA system can be defined as

$$\tilde{\mathbf{w}}_{S,qm} = \hat{z}_{qm} \mathbf{U}_{S,qm} \mathbf{\Lambda}_{S,qm}^{-1} \mathbf{U}_{S,qm}^\dagger \mathbf{s}_q. \quad (4.3.17)$$

### 4.3.6 Simulation Examples

In this section, we present simulation examples to demonstrate the performance of the proposed non-coherent blind MUD detection schemes for differential STBC. In our simulations, we consider a DS-CDMA system with  $K = 8$  users and generate the signature waveforms as random sequences with spreading gain  $P = 32$ . The differential Alamouti's code with BPSK constellation (Rate=1) and the differential Quaternion code [57] with QPSK constellation (Rate=1.5) are studied as examples of the differential STBC based on orthogonal designs and unitary group codes respectively. The Quaternion unitary group matrix  $\mathcal{G}$  with QPSK constellation is defined as the following set

$$\left\{ \pm \begin{bmatrix} 1 & 0 \\ 0 & 1 \end{bmatrix}, \pm \begin{bmatrix} j & 0 \\ 0 & -j \end{bmatrix}, \pm \begin{bmatrix} 0 & 1 \\ -1 & 0 \end{bmatrix}, \pm \begin{bmatrix} 0 & j \\ j & 0 \end{bmatrix} \right\},$$

and the initially transmitted codeword is

$$\mathbf{C}_k(1) = \begin{bmatrix} \frac{1}{\sqrt{2}} & -\frac{1}{\sqrt{2}} \\ \frac{1}{\sqrt{2}} & \frac{1}{\sqrt{2}} \end{bmatrix}.$$

Fig. 4.5 and Fig. 4.7 present the convergence speed of the proposed non-coherent blind MUD detection scheme at  $SNR = 14dB$  for differential Alamouti's code and differential Quaternion code respectively. It shows that the non-coherent blind MUD detection scheme overwhelms the non-coherent matched filter scheme when a very short block is used to do the estimation (here less than  $LT = 60$  symbol intervals). Also, we can see that convergence speed is fast, within about  $LT = 400$  symbol intervals, the proposed non-coherent blind MUD detection scheme almost reaches the best performance. Unlike coherent blind detection scheme, which needs a longer block in MIMO system than in MISO system even assuming channel state information known at receive, the proposed non-coherent blind scheme does not need extra symbols as we increase the number of receive antennas. In Fig. 4.6 and Fig. 4.8, we show the bit error rate (BER) performance of proposed non-coherent blind MUD detection scheme for aforementioned two example differential STBC respectively with the frame length  $LT = 400$  symbol intervals. It shows that proposed scheme possesses high performance: in DS-CDMA system with  $N_r = 1$  receive antenna, which only has about 1dB performance loss relative to the single user case;

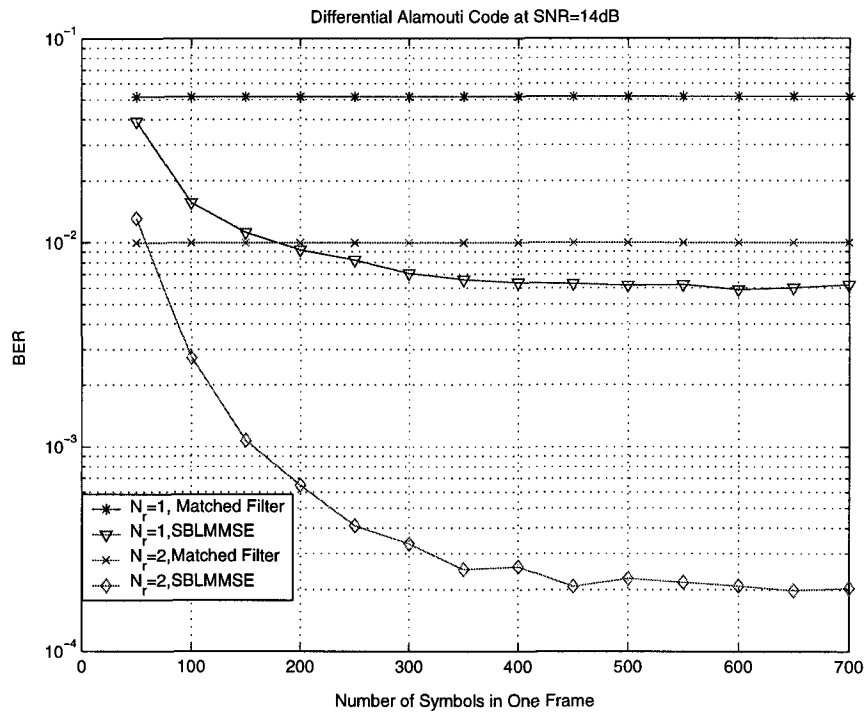


Figure 4.5: Convergence speed of non-coherent detection of the differential Alamouti's STBC with Rate=1 (BPSK constellation), in K=8 users DS-CDMA system.

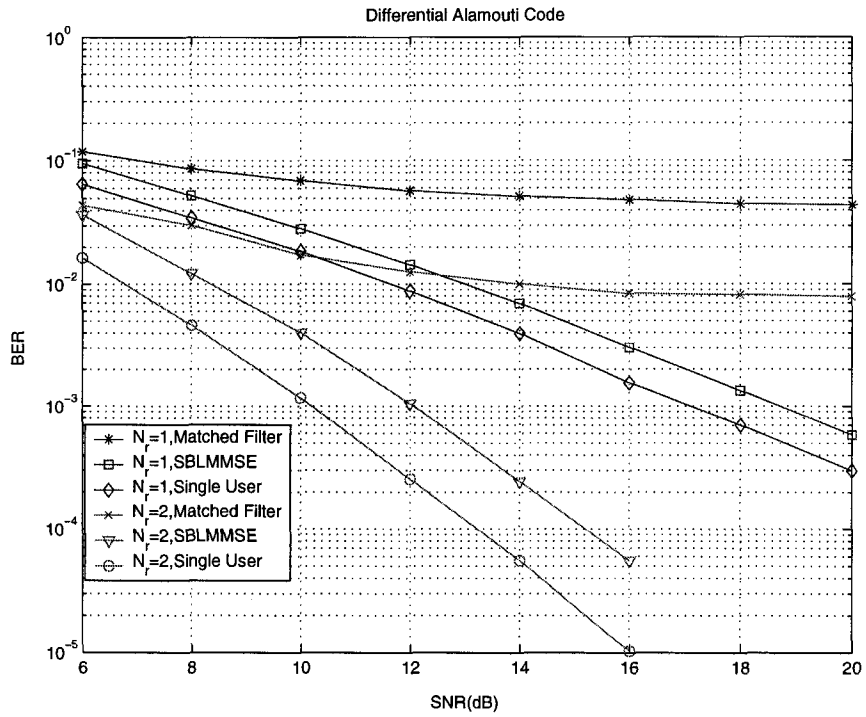


Figure 4.6: Performance of Non-coherent detection of the differential Alamouti's STBC with Rate=1 (BPSK constellation), in K=8 users DS-CDMA system.

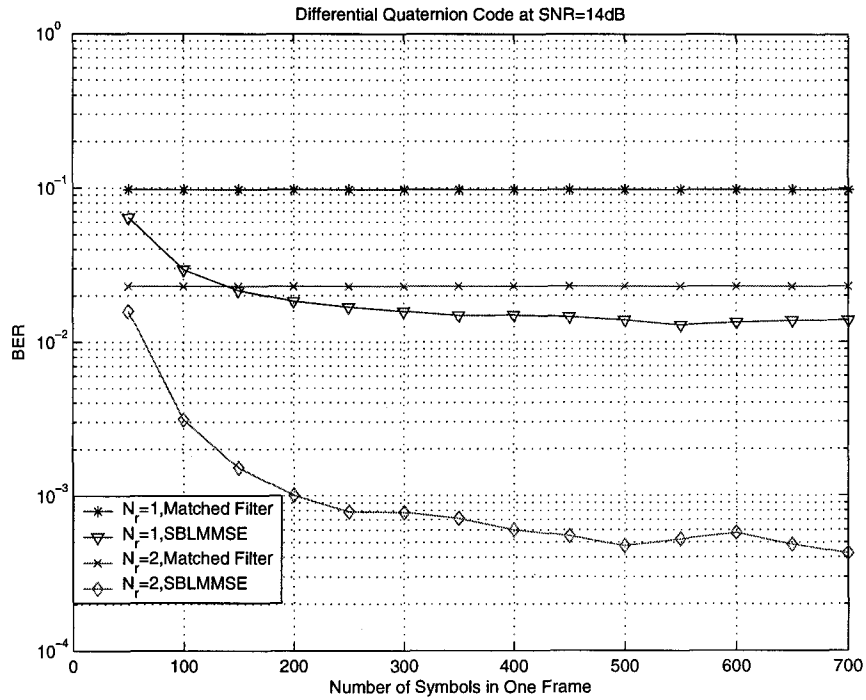


Figure 4.7: Convergence speed of non-coherent detection of differential Quaternion STBC with Rate=1.5 (QPSK constellation), in K=8 users DS-CDMA system.

in DS-CDMA system with  $N_r = 2$  receive antennas, which has about 1.7dB performance loss relative to the single user case.

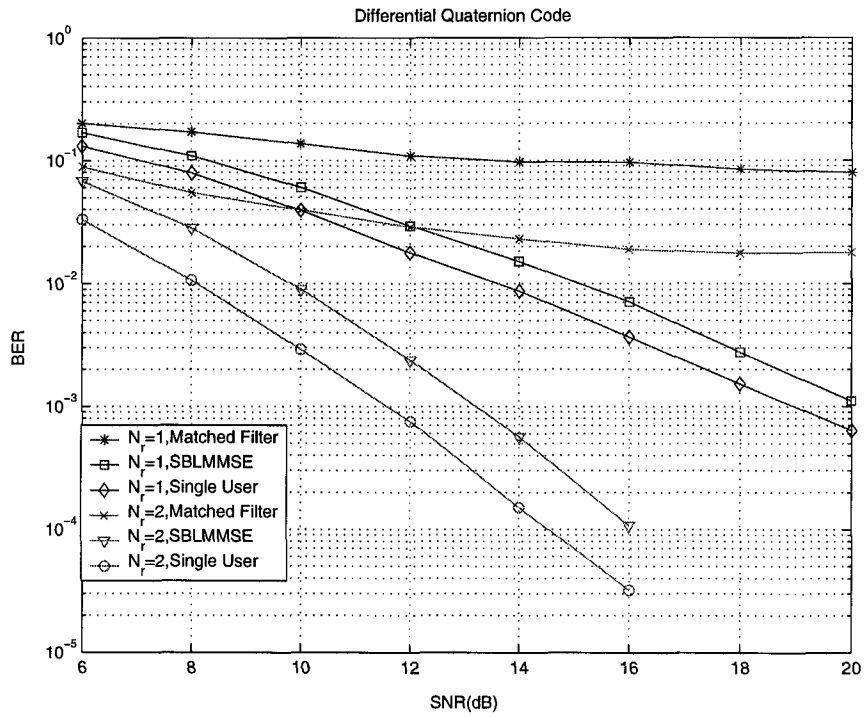


Figure 4.8: Performance of non-coherent detection of differential Quaternion STBC with Rate=1.5 (QPSK constellation), in K=8 users DS-CDMA system.

# Chapter 5

## Conclusions

We investigated power adaption and coding/decoding schemes in MIMO Rayleigh flat fading channels under the assumption that CSI is available at both the transmitter and the receiver. We suggested three coding methods that provide a tradeoff between coding/decoding complexity and performance: beamforming with channel partitioning, unordered multiple eigen-beamforming with channel partitioning, and ordered multiple eigen-beamforming with truncated channel inversion. Based on our numerical results, we showed that the capacities achieved by using the proposed multiple coding/decoding schemes can closely approach channel capacity and that the proposed schemes achieve a good tradeoff between coding/decoding complexity and capacity penalty. We also extended the conclusion [29] for SIMO system into MIMO system and restated it in a more general claim, i.e., the capacity penalty by using truncated channel inversion scheme diminishes as the maximum of the number of antenna increases while the minimum of number of antennas is fixed.

The main advantage of the proposed schemes is that they can approach channel capacity for MIMO systems with a moderate coding/decoding complexity. Implementing the optimum water-filling scheme would in principle require the use of an infinite number of codes. On the other hand, beamforming with channel partitioning requires only  $N$  different codes, matched to  $N$  different SNR values, where  $N$  need be only in the order of 2 or 3. Unordered multiple eigen-beamforming uses  $m$  coders/decoders in parallel, but these  $m$  coders use the same selection of  $N$  codes, i.e., also here only  $N$  different codes are

needed. Ordered multiple eigen-beamforming uses  $K$  coders/decoders in parallel, and each coder/decoder uses a different code, so  $K$  codes are used. Notice that all channels have been reduced to Gaussian channels, and many code design methods for the Gaussian channel can therefore be used to design practical coding schemes based on the methods developed here.

We also evaluated the capacities and the achievable rates of different power adaption schemes in correlated MIMO fading channels base on knowing the CSI at both the transmitter and the receiver. We showed that knowing the CSI at the transmitter is more crucial in highly correlated MIMO systems than in slightly (or uncorrelated) MIMO systems. We also showed that the capacity achieved by optimal power adaption can be approached by a simple beamforming TCI scheme in highly correlated MIMO systems.

Under the assumption that the CSI is only known at the mobile station, we applied the *group-blind* detection principle to develop the subspace-based blind multiuser decoders for space-time block codes in the downlink of a DS-CDMA system. We found out that the decoding of orthogonal STBC can still be decoupled and we combined sphere decoding with the subspace-based blind decoder for non-orthogonal STBC to obtain the best performance. We also proposed a decimation-combining processing to reduce the complexity. We showed that our proposed schemes can significantly outperform the traditional methods and the decimation-combining processing reduces the complexity with slight performance loss.

Under the assumption that the CSI is known neither at the base station nor at the mobile station, we developed non-coherent blind decoders for the differential STBC for the downlink of a DS-CDMA system. We presented the required structure of differential STBC to be suitable for blind decoding. We showed that in the MISO case, the decoding can be totally blind, however, in the MIMO case, one scalar is need to be estimated blindly to achieve better performance. We demonstrated that our non-coherent blind decoders can approach closely to the performance of a single user system.

# Bibliography

- [1] M. S Alouini and A. J. Goldsmith, "Comparison of fading channel capacity under different CSI assumptions," in *Proceedings of VTC 2000 fall*, vol. 4, pp. 1844-1849, Sep. 2000.
- [2] G. Foschini and M. Gans, "On limits of wireless communications in a fading environment when using multiple antennas," *Wireless Personal Communications*, vol. 6, pp. 311335, 1998.
- [3] E. Telatar, "Capacity of multi-antenna Gaussian channels," *European Trans. on Telecommunications*, vol. 10, no. 6 pp. 585-596, Nov. 1999.
- [4] G. J. Foschini, "Layered space-time architecture for wireless communication in fading environments when using multi-element antennas," *Bell Labs Tech. Journal*, pp. 41-59, 1996.
- [5] T. L. Marzetta and B. M. Hochwald, "Capacity of a mobile multiple-antenna communication link in Rayleigh flat fading," *IEEE Trans. Information Theory*, vol. 45, no. 1, pp. 139-157, Jan. 1999.
- [6] E. Biglieri, J. Proakis, and S. Shamai (Shitz), "Fading channels: Information-theoretic and communications aspects," *IEEE Trans. on Information Theory*, vol.44, no. 6, pp. 2619-2692, Oct. 1998.
- [7] N. Balaban and J. Salz, "Dual diversity combining and equalization in digital cellular mobile radio," *IEEE Trans. Veh. Technol.*, vol. 40, pp. 342354, May 1991.
- [8] G. G. Raleigh and J. M. Cioffi, "Spatio-temporal coding for wireless communication," *IEEE Trans. Commun.*, vol. 46, pp. 357366, Mar. 1998.

- [9] S. M. Alamouti, "A simple transmitter diversity scheme for wireless communications," *IEEE JSAC*, vol. 16, pp. 1451-1458, Oct. 1998.
- [10] V. Tarokh, N. Seshadri, and A. R. Calderbank, "Space-time block codes for high data rate wireless communications: Performance, criterion and code construction," *IEEE Trans. Information Theory*, vol. 44, pp. 744-765, Mar. 1998.
- [11] V. Tarokh, H. Jafarkhani, and A. R. Calderbank, "Space-time block coding from orthogonal designs," *IEEE Trans. Information Theory*, vol. 45, pp. 1456-1467, July 1999.
- [12] L. Zheng and D. N. C. Tse, "Diversity and multiplexing: a fundamental tradeoff in multiple-antenna channels," *IEEE Trans. Information Theory*, vol. 49, no. 5, pp. 1073-1096, May 2003.
- [13] C. A. Balanis, "Antenna Theory: Analysis and Design", Wiley, 1997.
- [14] D. Shiu, G. J. Foschini, M. J. Gans, and J. M. Kahn, "Fading correlation and its effect on the capacity of multielement antenna systems," *IEEE Trans. on Commun.*, vol. 48, pp. 502-513, Mar. 2000.
- [15] R. Janaswamy, "Effect of element mutual coupling on the capacity of fixed length linear arrays," *IEEE Antennas and wireless Propagation Lett.*, vol. 1, pp. 157-160, 2002.
- [16] L. Zheng and D. N. C. Tse, "Communication on the Grassmann manifold: a geometric approach to the noncoherent multiple-antenna channel," *IEEE Trans. Information Theory*, vol. 48, no. 2, pp. 359-383, Feb. 2003.
- [17] H. Yao, G. W. Wornell, "Structured space-time block codes with optimal diversity-multiplexing tradeoff and minimum delay," *IEEE Globecom'03*, vol. 4, Dec. 2003.
- [18] J. Yuan, Z. Chen, B. Vucetic, and W. Firmanto, "Performance and design of space-time coding in fading channels," *IEEE Trans. on Commun.*, vol. 51, no. 12, pp. 1991-1996, Dec. 2003.

- [19] A. R. Hammons and H. E. Gamal, "On the theory of space-time codes for psk modulation," *IEEE Trans. Information Theory*, vol. 46, no. 2, pp. 524-542, Mar. 2000.
- [20] A. Narula, M. J. Lopez, M. D. Trott and G. W. Wornell, "Efficient use of side information in multiple-antenna data transmission over fading channels," *IEEE JSAC*, vol. 16, pp. 1423-1436, Oct. 1998.
- [21] S. K. Jayaweera and H. V. Poor, "Capacity of multi-antenna systems with adaptive transmission techniques," *Proc. 5th Intl. Symp. on WPMC*, vol. 2, pp. 392-396, Honolulu, Hawaii, Oct. 2002.
- [22] S. K. Jayaweera and H. V. Poor, "Capacity of multiple-antenna systems with both receiver and transmitter channel state information," *IEEE Trans. Information Theory*, vol. 49, no. 10, pp. 2697-2709, Oct. 2003.
- [23] T. M. Cover and J. A. Thomas, "Elements of information theory," *John Wiley & Sons, Inc*, 1991.
- [24] W. Yu and J. Cioffi, "On constant-power waterfilling," *IEEE International Conference on Communications (ICC)*, vol.6, pp. 1665 -1669, June 2001.
- [25] A. J. Goldsmith and P. P. Varaiya, "Capacity of fading channels with channel side information," *IEEE Trans. Information Theory*, vol.43, no.6, pp. 1986-1992, Nov. 1997.
- [26] G. Caire and S. Shamai (Shitz), "On the capacity of some channels with channel state information," *IEEE Trans. Information Theory*, vol. 45, no. 6, pp. 2007-2019, Sept. 1999.
- [27] E. Biglieri, G. Caire, and G. Taricco, "Limiting performance of block-fading channels with multiple antennas," *IEEE Trans. Information Theory*, vol. 47, no. 4, pp. 1273-1289, May 2001.
- [28] S. Chung, G. D. Forney, T. J. Richardson, and R. Urbanke, "On the Design of Low-Density Parity-Check Codes within 0.0045 dB of the Shannon Limit," *IEEE Commun. Letters*, vol. 5, no. 2, pp. 58-60, Feb. 2001.

- [29] M. S. Alouini and A. J. Goldsmith, "Capacity of Rayleigh fading channels under different adaptive transmission and diversity-combining techniques," *IEEE Trans. Vehicular Technology*, vol. 48, no. 4, pp. 1165-1181, Jul. 1999.
- [30] L. Lin, R. D. Yates, and P. Spasojevic, "Adaptive transmission with discrete code rates," *IEEE International Conference on Communications (ICC)*, vol. 3, pp. 1424-1428, May 2002.
- [31] A. T. James, "Distributions of matrix variates and latent roots derived from normal samples," *Ann. Math. Statist.*, vol. 35, pp. 475-501, 1964.
- [32] S. A. Jafar and A. J. Goldsmith, "Beamforming capacity and SNR maximization for multiple antenna systems," VTC 2001 Spring, *IEEE VTC 53rd*, vol. 1, pp. 43-47, May 2001.
- [33] R. Knopp and G. Caire, "Power control and beamforming for systems with multiple transmit and receive antennas," *IEEE Trans. Wireless Commun.*, vol. 1, no. 4, pp. 638-648, Oct. 2002.
- [34] "Special issue on codes on graphs and iterative algorithms", *IEEE Trans. Information Theory*, vol. 47, no. 2, Feb. 2001.
- [35] "The turbo principle: from theory to practice, part I", *IEEE JSAC*, vol. 19, no. 5, May 2001.
- [36] "The turbo principle: from theory to practice, part II ", *IEEE Journal on Selected Areas in Commun.*, vol. 19, no. 9, Sept. 2001.
- [37] "Capacity approaching codes, iterative decoding algorithms and their applications", *IEEE Communications Magazine*, vol. 41, no. 8, pp. 100-140, Aug. 2001.
- [38] C. Chuah, D. N. C. Tse, J. M. Kahn, and R. A. Valenzuela, "Capacity scaling in MIMO wireless systems under correlated fading," *IEEE Trans. Information Theory*, vol.48, pp. 637-650, Mer. 2002.
- [39] P. J. Smith, S. Roy and M. Shafi, "Capacity of MIMO systems with semicorrelated flat fading," *IEEE Trans. Inform. Theory*, vol. 49, no. 10, pp. 2781-2788, Oct. 2003.

- [40] M. Chiani, M. Z. Win and A. Zanella, "On the capacity of spatially correlated MIMO Rayleigh-fading channels," *IEEE Trans. Inform. Theory*, vol. 49, no. 10, pp. 2363-2371, Oct. 2003.
- [41] M. T. Ivrlač, W. Utschick and J. A. Nossek, "Fading correlatiions in wireless MIMO communication systems," *IEEE Journal on Selected Areas in Commun.*, vol. 21, no. 5, pp. 819-828, June 2003.
- [42] V. A. Aalo, "Performance of maximal-ratio diversity systems in a correlated Nakagami-fading environment," *IEEE Trans. on Commun.*, vol. 43, no. 8, pp. 2360-2369, Aug. 1995.
- [43] S. Verdu, "Multiuser Detection," Cambridge university Press, 1998
- [44] J.Geng, U.Mitra and M.P.Fitz, "Space-Time block codes in multipath CDMA systems", *IEEE ISIT 2001*, Washington, D.C., June 24-29, 2001.
- [45] J. Geng, U. Mitra and M. P. Fitz, "Optimal space-time block codes for CDMA systems", *Milcom 2000*, Los Angeles, CA, October 2000.
- [46] G. Klang and A. Naguib, "Transmit diversity based on space-time block codes in frequency selective Rayleigh fading DS-CDMA systems," *In Proc. of VTC 2000, IEEE*, vol. 1, pp. 264-68, May 2000.
- [47] B. Hassibi and B. M. Hochwald, "High-rate codes that are linear in space and time," *IEEE Trans. on Information Theory*, vol. 48, no. 7, pp.1804-1824, July 2002.
- [48] H. Li, X. Lu and G. B. Giannakis, "Capon multiuser receiver for CDMA systems with space-time coding," *IEEE Trans. on Signal Processing*, vol. 50, no. 5, May 2002.
- [49] X. Wang and A. Høst-Madsen, "Group-blind multiuser detection for uplink CDMA", *IEEE Journal on Selected Areas in Commun.*, vol. 17, No. 11, Nov. 1999.
- [50] J. Conway and N. Sloane, "Sphere packings, lattices and graphs", Springer-Verlag, 1993.

- [51] B. Hassibi and H. Vikalo, "On the sphere decoding algorithm: Part I, the expected complexity" submitted to *IEEE Trans. on Signal Processing*.
- [52] E. Viterbo and J. Boutros, "A universal lattice code decoder for fading channels", *IEEE Trans. Inform. Theory*, vol. 45, no. 5, Jul. 1999.
- [53] B. M. Hochwald and T. L. Marzetta, "Unitary space-time modulation for multiple-antenna communication in Rayleigh flat-fading," *IEEE Trans. Inform. Theory*, vol. 46, pp. 543564, Mar. 2000.
- [54] B. M. Hochwald, T. L. Marzetta, T. L. Richardson, W. Sweldens, and R. Urbanke, "Systematic design of unitary space-time constellations," *IEEE Trans. on Infomation theory*, vol. 46, pp. 19621973, Sep. 2000.
- [55] V. Tarokh and H. Jafarkhani, "A differential detection scheme for transmit diversity," *IEEE Journal on Selected Areas in Communications*, vol.18, no.7, pp.1169-1174, July 2000.
- [56] H. Jafarkhani and V. Tarokh, "Multiple transmit antenna differential detection from generalized orthogonal designs," *IEEE Trans. on Infomation theory*, vol. 47, no. 6, pp. 2626-2631, Sep. 2001.
- [57] B. Hughes, "Differential space-time modulation," *IEEE Transactions on Information Theory*, vol. 46, no. 7, pp. 2567-2578, Nov. 2000.
- [58] B. M. Hochwald and W. Sweldens, "Differential Unitary SpaceTime Modulation," *IEEE Trans. on Commun.*, vol. 48, no. 12, pp. 2041-2052, Dec. 2000.
- [59] C. Gao and A .M. Haimovich, "A Differential Detection Scheme for DS/CDMA Spatial Diversity," *IEEE ICC*, vol. 1, pp. 465-469, May 2002.
- [60] X. Wang and H. V. Poor, "Blind Multiuser Detection: A Subspace Approach," *IEEE Trans. on Information Theory*, vol. 44, no. 2, pp.677-690, Mar. 1998